EFFECTS OF CYCLIC COMPRESSIVE LOADING AND SELF HEALING ON THE MECHANICAL AND PERMEABILITY PROPERTIES OF CONCRETE

by

Tümer Akakın

B.S., Civil Engineering, Boğaziçi University, 1998

M.S., Civil Engineering, Boğaziçi University,2001

Submitted to the Institute for Graduate Studies in
Science and Engineering in partial fulfillment of
the requirements for the degree of
Doctor of Philosophy

Graduate Program in Civil Engineering

Boğaziçi University

2008

ACKNOWLEDGEMENTS

I would like to thank my thesis supervisor Prof. Turan Özturan for providing me with the opportunity to complete my PhD thesis. I also especially want to thank my thesis advisory committee Prof. Mehmet Ali Taşdemir and Ass. Prof. Cem Yalçın whose support and guidance made my thesis work possible.

I want to thank present and past members of the laboratory technicians and assistants for helping me in the researches. Onur Ertaş for his continuous support.

I would also like to acknowledge Boğaziçi University Scientific Research Project (BAP 04A401) for their support to the project.

For the non-scientific side of my thesis, I particularly want to thank my wife Hatice Çınar Akakın and my little boy Çınar for their support.

ABSTRACT

EFFECTS OF LOW CYCLIC COMPRESSIVE LOADING AND SELF HEALING ON THE MECHANICAL AND PERMEABILITY PROPERTIES OF CONCRETE

Cyclic loading causes progressive and permanent process of the change of the internal structure of the material. Concrete, when subjected to repeated loads, may exhibit excessive cracking and may eventually fail after a sufficient number of load repetitions, even if the maximum stress applied is less than the static strength of a similar specimen.

Behavior of concrete under cyclic loading becomes important because of the widespread adoption of the ultimate strength design procedures and the use of higher strength material requires structural concrete members perform satisfactorily under high stress levels. With high stress ratios (applied stress/ultimate stress) low cycle and with lower stress ratios high cycle tests are applied. A study of the behavior after a certain number of cycles of a pre-fatigue represents a more realistic approach to measure the properties. The curing conditions which the concrete is exposed to after the cycles of pre-fatigue become important in determining the effect of cyclic loading on mechanical and permeability properties of concrete. Changes in the mechanical properties of concrete due to cyclic loading have been investigated in this study, taking into account the characteristics of the cyclic loading and curing conditions applied to concrete after pre-fatigue.

In this study, up to 100 cycles of compression loading is applied to 100x200 mm concrete cylinders with an average 28 day compressive strength of 38 MPa. The stress ratios (applied stress/ultimate stress) were 0.9, 0.8 and 0.6. Stress-strain behavior and modulus of elasticity were determined during cyclic loading, and ultrasonic pulse velocity and splitting tensile strength tests were carried out on cyclically loaded specimens. For the stress ratio $0.9f_{max}$ the modulus of elasticity, splitting tensile strength, ultrasonic pulse

velocity and compressive strength decreased as 47, 30, 8 and 6 percentages respectively after 100 cycles of loading. After water curing applied on the cyclic loaded specimens, 62, 5, 22, and 8 percentages increases were obtained for the modulus of elasticity, compressive strength, tensile splitting strength and ultrasonic pulse velocity, respectively, due to self healing.

The permeability properties were investigated through rapid chloride permeability, water absorption, sulphate attack and mercury intrusion tests. Mercury intrusion tests revealed that total pore volume and total pore area were higher for cyclically loaded specimen compared with the unloaded specimen. Mass losses due to sulphate attack for $0.9f_{max}$ loaded specimen were higher than those of control specimen and water cured specimens had lower mass losses.

The crack sizes for higher loading ratios were found larger and with self healing effect the cracks could get closer. The post peak responses were investigated and the change in behavior was found to change with cyclic loading.

ÖZET

BETONDA TEKRARLI BASINÇ YÜKLEME SONRASI BETONUN MEKANİK VE GEÇİRİMLİLİK ÖZELLİKLERİ VE KENDİNİ İYİLEŞTİRMESİNİN İNCELENMESİ

Tekrarlı yükleme malzemenin iç yapısında sürekli artarak ilerleyen ve kalıcı değişikliklere sebep olan hasarlara neden olur. Beton tekrarlı yüklemeye maruz kaldığında aşırı bir çatlama oluşabilir ve belli bir tekrarlı yüklemeden sonra benzer numunedeki dayanıma ulaşılmadığı halde çökebilir.

Tekrarlı yüklemelerin önemli olmasının nedenlerinden biri günümüzde kullanılan taşıma gücüne göre yapı tasarımı nedeniyle malzemelerin servis yüklerinde bile yüksek gerilmelere maruz kalabilmesidir. Yüksek gerilme oranlarında düşük tekrarlı ve düşük gerilme oıranlarında ise yüksek tekrarlı deneyler uygulanarak özellikleri incelenmektedir. Tekrarlı yüklemeye maruz kalacak malzemelerin özelliklerinin incelenmesinde yorulma öncesi belli bir tekrarlı yüklemeye maruz bırakılması daha gerçekçi bir yaklaşım olacaktır. Ayrıca tekrarlı yükleme sonrası betonun maruz kalacağı kür koşulları tekrarlı yüklemenin mekanik ve geçirgenlik üzerine etkisinin incelenmesinde önemlidir. Tekrarlı yüklemeden dolayı betonun mekanik ve geçirgenlik özelliklerini tekrarlı yüklemenin karakteristiği ve kür koşulları dikkate alınarak bu tezde incelenmiştir.

Bu çalışmada 100x200mm boyutlarında 28 günlük basınç dayanımı 38 MPa olan silindir beton numuneleri üzerinde 100 kez tekrarlı basınç gerilmesi uygulanmıştır. Gerilme oranları (uygulanan gerilme/ dayanım gerilmesi) 0.9, 0.8, 0.6 olarak uygulanmıştır. Gerilme- şekil değiştirme ve elastisite modulleri tekrarlı yükleme sırasında elde edilmiş ve ultrases hızı, yarmada çekme dayanımı, basınç dayanımı tekrarlı yükleme uygulanmış numuneler üzerinde ölçülmüştür. $0.9f_{max}$ oranında yüklenmiş numunelerde yüzde 47 oranında elastisite modulu , yüzde 30 oranında yarmada çekme dayanımı, yüzde 8 oranında ultrases dayanımı ve yüzde 6 oranında basınç dayanımı 100 kez tekrarlı

yükleme sonrası azalmıştır. Betonun kendini erken yaşlarda iyileştirmesi özelliği ile de elastisite modulu yüzde 62, basınç dayanımı yüzde 5, yarmada çekme dayanımı yüzde 22 , ultrases dayanımı yüzde 8 oranında su kürü koşullarında artmıştır.

Geçirgenlik özelliklerindeki değişim hızlı klor geçirgenliği, su emme, sülfat etkisi ve civalı porozimetre deneyleri ile incelenmiştir. Su emme oranı $0.9f_{max}$ oranında yüklenmiş numunelerde yüzde 50 oranında artmış , su kürü ile bu oran azalmıştır. Civalı porozimetre deneyinde ise tekrarlı yükleniş numunelerde toplam toplam boşluk hacmi ve toplam boşluk yüzey alanları artmıştır. Hızlı klor geçirgenliği deneyleri $0.9f_{max}$ oranında yüklenmiş numunelerde yüzde 26 oranında artmıştır. Ayrıca sülfat etkisi altında numunelerin kütle kayıpları daha yüksek oranda gerçekleşmiştir.

Ayrıca çatlak boyutlarının tekrarlı yükleme ile arttığı ve su kürü ile boyutlarının azaldığı belirlenmiştir. Kırılma sonrası özellikleri de incelenmiş ve tekrarlı yükleme etkisi gözlemlenmiştir.

TABLE OF CONTENTS

LIST OF FIGURES

LIST OF TABLES

LIST OF SYMBOLS/ABBREVATIONS

A	Area of the specimen
D	Diameter of the specimen
d_c	Pore diameter
E	Modulus of elasticity
E_{cm}	Secant modulus of elasticity
f_{ck}	Characteristic strength
f_{max}	Loading ratio compared with peak stress
f_r	Rupture strength
f_c	Stress during loading
f_{cm}	Target mean cylinder compressive strength
f_{ctm}	Mean axial tensile strength
$f_{ctm,fl}$	Mean flexural strength
f_{ct}	Axial tensile strength
$f_{ct,sp}$	Tensile splitting strength
f_{ult}	Peak stress
G_f	Fracture energy
K	Sorptivity
k	Coefficient of permeability
L	Length of specimen
N	Number of cycles
N_f	Cycles up to failure
n_u	Ultimate number of cycles during fatigue loading
t	Time
u_p	Plastic strain
Q	Total flow
P	Applied load
P_m , V	Pore volume
S_{max}	Maximum loading during cyclic loading
S_{min}	Minimum loading during cyclic loading
Å	Pore radius

ε	Axial strain
ε_{max}	Maximum strain
σ	Axial stress

1 . INTRODUCTION

Concrete became the most used engineering material over the last century because of its being economic, easily available and structurally advantageous. However, the widespread use of ultimate strength design procedures and the use of higher strength materials cause cyclic loading to be an important problem in concrete structures such as pre-stressed concrete railroad ties, marine structures, airport concrete pavements and continuously reinforced concrete pavements. When concrete is subjected to cyclic loading mechanical and permeability properties of concrete are adversely affected which causes structural safety and durability problems. Since cyclic loading is a common problem the changes in concrete properties should be investigated to determine the service life and structural stability. Considering the autogenous healing of concrete under appropriate conditions, the mechanical and permeability properties of concrete after self healing should also be investigated to observe the effectiveness of this process the repair of the damage caused by cyclic loading.

Stress repetition is called as cyclic loading which can be caused by external loads or by temperature variation. As a result of cyclic loading a progressive and permenant damage is caused in the material. In static loading, increasing stress cracks are developed in the material, but these cracks are recoverable as long as the material's behavior is elastic. As the loading level increases the solid material's response becomes nonlinear which is because of irreversible energy dissipation. This nonlinear behavior can either be ductile or brittle changing with the crystallization of the solid. This behavior in brittle materials like concrete is nonlinear which is related to the opening and growth of the pre existing cracks and voids. In contrast to static loading, there is irreversible energy dissipation in each cycle of repeated loading so cracks propagate, which results in redistribution of stresses and increased deformations. [1]

The damage evaluation and the failure of concrete in cyclic compression are very complex. Damage in concrete by cyclic loading develops in two stages. In the first phase, micro cracking occurs as a result of cementation breaking between the aggregates and the cement paste. In the second phase, micro cracks grow, propagate and unite to form the

major cracks. As a consequence, the gradual weakening of the material occurs and, if a great number of repeated loads are applied, both layers and structure may collapse. [2]

The amount of damage in concrete due to cyclic loading is related with cyclic loading stress levels and the number of cycles. As the stress level decreases the number of cycles to failure increases and in contrast as the stress level increases the number of cycles to failure decresases. As a result of cyclic loading failure occurs which is also known as fatigue. Concrete is known to have no fatigue limit which means there is no maximum ratio of the applied stress below which concrete can withstand an infinite number of loading cycles without failure. [3]

Concrete structures subjected to cyclic loading need to be evaluated whether the serviceability limit is reached due to excessive damage. Thus concrete subjected to cyclic compressive loading should be evaluated for its mechanical properties used in the design of structures such as compressive and tensile strengths and modulus of elasticity as well as the permeability properties related to durability of this structure. So, the objective of this study is to evaluate the changes of mechanical and permeability properties of concrete under low cyclic compressive loading at different loading ratios and under self healing conditions.

In literature the cyclic tests are generally done on the mechanical properties of concrete. But testing done on the permeability properties of the concrete is very rare. Permeability of concrete from bridges or dynamically loaded members is not the same as the permeability of concrete under static loading. In designing such concrete structures permeability of concrete should be measured on dynamically loaded samples.

So a study of the behavior of concrete after a certain number of cycles of a pre-fatigue loading represents a more realistic approach to measure the properties of a cyclically loaded structural concrete. During cyclic loading it was found out that most of the damage occurs in the first cycles of loading. Normalized strain value which gives us information about the deformation that the specimen experiences actually gives us valuable data on the damage that the specimen experiences.

In this thesis the changes in concrete properties with up to 100 cyclic compressive loading will be measured. The changes in the permeability and mechanical properties of concrete under cyclic compressive loading will be observed at load levels of $0.6f_{max}$, $0.8f_{max}$ and $0.9f_{max}$. In this research after cyclic loading, mechanical and permeability properties of concrete were measured. Mechanical tests applied were compressive strength, modulus of elasticity, ultrasonic pulse velocity, post peak response analysis, and permeability properties were measured applying the tests of water absorption, rapid chloride permeability, magnesium sulphate effect, optical analysis. The tests were applied before and after cyclic loading so that cyclic loading effects were investigated. Also to observe self healing effects some of the specimen after cyclic loading application were kept in water and laboratory cure conditions.

Post peak response was conducted to investigate the property changes after cyclic loading. As well as other mechanical properties cyclic loading would also change the post peak response of the concrete.

2 . LITERATURE REVIEW

Cyclic loading effects on materials were first observed and documented for iron. The first study of metal fatigue is believed to have been conducted around 1829 by the German engineer Albert [4]. He performed repeated load proof tests on mine-hoist chains made of iron. The interest in the study of fatigue expanded later on due to the increasing use of iron particularly in wheel axels in bridges and railway systems. The first fatigue curve for concrete cubes in compression was published by Van Ornum [3]. He found no endurance limit for concrete similar to that which had been assumed for steel. On the development of highway systems in the 1920s led to further interest in the fatigue of concrete, since the concrete pavements used for the highways are subjected to millions of load cycles from axle loads of cars and trucks. In numerous applications, concrete is subjected to repeated cyclic loads under which concrete gets unrecoverable damage and eventually may fail. As concrete is subjected to loads at increasing intensity damage occurs as ranging from micro cracking to ultimate failure [5].

First systematic cyclic loading tests on concrete were done at few laboratories notably by August Wöhler [6]. One of the results of these studies was that the fatigue strength of concrete was defined as a fraction of the static strength that can be repeatedly applied for a given number of cycles without failure of the material changes in the properties of concrete.

During the last few decades the concrete fatigue phenomenon has once again gained interest, especially for railway bridges, due to more slender structures, higher traffic speeds and higher axle loads. For example, the increased axle loads on the existing railway lines have caused problems with the bridges since it has led to a change of the conditions for the bridges compared to the ones when they were built. One of the problems is that the bridges are often predicted to fail in the fatigue analysis when they are evaluated with the present concrete codes [4].

Basic theory of cyclic compressive loading will be investigated in this section. First, the behavior of concrete under compression will be discussed. Then, how the failure

mechanism works in static and cyclic compression will be studied, and the mechanical and permeability properties of concrete after cyclic loading will be investigated. Finally, the effects of self healing on mechanical and permeability properties of cyclically loaded concrete will be reviewed.

2.1. Failure Mechanisms of Concrete Under Compression

The behavior of concrete under uniaxial compression loading has been investigated by numerous researchers since compressive strength is the primary parameter in the design of concrete structures and significant information on stress strain behavior of concrete exists in literature.

Concrete behavior is complex under compression at both microscopic and macroscopic levels because; the concrete is a heterogeneous material with multiple phases consisting of portland cement, aggregate and water. One of the ingredients of this heterogeneous material, namely cement, undergoes a chemical hydration process after contacting with water, which produces microscopic hydration products to form a matrix that holds aggregate particles together after hardening. So, there are two phases; namely cement paste and aggregate, which forms concrete known as one of the most complex multiphase materials in engineering [7,8].

Cement matrix is porous and there are additionally micro cracks between the aggregates and cement paste which can be the result of bleeding, shrinkage and thermal stresses between them. Also some pores can be the remains of water after hydration of cement. So, concrete has cracks inherently. Since there are two phases in concrete material the fracture of concrete may start by fracture of cement paste or fracture of aggregate or failure of bond in the interface between the paste and the aggregate.

Figure 2.1 summarizes failure modes of concrete under compression proposed by different researchers. There are pores inherently in concrete and stress concentrations under compression forms micro cracks resulting in axial tensile splitting as shown in (a) section of Figure 2.1. Some researchers model the failure of concrete, in terms of inclusions like stiff aggregates which have different stiffness parameters and the tensile

cracks between inclusions, as shown in (b) and (c) section of Figure 2.1. On the other hand, in the absence of inclusions or pores, the inclined cracks may form depending on the direction and intensity of loading which leads to total failure [9].

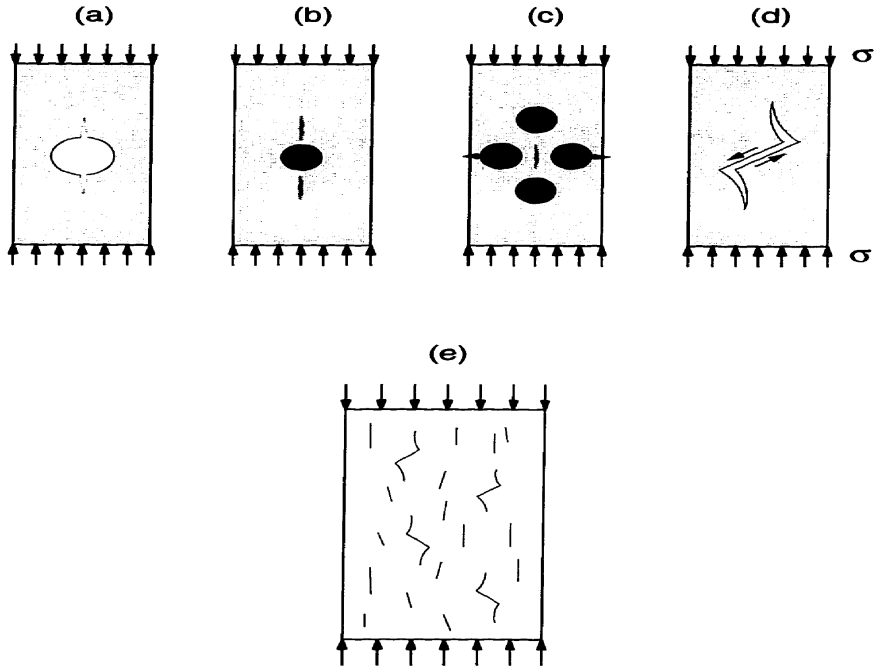

Figure 2.1. Failure modes of concrete under compression [9]

In the uniaxial case failure occurs by progressive microcracking, starting at the aggregate mortar interface, later extending as tensile cracks through the mortar. In the uni axial case ultimate failure occurs by splitting in planes perpendicular to the face of the specimen and parallel to the load [10]. Under compression and tension there is a similar mechanism in the concrete between aggregates and mortar [11].

When the concrete is under uniaxial compression, recoverable elastic and irrecoverable inelastic deformations can be observed because of increased cracking [12]. These cracks occur because aggregates and hardened cement paste show different mechanical behaviors as illustrated by the difference in their moduli of elasticity. As shown in Figure 2.2, the cement paste which has no aggregates has a different behavior than mortar which has fine aggregates. So, these differences lead to stress concentrations and eventually to cracking at the contact surface of these materials for normal strength

concrete. As a consequence, there is a nonlinear behavior of concrete under compression which can be observed in the stress strain behavior[9, 13].

In concrete subjected to compression stress, stress concentrations occur because of the above mentioned causes and microscopic flaws invariably grow and combine with each other and propagate in cement aggregate interface or in cement paste[14]. So, failure of concrete is a result of the start and growth of micro cracks which can be later observed as macro cracks. The compression damage can start at very low stress levels as shown in Figure 2.3 [15]. For normal strength concrete, negligible bond cracks start for stress levels upto 30 per cent of f_{max} where as between 30 per cent and 50 per cent of ultimate stress bond cracks start to increase. Then, matrix cracks start to grow after 50 per cent stress level and more extensive and continuous macro crack system develops. After 75 per cent stress level the matrix cracks start to grow faster as shown in Figure 2.3. With increasing load, macro cracking increases and becomes unstable leading to failure which is also called critical load for crack formation of concrete [14]. On the other hand, most of the cracks that are opened while loading may recover after unloading depending on the level of bonding and damage occurred [16]. Also some researchers found out that sustained loading has a remedial effect where sustained load causes Van der Walls forces to be active an attraction between hydration products of cement [17].

Because of the increased macro cracks an increase in volume can be observed after 75 per cent of maximum load. Also, microscopic internal splitting throughout the specimen occurs [18]. The increase of volume occurs at peak or near peak loads at which the damage is localized. After that, the peak stress failure is immediate. Also, after peak stress, the strain distribution along the specimen is not uniform since failure occurs in localized finite dimensions and in the damage zone there is an increase of damage where the other part of the specimen unloads [18].

This cracking mechanism softens the material and nonlinear stress-strain relationship starts [14]. As the cracks increase in number and size with the increasing stress, the cracks are also aligned towards the direction of the applied stress as shown in Figure 2.4 [19].

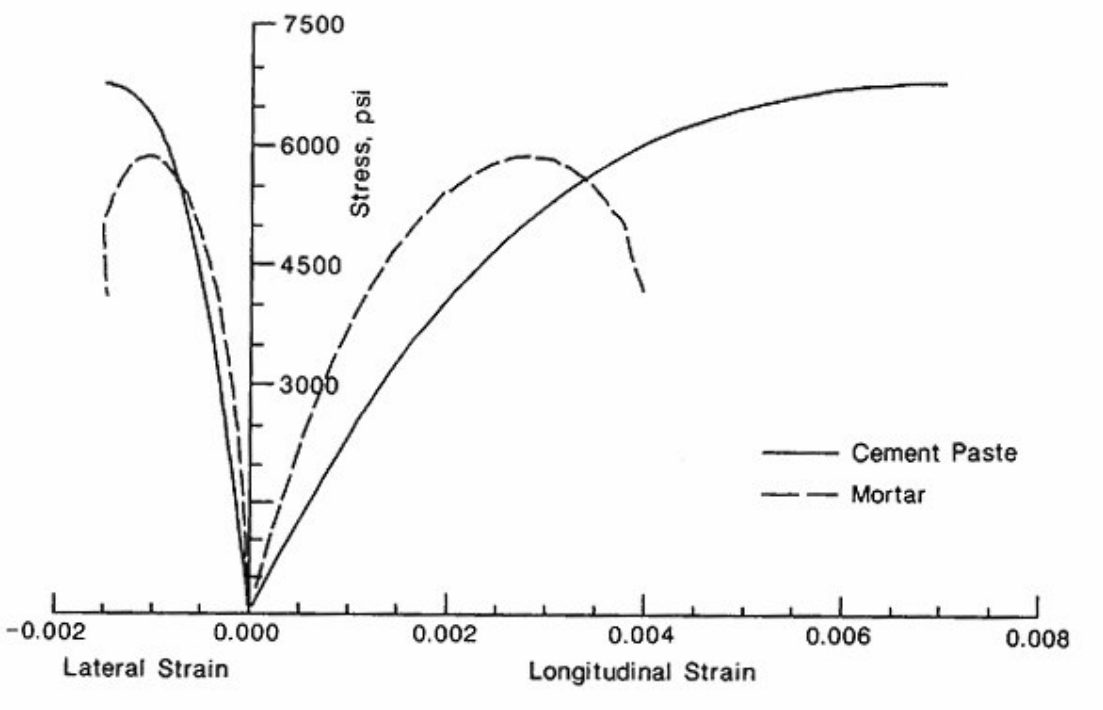

Figure 2.2. Stress strain behavior of monolithically loaded specimen[20]

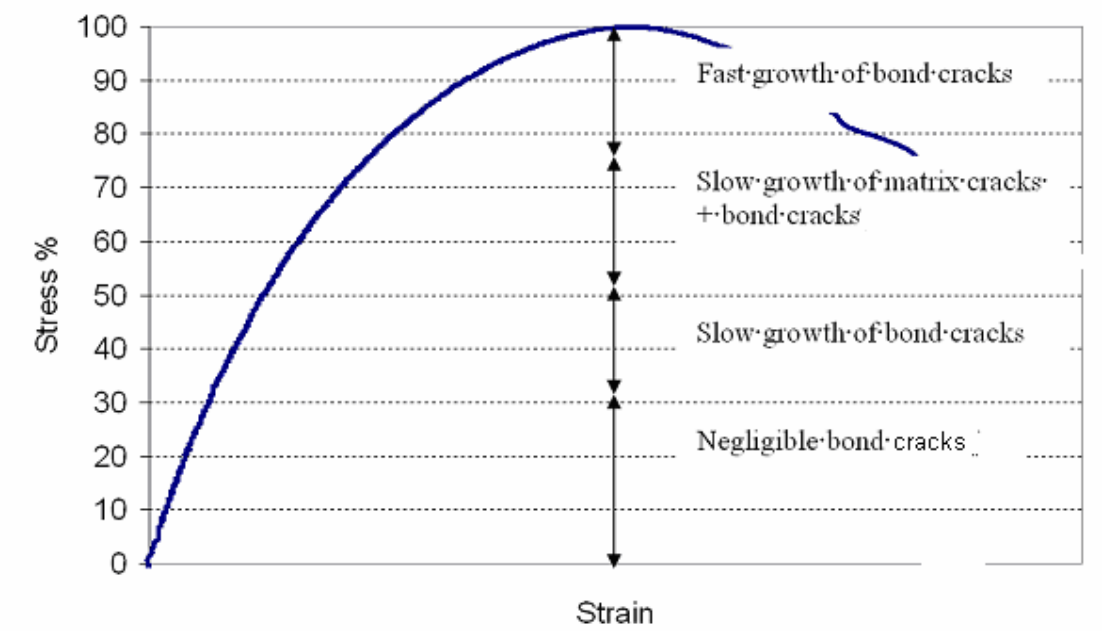

Figure 2.3. Stress strain diagram and its relation with damage cracking [15]

In compression failure of concrete, the formation of this damage is generally limited to a zone called “Damage Zone”. The deformations and cracks increase within this region.

Once the strain is localized strain is no longer constant through out the specimen and depends on the length of the specimen where the deformation is recorded [15]. Under compression actually the splitting forces occur and results in cracking of the sample as given in Figure 2.4. However, in the restrained volume due to boundary conditions of the tested specimens these deformations are not observed as given in Figure 2.4. The readings for damage are to can be taken between the restrained volumes, as shown in Figure 2.5 [19].

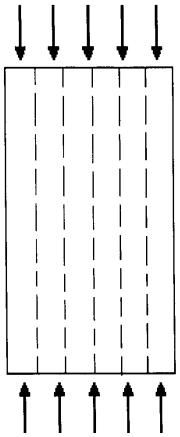

Figure 2.4. Crack alignments under compression stress [19]

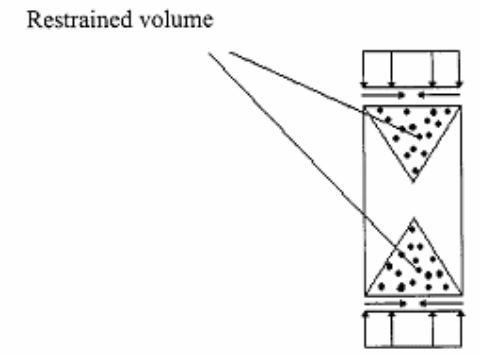

Figure 2.5. Restrained volume at ends for height/diameter ratio 2 [19]

2.2. Cyclic Loading of Concrete

During cyclic loading the crack formation causes localized plastic deformation which results in permanent damage to the component. As concrete experiences increasing number

of cycles, cracks (and damage) increase. After certain number of cycles, these cracks will cause the component to fail [2].

Fatigue is a damage process produced by cyclic loading which results in the cumulative process of failure consisting of crack initiation, propagation and the final fracture of the component. Loading on a material in a structural member can be either tension ,compression , bending or torsion. So, the fatigue damage can be in either of these loading conditions. The fatigue behavior can be investigated on the materials by several methods, such as only compression, only tension etc. The bending tests generally simulate the behavior of the concrete without reinforcement, which is the case especially for the concrete pavements. In concrete pavements concrete is solely subjected to cyclic loading in bending. besides compression concrete is also subjected to tension. On the other hand, tension property can be investigated by indirect tension methods like splitting tests. For example, in a regular concrete bridge, beam is reinforced and concrete is subjected to compression and reinforcement to tension. As the first load is applied and during the first cycles of compression the defects oriented in the direction of compression [21]. Bending and compression fatigue tests have strong relations [22]. It is also found out that the compressive and bending fatigue properties are very similar.

2.2.1. Cyclic Compression Loading of Concrete

It was found out by several researchers that resistance against cyclic loading is affected by concrete composition, environmental conditions, loading conditions and mechanical properties of concrete. However, concrete is known to have no fatigue limit which means that there is no maximum ratio of the applied stress below which concrete can withstand an infinite number of loading cycles without failure. The investigations prove that there is no endurance limit as in steel. The concrete subjected to cyclic loading eventually breaks down whatever the stress level is. However, for concrete 10.000.000 cycles is practically accepted as the endurance limit [23].

Cyclic loading is a process causing permanent internal damage which increases with cycles. Through cyclic loading, internal micro cracks increase resulting in significant increase of irrecoverable strain. It is found out that as the internal structure of concrete

becomes more porous, that is to say with higher water cement ratios, it took longer time to develop cracks [21]. This can be related to the higher ductility of concretes with higher water/cement ratios. However, high strength concrete fails in a more brittle way. Behavior of cement-based materials is controlled by the deformation capacity of the structure. When this capacity is fulfilled during cyclic loading, the specimen will fail because of fatigue [21].

In previous section behavior of concrete under compression loading has been explained. Under compression cracks start to form in concrete and in cyclic compressive loading formation of cracks start according to the level of applied load. Eventually concrete fails in a brittle way after application of the load repeatedly [24]. Failure mechanisms for concrete during cyclic loading and under compressive loading are similar. Stress applied affects the defects in the same way as in crack formation in compression loading. So in each cycle of loading, diminution and extension of the defects are to be examined. Defect generation is like the formation of micro cracks. Some defects get smaller like closing of micro cracks during compression loading (generally in cracks that are inherently between the aggregate and cement interface). There is also defect extension like propagation or enlargement of micro cracks during compression unloading [25, 26, 27]

Therefore concrete material subjected to cyclic loading experiences progressive deterioration of its mechanical properties. However, some researchers found out that there is an increase in compressive strength of concrete subjected to low intensity compressive cycles [28]. Specimens subjected to low strength ratio cyclic compression loading have strengths which are upto 20 per cent higher than those that are not subjected to cyclic loading [28]. The reason for this increase in strength can be due to the defects diminution at low stress levels. One example of the defect diminution is that cracks which are inherently in concrete get closed and compressive strength may be enhanced. According to Mehmel and Kern [3] this increase is approximately 10 per cent. This phenomenon can also be described as decrease in tensile stress singularities, developed in the material and redistribution of stresses arising from the creep induced by cyclic loads [28]. Hisdorf [28] observed an increase in static strength of cyclically loaded concrete compared to the specimen that were not loaded, and also in fatigue strength up to cycles applied at 20-30per cent of fatigue life.

The damage evolution and the failure of concrete in cyclic compression are very complex. The damage localizes at or close to the peak load. A mechanistic understanding of damage growth and failure of concrete subjected to fatigue loading in compression is still lacking [29].

Concrete composition effect on the behavior of concrete under uniaxial low cyclic loading was investigated by Moral [30]. In his research several types of cyclic loading effects was investigated under several cyclic loading conditions. The composition effects investigated were (i) the structure of hardened cement paste (ii) the particle size distribution of the aggregate (iii) the cement content.

In Moral's findings it was found out that post peak response under compressive loading is effected by the composition of the concrete. As the aggregate sizes decreased the specimens were less effected by the cyclic loading. As the water cement ratio decreased, at the same level of cyclic loading the compressive strength after cyclic loading decreased more. With the increase in compactity of cement paste the stress at which the significant damage and the rate of damage increases.[30]

It was also observed in Moral's research that with increasing cyclic loading ratio the compressive strength and fracture energy has decreased. The decrease for $0.9f_{max}$ loading for 0.7 water/cement ratio concrete was 10 per cent. With decreasing w/c ratio the decrease was smaller. [30]

2.2.2. Fatigue Strength

First cyclic loading tests and S-N curves were done in 19th century; S showing the stress magnitude normalized with maximum stress and N showing the number of cycles. An example of S-N curves is illustrated in Figure 2.6. The fatigue strength of concrete is defined as a fraction of the static strength that can support repeatedly for a given number of cycles [23]. It is accepted that there is a relationship between the load ratio and the number of cycles applied.

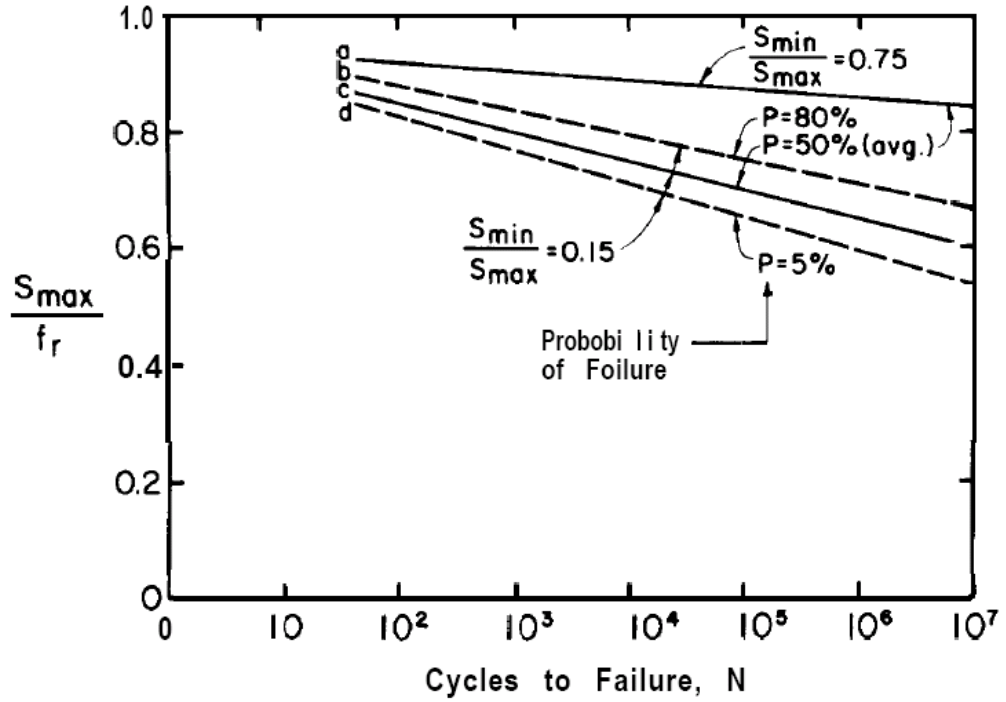

Figure 2.6. Fatigue strength of plain concrete beams[23]

Since 10.000.000 cycles is assumed generally as the endurance limit for concrete, design for fatigue may be done by the use of a modified Goodman diagram, as illustrated in Figure 2.7. The stress ratio for the design for fatigue loading can be found by this diagram. Also, tension, compression, and flexure loading modes are utilized in this diagram. For example, for no minimum stress level for a fatigue of 10.000.000 cycles, 50 per cent of peak stress level can be applied according to Figure 2.7. As the minimum stress level increases the stress that can be applied in cyclic loading also increases [23].

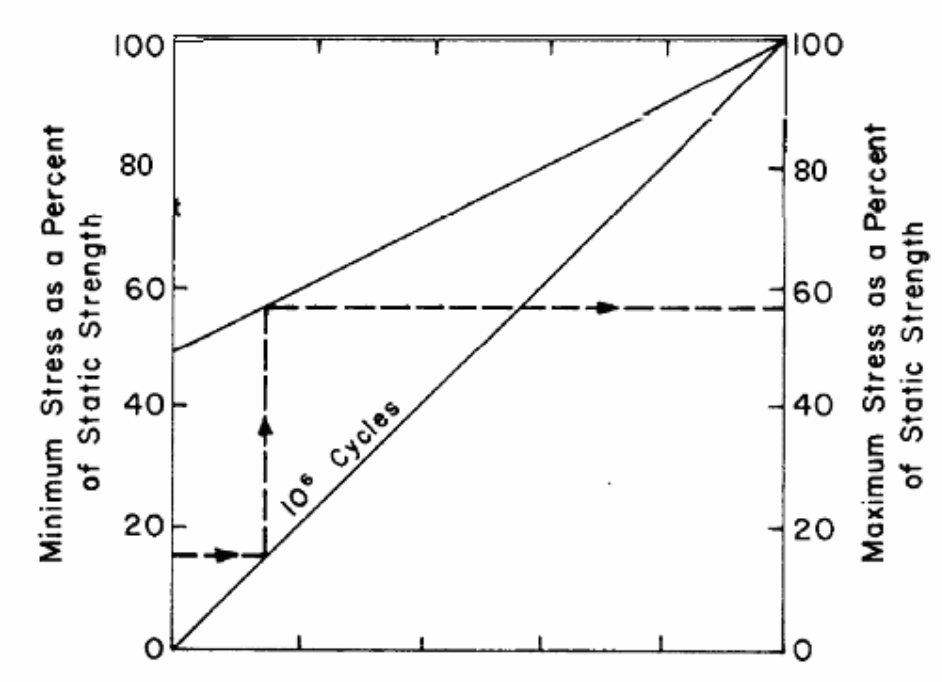

Figure 2.7. Fatigue strength of plain concrete [23]

In the literature [18], low cycle fatigue loading is attributed to 1-1000 cycles of loading, whereas 1000-10.000.000 cycles of loading is called as high cycle fatigue loading. Structures especially subjected to earthquake loading, or structures which are loaded above their service load only for a few cycles, as in airport pavements, bridges which are loaded above their service loads etc. are said to be subjected to low cycle fatigue as shown in Figure 2.8.

Low Cycle Fatigue			High Cycle Fatigue				Super High Cycle Fatigue		
Structures Subjected to Earthquakes			Airport Pavements and Bridges		Highway and Railway Bridges, Highway Pavements, Concrete Railroad Ties		Transit Structures	Sea Structures	
0	10^1	10^2	10^3	10^4	10^5	10^6	10^7	10^8	10^9

Figure 2.8. Fatigue life description according to Hsu [18]

Fatigue is also related with the rate of loading. As the loading rate increases cycles to failure increases, because there becomes relaxation in rapid loading and damage under sustained loading does not occur. The variation of the number of cycles with the rate of

loading is given in Figure 2.9. The response of concrete to repeated compressive loading is independent of the frequency of loading cycle above 1 Hz. Test results show that the loading frequency applied does not affect the fatigue behavior where the loading frequency applied on the specimen ranged from 1-20 Hz. In slow cycling below this range creep affects the test results [31].

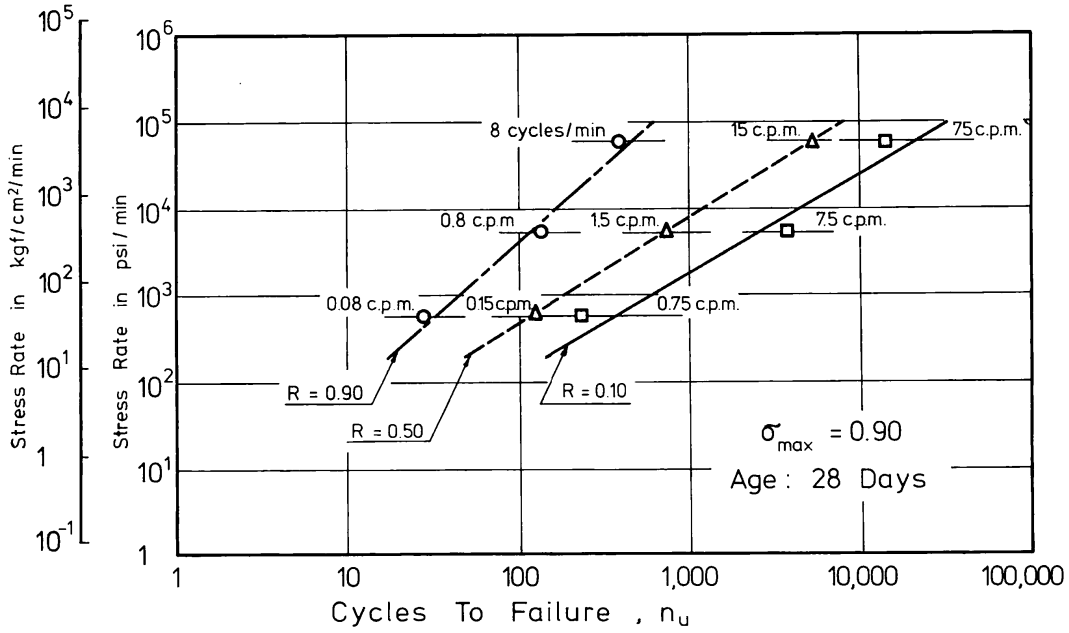

Figure 2.9. Effect of loading rate on fatigue strength [31]

As the minimum stress applied in fatigue, cyclic loading decreases as the number of cycles to failure decreases as well. As the minimum stress level is lowered the strains per each cycle is getting higher. The application of cyclic loading can be between two stress levels. In Figure 2.10 two examples of cyclic load application are given. In (a) section of Figure 2.10 maximum stress is $0.9f_{max}$ and minimum stress level is zero. In (b) section of Figure 2.10 maximum stress level is also $0.9f_{max}$ but the minimum stress level is not zero, but 0.4 f_{max} level of concrete. In the first case there is a larger damage of concrete in each cycle. As the minimum stress in the cyclic loading decreases the fatigue strength of the concrete decreases [13] as also shown in Figure 2.10.

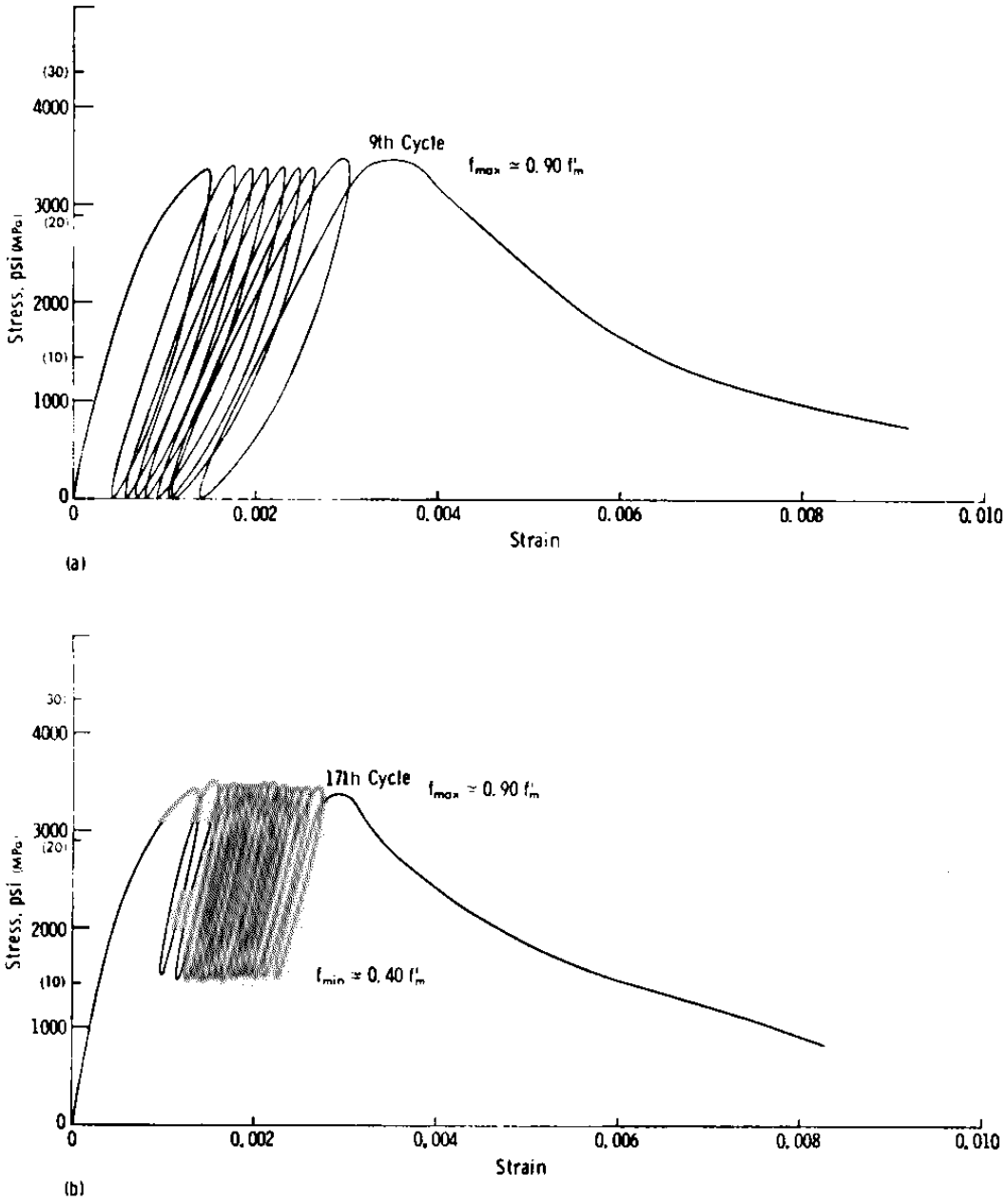

Figure 2.10. Effect of minimum stress during cyclic loading [13]

The environmental conditions are also effective in cyclic loading. Frost damaged concretes have larger degradation under cyclic loading [32]. Thus we can say that any environmental condition that will affect concrete properties will also affect the cyclic loading characteristics of concrete. These environmental conditions should also be taken into account in design procedures.

2.3. Mechanical Properties of Cyclically Loaded Concrete

Cement composites fail under the repetitions of load below ultimate stress. During such as cycling loading process the properties of concrete also change due to the cyclic loading damage.

Cyclic loading increases elastic deformations and stress-strain curve becomes linear with increased linear region. As the number of cycles increase the strain at ultimate stress increases gradually as given in Figure 2.11. With the increase in number of cycles, the cracks also increase gradually in size and number and elasticity modulus decreases. As the cycles come nearer to the fatigue life limit the cracks and strains start increasing very rapidly and the structure breaks down. But total strain does not pass the level of strain at failure during static loading.

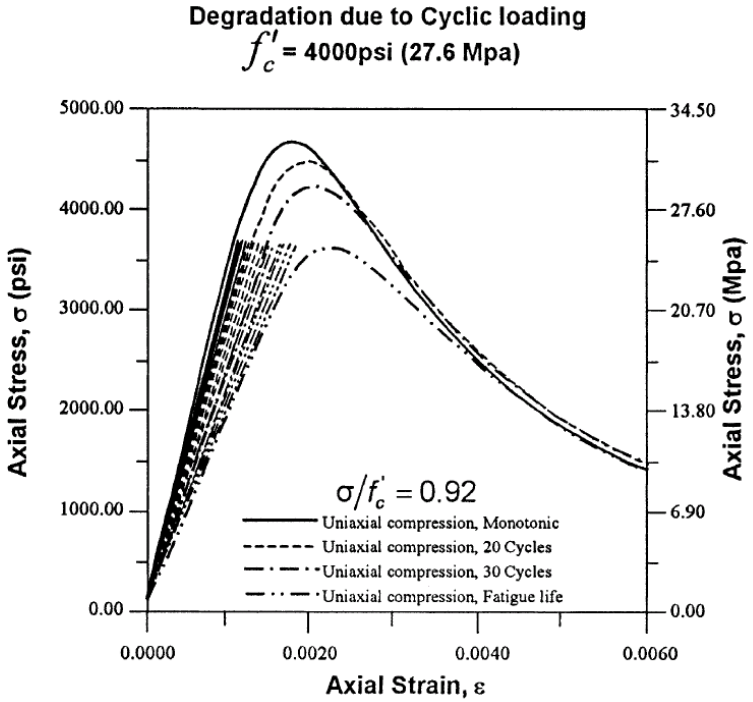

Figure 2.11. Post cyclic stress-strain response [33]

Progressive damage under fatigue loading is also indicated by reduction of the slope of the compressive stress-strain curve with an increasing number of cycles. In addition to

internal micro cracking, cyclic loading is also likely to cause changes in the pore structure of the hardened cement paste. Modulus of elasticity of the concrete specimen decreases gradually with cyclic loading [13].

The concrete strength is another parameter in cyclic loading damage. The strain decreases with the increasing concrete strength so a more brittle failure occurs. With increasing concrete strength, the fatigue life cycle decreases and the cracks increase more rapidly. Total strain at failure is found to be approximately the same as the strain of descending part in monotonic stress strain curve. It is reasonable that the fatigue strain at failure decreases with increasing concrete strength. Also, the rate of strain increment increases with the strength of concrete. Therefore the fatigue life should decrease with increasing concrete strength. As a result it can be said that high strength concrete is more brittle than low strength concrete also in cyclic loading [24].

The deformations of the specimens during fatigue in compression display three stages as given in Figure 2.12. At the first $1/10^{th}$ cycles of failure the damage is significant since most of the strain occurs both in axial and radial directions. During the second phase, which covers most of the fatigue life, the rate of longitudinal deformation remains constant while there is almost no radial deformation. A very good correlation exists between the rate of longitudinal deformation and the fatigue life, allowing a precise prediction of this characteristic [21]. At the third stage the fatigue damage and strain increase very much. Also, the elasticity modulus decreases very rapidly at the very first cycles after which it decreases at a constant rate which is followed by a rapid decrease again with the increase of cycles coming near to the fatigue life. Ultrasonic pulse velocities follow the same situation as the deformations [21,34]. Also the energy absorbed is very large at the first few cycles where the damage is larger. The area between loading and unloading in stress strain diagram shows the energy absorbed. The energy absorbed gets smaller at the second phase. Then the absorbed energy gets very large again when it comes to the end of cyclic life. As the cycles come near to the fatigue life limit the number and size of cracks and measured strains increase very rapidly and the structure breaks down. But the total strain does not exceed the level of failure strain for the static loading [35].

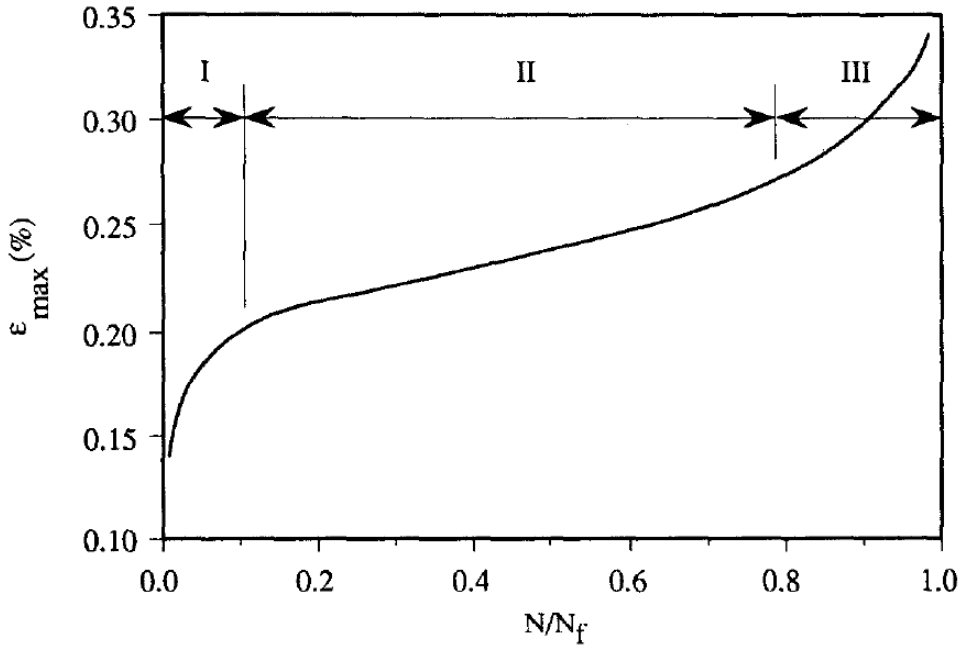

Figure 2.12. Typical strain development curve [34]

While cyclic loading results in cracks growing in size and number pulse velocity of the concrete decreases as compared with the velocities obtained in undamaged concrete [36,37]. Ultrasonic pulse velocity is consistent to number and size of the cracks and tests show that ultrasonic pulse velocity decreases with cyclic loading [21]. This decrease in ultrasonic pulse velocity can be used to monitor the crack formation during cyclic loading. A damage coefficient can be obtained from measuring the ultrasonic pulse velocity with cyclic loading .So, damage accumulation can also be estimated by ultrasonic pulse velocity. Length of cracks generated by cyclic loading also increases with the intensity of loading [21]. Cyclic or sustained stresses cause progressive internal microcrack propagation as observed by ultrasonic, volumetric and microscobic measurements [17,29].

There is a loss in transverse tensile strength after damage due to the compressive loading of concrete. Splitting test can be used as a simple and reliable method for quantifying the damage. The tensile strength of concrete can be reduced by 25 per cent due to compressive loads applied along the perpendicular direction, even in high-strength concretes [38]. However, damage in high-strength concrete due to uniaxial compressive stress is negligible as long as the monotonically applied stress is less than 60 per cent of its strength. Under the cyclic loading applied in this study [38], damage is negligible when

the maximum stress is lower than 60 per cent. Also as the strength of concrete increases damage evolution in high-strength concrete seems to occur at a significantly lower rate than in normal concretes [38].

2.4. Permeability Properties of Cyclically Loaded Concrete

Concrete under repeated loading sustains gradual fatigue damage as explained previously. This damage not only affects the mechanical properties of concrete but also the permeability properties.

Permeability of concrete is related with the durability of concrete. With the increase of permeability properties of the concrete the deteriorating mechanisms of concrete progress at an accelerated rate. However, the permeability properties of concrete are mostly measured not on specimens that are in service but on specimens that are not loaded. Thus, the use of strength and durability tests on undamaged specimens may be misleading. In particular, service-life prediction models of new and existing concrete structures must account for the changes in the microstructure due to imposed loading and environmental conditions. Some studies show a slight increase in the water permeability of specimens after unloading. External load causes microcracks which increase overall porosity of the system [39]. At macro level mechanical properties are affected negatively and at micro level internal micro structure degenerates and micro defects form. Micro level investigation will help to identify the macro properties of concrete's fatigue behavior [40]. Pore structure is one of the important properties, which will also change strength, elasticity, shrinkage, and durability. Porosity, pore size distribution and specific surface area can be used as micro damage parameters to evaluate macro damage of concrete.

Permeability is caused by the porous medium. The total pore volume, size of the pores and their continuity are important parameters. In an undamaged concrete, volume and continuity of the pores are affected by water cement ratio, aggregate distribution and etc. Micro cracks in concrete are considered to be the primary cause of permeability. Structural loads, temperature and moisture gradient, drying shrinkage, freeze-thaw cycles, and chemical expansions can be some causes of this damage. Uniaxial compressive loading is increased up to a particular stress level expressed as a percentage of the ultimate

load before the measurement of permeability is carried out on the preloaded concrete. The increase in permeability of concrete is attributed to microcracks developed in the concrete due to the compressive loads. The occurrence and subsequent propagation of micro cracks in concrete are usually related to the level of applied compressive stress [41]. As discussed in previous sections that concrete has cracks inherently. These effects cause cracks to form which increases the permeability of concrete. Cracks in the damaged concrete interconnect and increase permeability. As there is more deterioration there is a higher increase in cracks and in permeability [42]. On the other hand, cracks that are opened during loading may close during unloading. For wide opened cracks it is desirable to use opened cracks. Water permeability of the specimen increases with the increase in the size of cracks [42]. Micro cracking of concrete affects its mechanical behavior and barrier characteristics because such damage modifies the pore structure and, in particular, increases its continuity [43,44].

The durability of concrete depends upon its ability to prevent the ingress of aggressive deteriorative materials. Permeability can also be defined either by liquid intrusion or gas intrusion as in the case of gas permeability [45].

At low level compressive stress, micro cracking increases only within the interface between the aggregate and cement paste. Until the external load is 75 per cent of the compressive strength, the micro cracks do not interconnect and form a continuous network that will transport liquids and gases. This damage is not only within the bond areas but more extended in the volume [46]. The severity of mortar crack cause permeability to increase. Also higher rate of increase is viewed as the external load increases. Non cyclic loading below 75 per cent did not increase ion transport and permeability [46].

There are investigations done on the porosity strength relationships for concrete [47]. But very few papers have been published about the development of porosity and changes in the pore system of concrete under cyclic loading. In some researches [40] measured porosity of cement paste after uni-axial compressive low cycles.

Mercury intrusion, helium flow, and nitrogen adsorption methods are used to measure porosity, pore size distribution and specific surface area of pores of ordinary

concrete at different bending fatigue stages as investigated by Zhang [40]. These properties can be used to measure damage level and fatigue life. At different stages of fatigue loading the permeability is measured and it is found out that it linearly increases with increasing number of cycles as shown in Figure 2.13 [40].

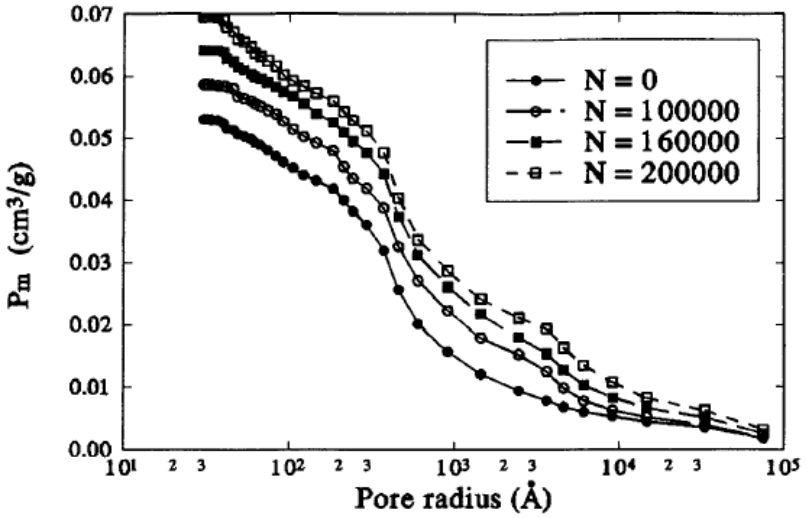

Figure 2.13. Cumulative pore volume of mortar at different fatigue stages [40]

There is also a test done on cyclic loaded concrete which evaluates the damage by water absorption. Application of external loads increases water absorption with especially loads below critical stress [46].

Permeability on micro cracked concrete has been investigated by several researchers. Researches on water permeability showed that the permeability of concrete increased significantly as the concrete was subjected to a cyclic compressive load above 40 per cent of ultimate strength [41]. Also a significant increase in air permeability of concrete was observed when compressive stress was in excess of 80 per cent of the maximum load. Also in a research with the rapid chloride permeability test, results were not generally affected after 1 cycle of uniaxial compressive loadings below 75 per cent of the maximum load. Flow rate of electrically transported chloride ions increased noticeably when the sustained stress level was increased to 65 per cent of ultimate strength Figure 2.14 [41].

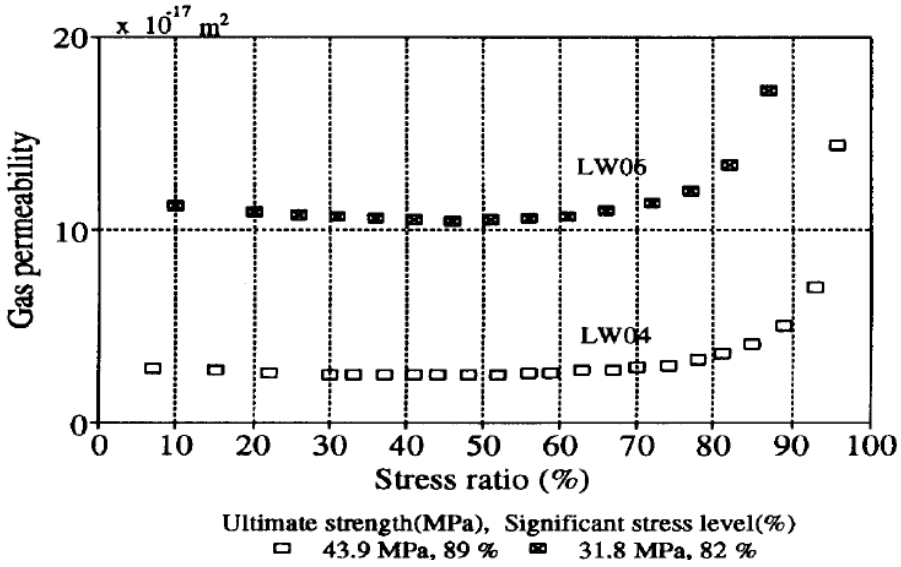

Figure 2.14. Gas Permeability of concrete with applied stress ratio [41]

Figure 2.15 shows that the stress level applied for cyclic compressive loading change the mass transfer properties of the concrete, causing increase in the permeability coefficient. Service life prediction can also be made from such a relationship [48].

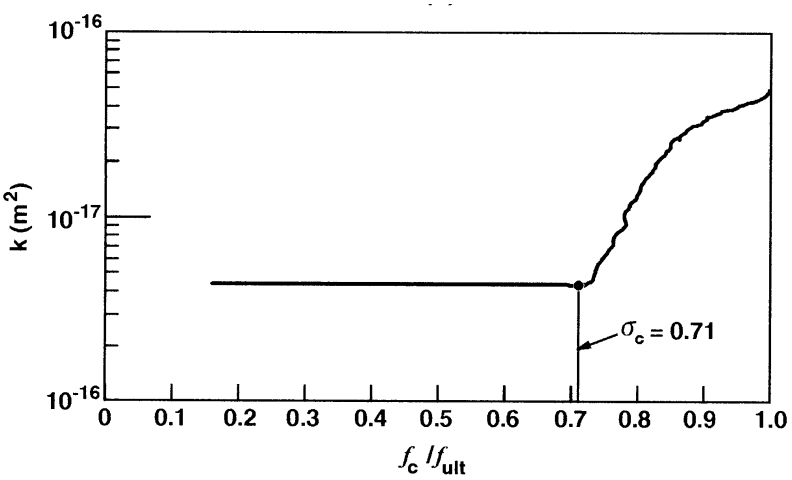

Figure 2.15. Typical permeability versus applied stress [48]

Cracking of the mortar matrix is the cause of the deteriorations of concrete. Deterioration process results in uniformly distributed cracks. Although permeability tests have been naturally done on the uncracked specimens, concrete initially has cracks due to load, shrinkage, alkali aggregate reactions, and freezing and thawing cycles. Some

researchers investigated flexural elements and flexural cracks. Overall micro cracking have been found to be very minimal [48].

The degree of permeability depends also on the crack opening. Cracks below 50 microns have little effect on permeability. If the cracks are open about 50 to 200 microns the concrete permeability increases rapidly [16]. With increasing load and opening of cracks the weight loss of specimens subjected to sulphate conditions increase are given in Figure 2.16.

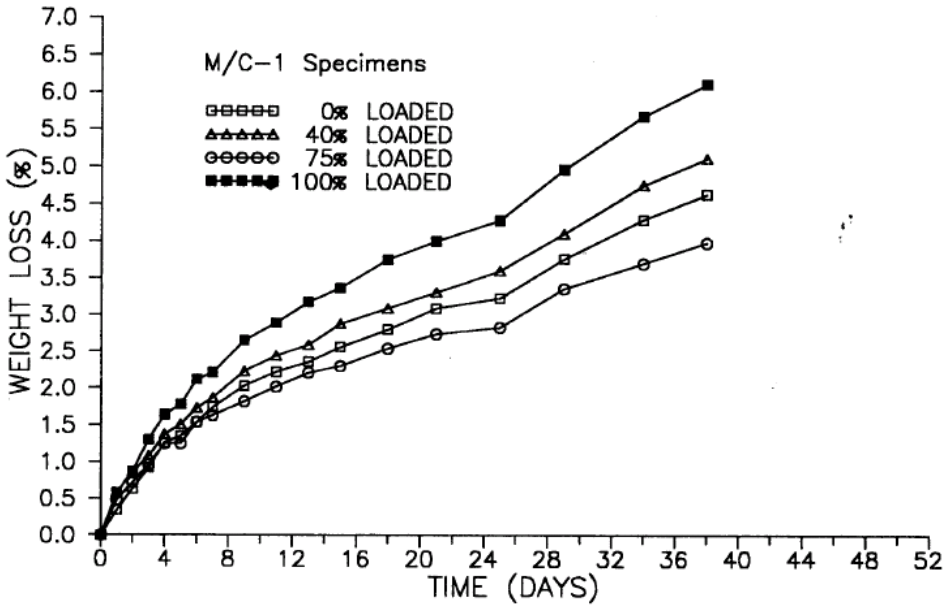

Figure 2.16. Weight loss of specimen with loading ratio[46]

But it was found out that the Rapid Chloride Permeability Test (RCPT) results did not differ with water cure [46] The chloride permeability of plain concrete subjected to loads up to 70 per cent of maximum load is generally unaffected by uniaxial compressive loading.

2.5. Effects of Self Healing on Mechanical and Permeability Properties of Concrete

Concrete has an autogenously healing property. Self healing property of concrete is important because after damage the self healing characteristics of concrete will be needed to evaluate the changes in service life of concrete.

It should be noticed, first of all, unloading of concrete has an effect of decreasing permeability. The effect of external load after unloading which is assumed to involve extensive damage in the specimen (near peak stress) is to cause macroscopic cracking and a sharp increase in permeability [5,42]. However, the crack size decreases with unloading [40]. As the crack size decreases the permeability of concrete also decreases.

Compared to the undamaged sample, a uniaxial compressive load at 90 per cent of the ultimate strength can increase the axial permeability by about one order of magnitude after unloading [40]. During loading, since the cracks are larger, the permeability is also higher. The increase in permeability is related with the unclosed cracks during unloading.

Strain is generally the first criterion for damage evaluation of concrete. As it can be observed from Figure 2.16, there is a correlation between damage and increase in permeability. Damage evaluation can be deduced from the stress– strain curves recorded during loading. A criterion resulting from a plastic-fracturing model is necessary for the consideration of the plasticity of material [46].

Also it is found out that concrete cracks, both dormant and active, subjected to water pressure are able to heal themselves with time. The greatest autogenous healing effect occurs within the first 3 to 5 days of water exposure, where the water leakage, depending on the crack width and water pressure, makes up to 20 per cent of the initial water leakage rate [46].

The mechanism for decreasing the crack size working with the precipitation of calcium carbonate crystals ($CaCO_3$) within the crack is almost the sole cause for the autogenous healing of the cracks as shown in Figure 2.17 [42]. So, curing conditions after static loading becomes effective on permeability. Drying effects on the other hand,

increases the permeability. In several researches it was found out that water cure decreases permeability and increases strength of concrete [26, 49, 50].

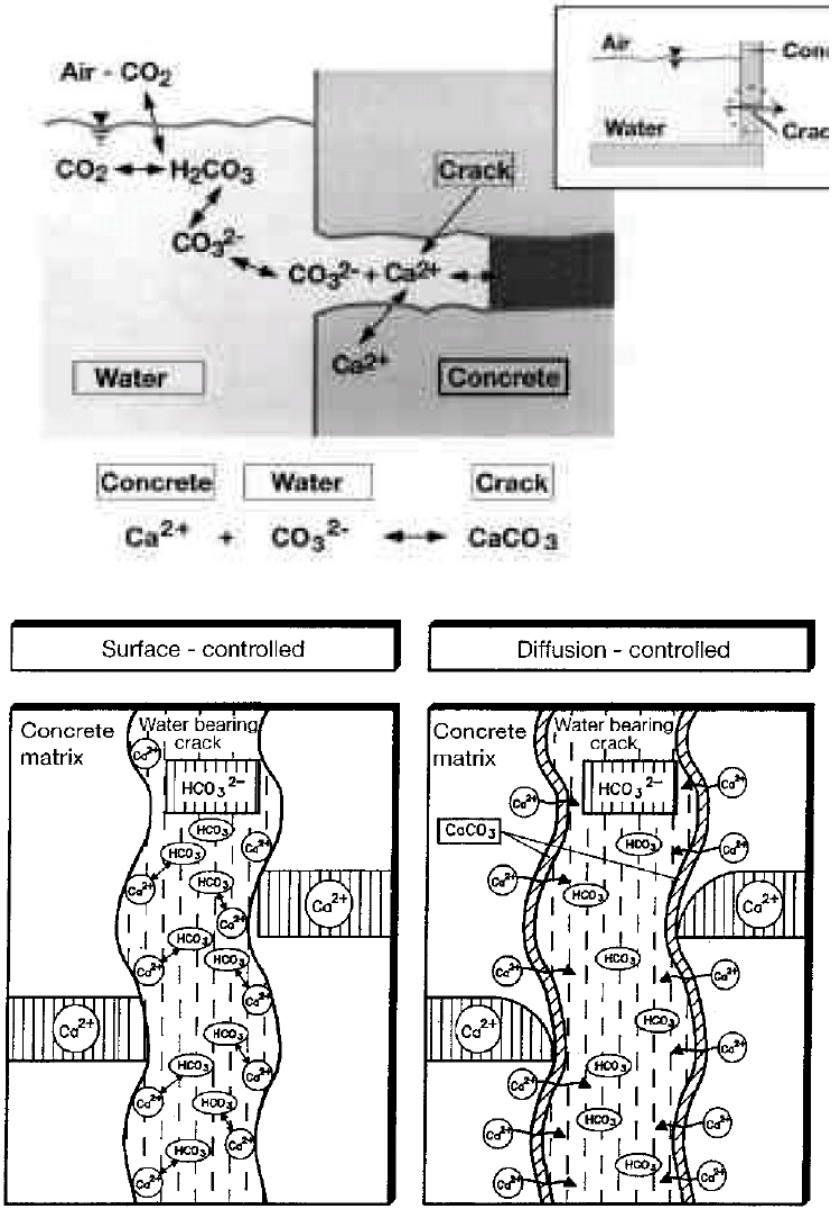

Figure 2.17. Crack filling mechanism of $CaCO_3$[42]

The autogenous healing occurs between opposing surfaces of narrow cracks. Healing can take place only in the presence of water because the healing consists of chemical reactions of compounds exposed at the cracked surfaces. These reactions produce new hydrates and other minerals. The opposing surfaces of a crack eventually bridges. The

cement, hydrated or unhydrated, is the essential element in autogenous healing. The chemical reactions of healing are not fully investigated. There are two possibilities; the formation of calcium hydroxide and of calcium carbonate. The former requires the presence of water only where as the second requires, in addition, the presence of carbon dioxide.

In a research done by Granger and et al [51] the self healing properties of concrete after damage is investigated. In this investigation the results of an experimental investigation on the mechanical behavior of self healed concrete specimens have been presented in Figure 2.18. Under three point bending test the specimen is damaged then prismatic specimens are aged, in air or in water, during various durations ranging from 1 to 20 weeks. In exclusively water cure, damaged beams tend to recover their initial global stiffness, and to improve slowly their flexural strength. This behavior was attributed to the self healing of mainly by hydration of anhydrous clinker on the crack surfaces. The improvement of strength was attributed the progressive development of the mechanical properties of the newly formed crystals primarily C–S–H [51].

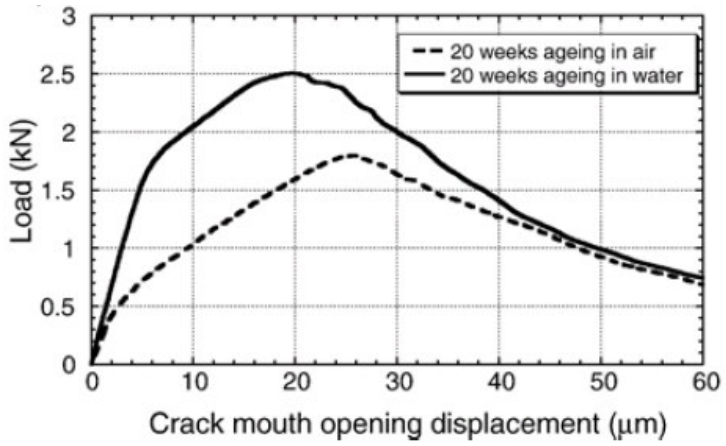

Figure 2.18. Crack mouth opening with load and in different cure conditions [51]

In an other research done by Wenhui Zhong and Wu Yao [52] acoustic emission analysis was performed in order to confirm that the specific response observed for healed specimen. It also shows the two phases of the cracking process of healed concrete, comprising damage inside the existing crack and continuation of the crack propagation.

The change in ultrasound velocities are given and showed a linear relation with this research findings Figure 2.19 [52].

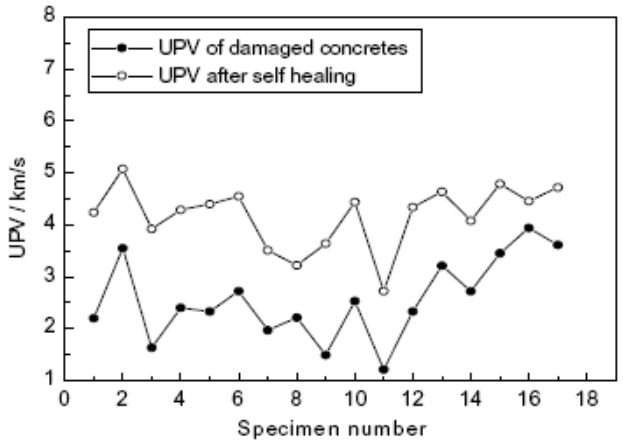

Figure 2.19. The change in ultrasonic pulse velocity velocities after damage and water cure [52]

Crack closing mechanism by self healing was investigated in research done by Hans-Wolf Reinhardt and Martin Jooss [53] the cracks are found to close by curing especially in water cure. An example of the research findings can be investigated in Figure 2.20. [53]

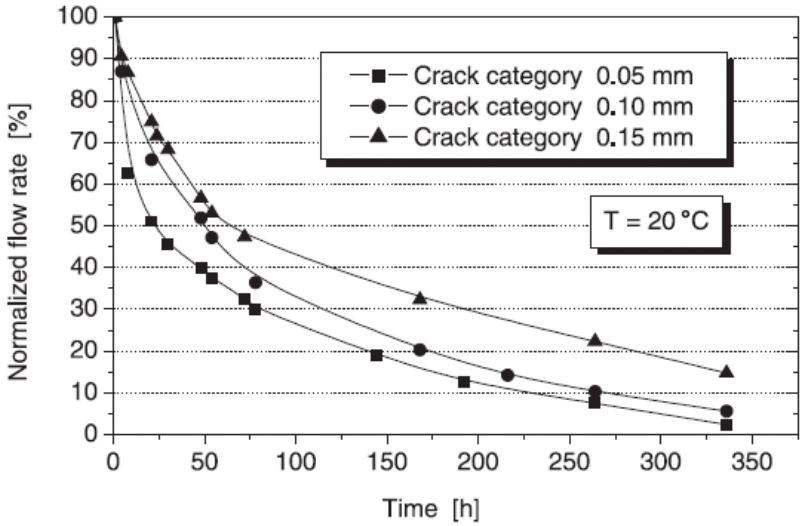

Figure 2.20. The flow rate change of concrete specimen with time for different crack openings [53]

As given in the Figure 2.20, with time the flow across the crack openings decreases. This is parallel to the results found in the experiments. It shows a faster healing of cracks that have a smaller crack width, whereas the curves have generally shifted to a lower level. So, Figure 2.20shows the normalized flow rate as function of crack width and temperature. The curves are the mean of all relevant specimens. The flow rate is normalized with respect to the initial flow rate at the beginning of the test. Cracks with an average crack width measured at the surface of 0.05 mm shows the fastest self-healing. Smaller cracks do heal faster than greater ones.

There are three ways in autogenously healing according to Neville[27]. (i) Formation of hydration products (ii)The formation of calcium hydroxide or the formation of calcium carbonate. The former requires the presence of water only; the second requires, in addition, the presence of carbon dioxide.(iii)A third mechanism that can contribute to healing, but cannot provide it by itself, is silting up of cracks or deposition of debris.

The healing consists of chemical reactions of compounds exposed at the cracked surfaces. These reactions produce new hydrates and other minerals. The opposing surfaces of a crack eventually bridges. The cement, hydrated or unhydrated, that is the essential element in autogenous healing. The chemical reactions of healing are not fully investigated.

2.6. Post Peak Properties of Cyclically Loaded Concrete

This part describes the experimental investigation of the development of the localized damage under cyclic loading of concrete tested in post peak compression zone. In the design of concrete structures maximum strength and initial modulus of elasticity are used. However, post-peak measurements of stiffness and strength degradation in uniaxial also compression are very important in elastic damage and plastic softening modeling of concrete. Stress-strain diagram is most frequently used for this purpose. The relationship between cyclic loading damage and the peak stress, the modulus of elasticity and the fracture energy should be evaluated. Focal points (pole) extracted from the test data of

concrete specimens cyclically loaded at different levels of f_{max} mean that different cyclic loaded specimens have different post peak behaviors.

In post peak analysis it was observed that there was a linear correlation between the mechanical fracture energy and the cyclic loading of the concrete. These results gave clues about how the damage developed to form a zone that influenced the stiffness degradation and the post peak response of the concrete subjected cyclic loading. After post peak response there is strength degradation with stiffness decrease. The lack of sufficient quantitative experimental data has started the development of elastic damage and plastic softening formulations for concrete.

When concrete is loaded in uniaxial compression there are two regions in the stress-strain diagrams; prepeak and postpeak. In prepeak region most often used material property is the modulus of elasticity. After a certain level (between 40-60 per cent) of ultimate stress the curve becomes nonlinear. And after peak stress level damage occurs with increasing strain and decreasing stress level which is called postpeak region. The modulus of elasticity after peak stress decreases and the lines drawn from peak points parallel to loading modulus of elasticity combine at a point so called focal point as shown in Figures 2.21 and 2.22.

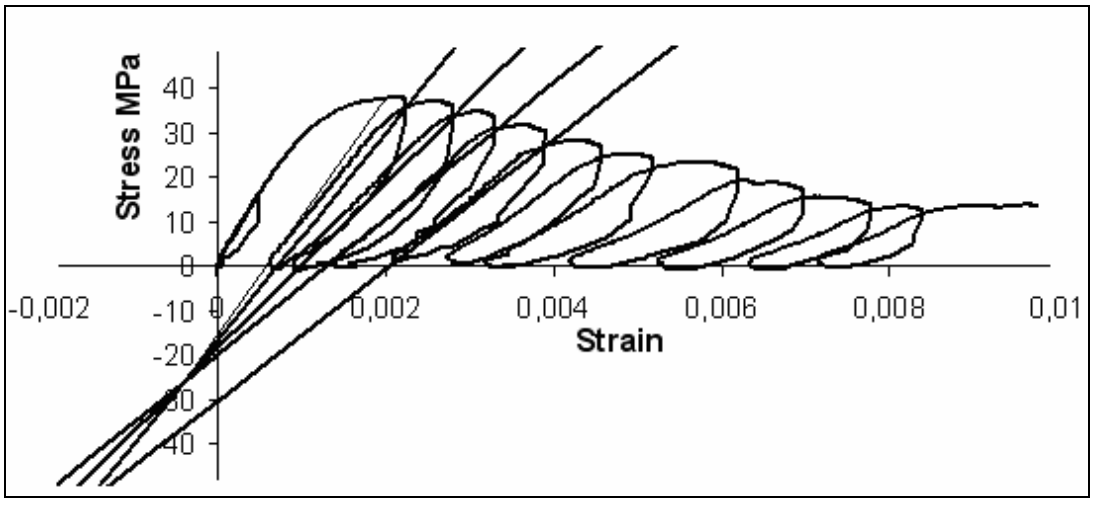

Figure 2.21. The change of modulus of elasticity after peak loading

When the material is unloaded, after peak stress, the modulus of elasticity is found to decrease. It is found out by many researchers this at a point which is called focal point[54,55]. This point is found out to be a material property which gets down in brittle materials and gets higher in ductile materials.

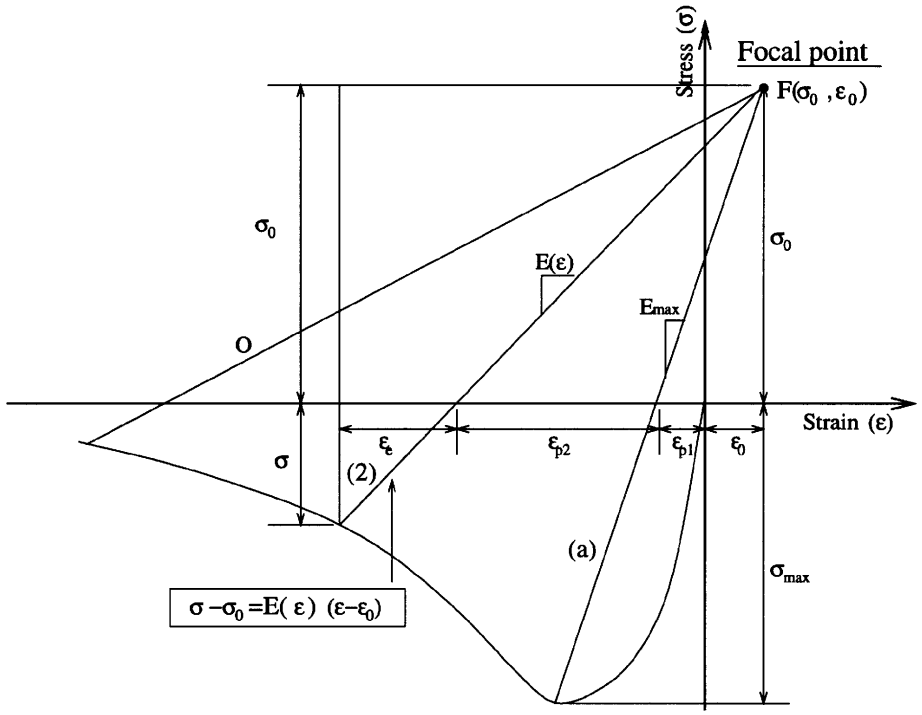

Figure 2.22. Illustration of focal point [55]

Figure 2.21 illustrates that for each specimen, the stiffness of the concrete decreases with increasing strain level. The slopes of the unloading curves can be approved to merge at a common point, which is termed as focal point (ε_0, σ_0) [54,55]. Figure 2.22 shows the focal point as a common point of intersection for all unloading slopes. The focal point provides a powerful resource which can be used for calculating stiffness of concrete at any point along the stress-strain curve. The term elastic strain describes the strain that is recoverable on unloading the specimen while the term inelastic strain is used to describe the permanent strain that develops in the specimen. Similarly, energy in the system can be divided into two components: elastic strain energy and fracture energy as also given in Figure 2.23. There are also some models developed to find fracture energy of concrete [56].

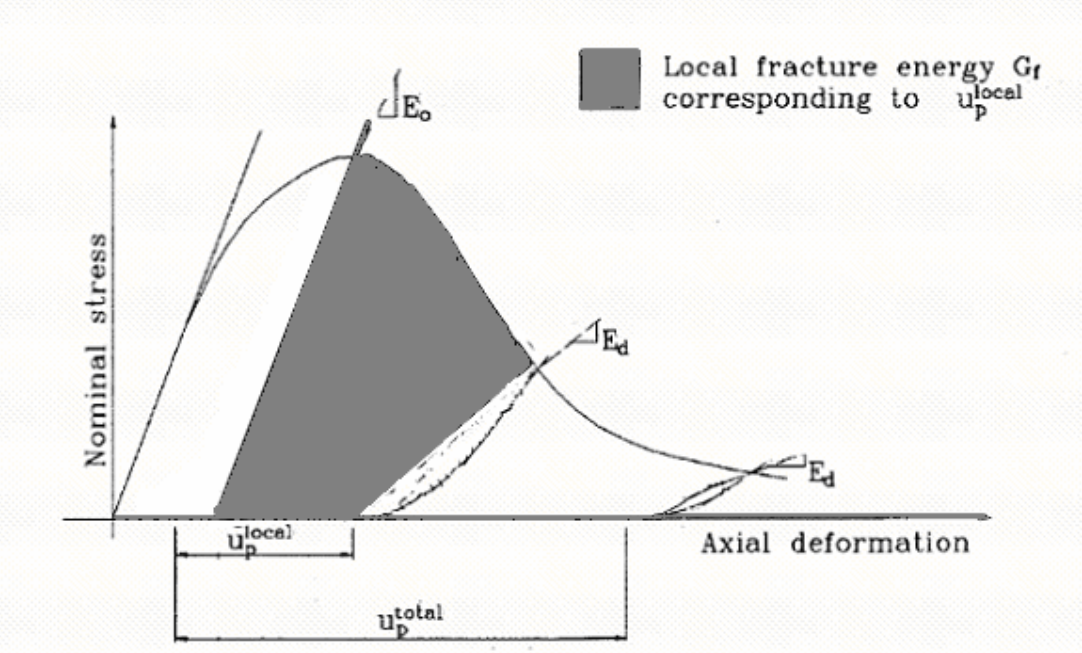

Figure 2.23. Fracture energy description [55]

The crack formation in concrete's mesostructure causes the non linear behavior of the concrete. Progressive crack formation causes reduction in the modulus of elasticity. There are three energy mechanisms: a) energy loss due to plastic deformation b) energy loss due to elastic damage c) energy conservation due to elastic deformation. debonding between aggregate and cement paste is responsible for stiffness degradation.

Post peak fracture energy and modulus of elasticity relations has been investigated by several researchers Tasdemir [54] and Lee[55] Figure 2.24 and Figure 2.25. It was found out by Tasdemir [54] that the normalized fracture energy and modulus of elasticity relation was independent of mixture in bending and by Lee[55] that it was also independent of the specimen dimensions in compression.

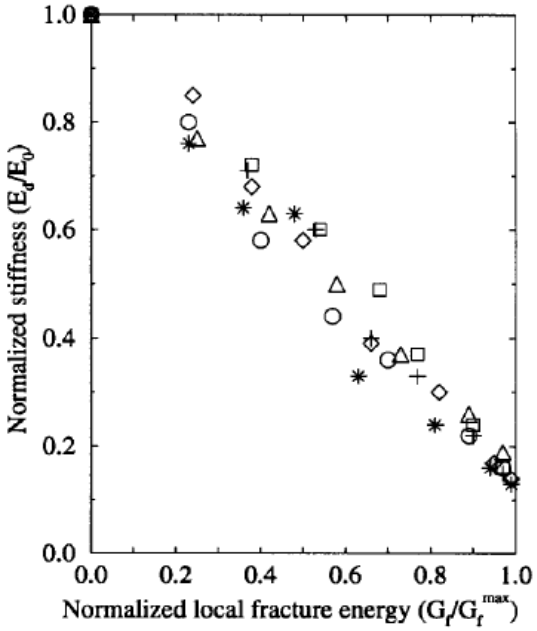

Figure 2.24 Fracture energy and modulus of elasticity relation in compression [55]

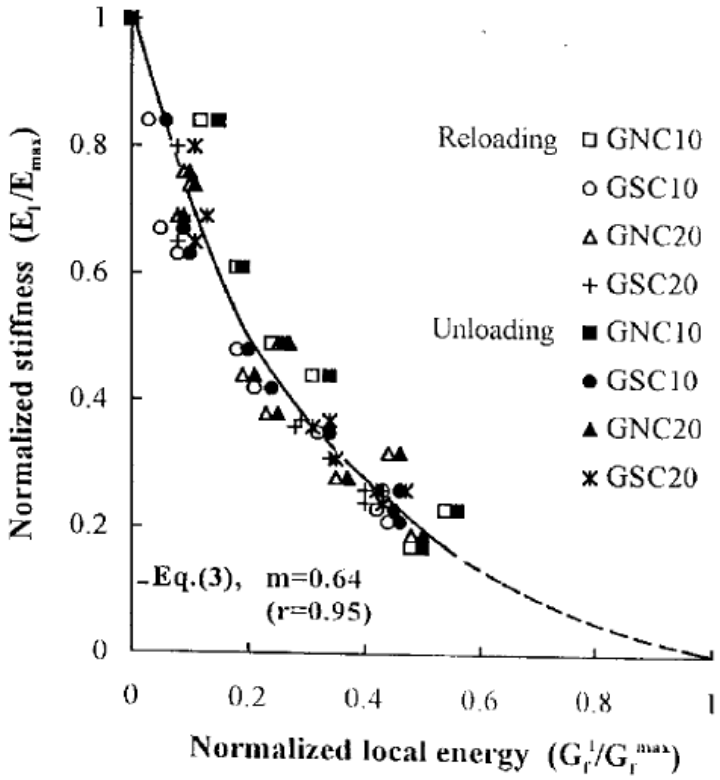

Figure 2.25 Fracture energy and modulus of elasticity relation under bending [54]

3 . EXPERIMENTAL STUDY

In this study effects of low cycle compressive fatigue loading on the mechanical and permeability properties of concrete were investigated. Concrete was produced with a water-cement ratio of 0.60, cement content of 330 kg/m^3 and an average 28 day compressive strength of 35 MPa. CEM I type Portland Cement with specific gravity of 3.19 gr/cm^3 and strength of 52.2 MPa was used. Crushed limestone coarse aggregate as well as crushed sand and natural sand fine aggregates with specific gravities of 2.71, 2.68 and 2.62 gr/cm^3, respectively, were used to give a mixture with a maximum particle size of 31.5 mm. Cylindrical specimens of 100x200 mm were cast. After demolding the specimens were water cured till one day before testing at 28 days. Then some of the specimens were subjected to low cycle compressive loading upto 0.6, 0.8 and 0.9f_{max} and afterwards tested for some mechanical and permeability properties to investigate the effects of cyclic loading. Further some of cyclically loaded concrete specimens were water or air cured for another 28 days to observe the self healing capacity of the micro-cracks in concrete through testing those specimens for the same mechanical and permeability properties.

Mechanical tests like compressive strength, splitting tensile strength, modulus of elasticity ultrasonic pulse velocity measurements, and focal point determination as well as durability tests like rapid chloride permeability, water absorption and sorptivity measurements, mercury intrusion porosity testing, sulfate resistance and microstructural analysis were done to evaluate the damage after cyclic loading of the concrete specimen.

3.1. Materials

3.1.1. Cement

Portland cement CEM I 42.5 conforming to the TS EN 197-1 was used in this thesis. Its physical and chemical properties are given in Table 3.1. The strength properties of this cement are given in Table 3.2.

Table 3.1. Properties of the portland cement used

Factory	Akçansa Büyükçekmece	Max in TS EN 197-1
Date of Production	25.11.04	
Insoluble Residue	0.29%	1.5%
MgO	0.95%	5%
SO_3	2.71%	3.5%
Loss On Ignition	1.39%	4%
Cl	0.0502%	0.1%
Specific Gravity	3.19g/cm^3	
Setting Time Initial	2:36	Min 1Hr
Setting Time Final	3:18	max 10Hr
Soundness (Lechatelier)mm	1mm	max 10mm
Blaine Specific Surface	3640cm^2/g	min 2800 cm^2/g
0.045mm sieve residue	10.2%	
0.09mm sieve residue:	0.8%	

Table 3.2. Compressive strength of portland cement used (EN 196-1)

Days	Test Results	TS EN 197-1 (Limits)
2	30.8N/mm^2	Min 20 N/mm^2
7	42.1 N/mm^2	Min 31.5 N/mm^2
28	52.2 N/mm^2	Min 42.5 N/mm^2

3.1.2. Aggregates

Crushed stone and sand aggregates conforming to TS EN 12620 were used in this study. Crushed stone aggregates were utilized in three different size groups, so there were totally four different size groups of aggregates being used. Dredged fine aggregate was between the sieve sizes of 0-3 mm, where as the crushed stone sand particles were between 0 and 5 mm. Also there were two coarse crushed stone aggregates between 5 and 12 mm and 12 and 20 mm, respectively. The properties and the grading of aggregates used are given in Tables 3.3 and 3.4, respectively. Aggregates are proportioned to obtain the grading curve given in Figure 3.1.

3.1.3. Admixtures

Superplasticizer POZZOLITH® MR 30 S supplied by YKS Degussa conforming to TS EN 934-2 was used. This admixture consisted of modified lignin sulphonate and had a density of 1.16 kg/lt. The admixture was used as 1 per cent fraction of cement by weight as specified in the user manual of the admixture.

3.1.4. Water

Tap water conforming to TS EN 1008 was used.

3.2. Mixture Composition, Specimen Preparation, Curing and Testing Program

Concrete, with an average 28 day cylinder compressive strength of 38 MPa, was used in this study. The workability of the fresh concrete was adjusted so that fresh concrete showed 18±2 cm slump. Aggregate mix proportions were chosen as 25 per cent for each one to give a grading as specified in Figure 3.1. Mixing water content was estimated as 198 kg/m^3 to give a plastic flowing consistency. Strength requirement was estimated to be achieved by a water – cement ratio of 0.60, which indicates that the cement content should be about 330 kg/m^3. Mix proportioning of the concrete used was given in Table 3.5.

3.2.1. Preparation of Specimens

Concrete mixtures were prepared in batches of 0.02 m^3 in a laboratory pan mixer, in accordance with ASTM C 192, which has a capacity of 0.04m^3. Moulds of 100x200 mm steel cylinders were used for specimens and compaction was done on a vibratory table. The specimens were prepared according to TS EN 480-1. Twelve specimens were taken from each batch.

The molded specimens were kept in laboratory environment for 24 hours. After removal of the moulds the test specimens were stored in water at a temperature of 20±2°C for 28 days.

3.2.2. Fresh Concrete Properties

Slump test was carried out just before casting the specimens according to TS EN 12350-2 Testing Fresh Concrete- Part 2: Slump Test in order to measure the workability of the fresh concrete. The average slump of fresh concrete obtained was 18±2cm.

Density of the fresh concrete was measured according to TS EN 12350-6 Testing Fresh Concrete- Part 6: Density. Fresh concrete density of the mixtures remained between 2360-2370 kg/m^3.

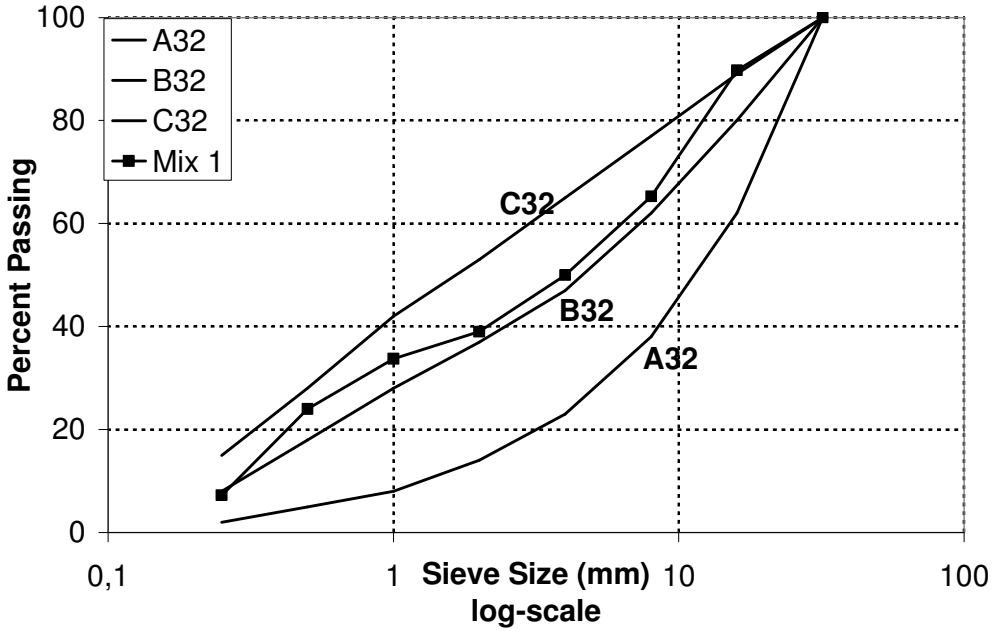

Figure 3.1. Chosen aggregate size distribution

3.3. Experimental Procedures

In this research the changes in the properties of hardened concrete after cyclic compression loading and after additional curing for self healing were investigated through the experiments given below. The testing methodology of cyclic loading under compression is given below. Each specimen was subjected to cyclic loading with different stress ratios up to 100 cycles. Then, some of the specimens were tested as below. Other specimens were kept to investigate the effects of self healing. The specimens kept for 28 days either in laboratory cure or water cure for self healing were later tested for the same properties.

Table 3.3. Crushed stone and natural sand properties

Agregate Production	Crushed and Sand
Production Place	Cebeci/İstanbul - Akpınar/İstanbul
Producer	Dalbay - Kum Seç Mad.
Sampling Place	Set Beton Ayazağa Plant

Experiments Applied	Experiment Standard	Agregate Sizes (mm)			
		Fine Aggregates		Coarse Aggregate	
		0-3 mm	0-5 mm	5-12 mm	12-20 mm
Density(gr/cm^3)	TS EN 1097-6/	2.62	2.68	2.70	2.71
Water absorption(%)	TS EN 1097-6/	1.1	1.4	0.6	0.4
Sand equivalent	TS EN 933-8/	90	80	-	-
Methylene Blue Test	TS EN 933-9/	0.7	0.6	-	-
Fine Material Content(%)	TS EN 933-1	0.6	14	-	-
Compacted Bulk Density (Kg/m^3)	TS EN 1097-3	1517	1886	1569	1538
Loose Bulk Density (Kg/m^3)	TS EN 1097-3	1374	1668	1308	1361
Freeze resistance ($MgSO_3$)-(%)	TS EN 1367-2	-	-	5.54	
Los Angeles (%)	TS EN 1097-2	-	-	19	
Flakeness Index(%)	TS EN 933-3	-	-	14	9

Table 3.4. Sieve analysis of aggregates

Sieve total pass (%)- (TS-3530 EN 993-1/1999)

	Fine Aggregates		Coarse Aggregates	
	0-3	0-5	5-12	12-20
31 mm	100	100	100	100
16 mm	100	100	100	59
8 mm	100	100	59	2
4 mm	100	93	6	1
2 mm	100	53	2	1
1 mm	99	34	2	0
0.5 mm	95	21	0	0
0.25 mm	15	14	0	0

Table 3.5. Mixture proportioning of concrete

Material	Proportion
Cement Content	330 kg/m^3
Water Content	198 kg/m^3
Superplasticizer	1%(of cement content)
No II	464 kg/m^3
No I	463 kg/m^3
No 0	459 kg/m^3
Sand	449 kg/m^3

3.3.1. Static and Cyclic Compression Loading Test

The concrete specimens were capped with sulfur mixture one day after removing from the water curing tank and tested in about an hour. Three specimens were used for compressive strength determination. Compressive strength of the specimens was determined according to TS EN 12390-3. The control specimens were loaded to failure to determine the stress strain behavior and static compressive strength. Cyclic loading tests were conducted on different concrete specimens up to maximum of 100 cycles. During cyclic loading the stress applied to the specimens were alternated between the minimum stress of 0 and maximum compressive stress levels of 0.6, 0.8 and 0.9 of f_{max} determined in the static compressive loading test.

During cyclic loading stress strain diagrams were also plotted for all cycles and thus modulus of elasticity of concrete could have been obtained for each cycle. Equipment in Figures 3.2. and 3.3. were used for determining the stress strain diagrams under both slow rate static and cyclic loading tests of the concrete specimens.

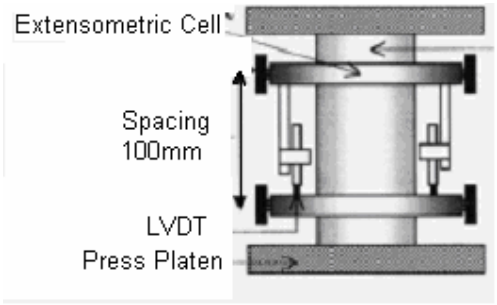

Figure 3.2. Compressmeter for strain measurements during cyclic loading

Figure 3.3. Data acquisition system of cyclic loading

Cyclic compression loading was applied on concrete specimens under a controlled loading rate compression testing machine. Test machine has a wide range of loading rate which can be managed manually. Applied loading rate was read from a computer. The computer can also record the data obtained from the two LVDT's which are on two opposite sides of the ring attached to the specimen. The axial compressive strain was taken as the average of these two readings. The axial strain was measured with a precision of 0.001 mm. The load was measured via a pressure transducer. The raw data for load measurements were calibrated through a load cell. The load measurements were done all through the test at a rate of 8 Hz.

The same setup was also used for plotting the stress strain diagrams and measuring the modulus of elasticity of the concrete. In measuring the modulus of elasticity of the control concrete under static loading, a loading rate of 0.25 MPa/sec was applied. While applying cyclic loading, on the other hand, for plotting the stress strain diagrams for each cycle a loading rate of 1.25 MPa/sec was used. Focal point findings and post peak response behavior analysis were also done using the data from this setup.

3.3.2. Determination of Modulus of Elasticity

The elastic modulus can be measured using either static or dynamic tests, and these two ways do not give the same result. The static modulus is measured by deforming of a

concrete cylinder under an applied compression load (usually up to 30-40 per cent of the ultimate load).

The modulus of elasticity was measured according to ASTM C 469-02 'Static Modulus of Elasticity and Poisson's ratio of concrete in compression'. Secant modulus of elasticity was utilized for determining the modulus of elasticity from the stress-strain plot. The modulus of elasticity and Poisson's ratio values were measured within the stress range of 0-40 per cent of the concrete strength. As the upper limit of the range of stress application was increased higher values of modulus of elasticity would have been obtained. Through out the full loading , actually, the first record was taken when the strain was about 50 millionths and the second reading was taken when the load was equal to 40 per cent of the concrete strength.

The modulus of elasticity is the ratio between stress (load/area) and strain (deformation, or change of length/length). Concrete is not a truly elastic material, the relationship between stress and strain is not constant. Three E-value conventions are used, the secant modulus, the tangent modulus and the initial tangent modulus, as shown Figure 3.4.

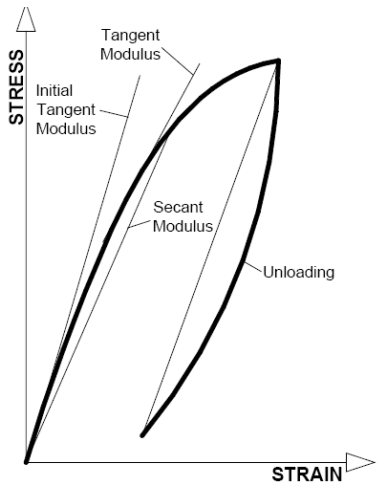

Figure 3.4. Stress – strain relationships for concrete [57]

The most useful measure is the secant modulus, and in EN 1992-1-1, it is the secant modulus, E_{cm}, that is used in reinforced concrete design. In the absence of experimentally

measured values, the secant modulus is mostly calculated, or assumed, from the characteristic compressive strength of concrete for the use in design.

If information is not available on the concrete that will be used, designers have to use the lowest common European value for the modulus of elasticity. For quartzite aggregates, the 'normal' static modulus (the secant modulus) is calculated from the specified characteristic compressive cylinder strength from the equation. [58]

3.3.3. Compressive Strength of Concrete

Compressive strength may be defined as the measured maximum resistance of a concrete specimen to an axial compressive loading.

Compressive strength is generally measured at the age of 28 days and expressed in megapascals (MPa). Seven-day strengths are often estimated to be about 75 per cent of the 28-day strength where as 56-day and 90-day strengths are about 10 to 15 per cent greater than 28-day strengths if not measured experimentally. The water-cement ratio, the curing and environmental conditions, and the age of the concrete affect compressive strength primarily. These factors also affect the flexural and tensile strengths of concrete and the bond of concrete to steel [59].

The rate and magnitude of the load can be manually changed in the testing machine. The compression machine's testing platens fit to requirements of Test Method ASTMC39. The constant rate of loading is supplied manually.

The compression test is done according to ASTM C 39 before measuring modulus of elasticity of the specimen. It is done to determine the ultimate strength of the specimen. There are three specimens used to determine the ultimate strength. The specimen is aligned carefully so that the load is acting axially. The top platen is to contact the specimen gently to provide a homogenous load distribution, and apply load at a rate of 0.25 MPa /sec.

3.3.4. Splitting Tensile Loading Test

In this study, splitting tensile test was done according to EN 12390 using the compression testing machine with the auxiliary equipment described in this standard (Figure 3.5). The water cured specimens were air dried for one day before applying the test. Splitting tensile test was done on control specimens and also on cyclically loaded specimens. The test was also done on water and air cured specimen which have been previously cyclically loaded to investigate the self healing effect. The splitting tensile strength was calculated from the Equation (3.1) after measuring the splitting load P in the test.

$$f_s = \frac{2P}{\pi DL} \tag{3.1}$$

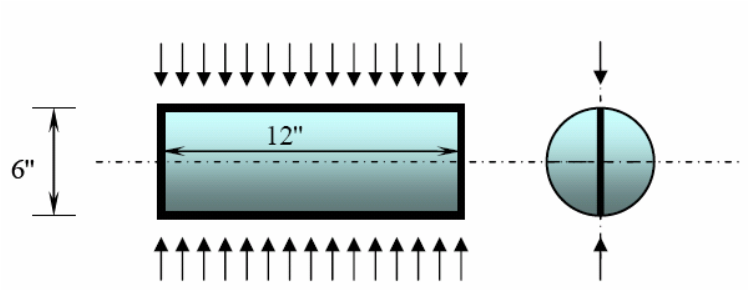

Figure 3.5. Splitting tensile stress specimen diagram

3.3.5. Ultrasound Velocity Test

Ultrasonic pulse velocity measurement was done according to TS EN 12504-2. The testing equipment was calibrated with the calibration tool provided with it. Ultrasonic pulse velocity measurements were done on control and cyclically loaded specimens for comparison. The test was also applied to cyclically loaded specimens after they have been subjected to additional air and water curing to investigate the effects of self healing.

3.3.6. Capillary Water Absorption and Sorptivity Test

Capillary suction occurs when water is drawn into the fine voids (capillaries) in concrete from the wet surfaces and is mainly caused by surface tension. The test setup is given in Figure 3.6. Concretes with finer pore structures will experience greater capillary suction pressures.

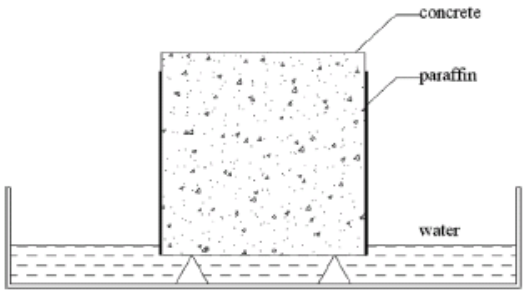

Figure 3.6. Water absorption test on concrete specimen

Concrete specimens which have been subjected to different cyclic loadings were cut to get slices of 75 mm thickness and put in an oven of 65 ℃ until gaining a constant mass. And then they were cooled to room temp in 3 hours in desiccators. The specimen's one face was exposed to water as seen in Figure 3.6. The water was 5 mm above the base of the specimen. The specimen's side face was sealed. The specimen was weighed at certain times (1, 4, 9, 16, 25, 36, 49, 64 minutes) to get measurements for capillary water absorption of concrete. Then the sorptivity was calculated by using the following Equation (3.2).

$$\frac{Q}{A} = k \times t^{(1/2)} \tag{3.2}$$

Q = Total Flow
A = Area
t = time
k = Sorptivity

3.3.7. Rapid Chloride Permeability Test

ASTM C 1202 gives the details of the rapid chloride permeability test. This test method covers the determination of the electrical conductance of concrete to provide a

rapid indication of its resistance to the penetration of chloride ions. This test method is applicable to the types of concrete where correlations have been established between this test procedure and long term chloride ponding procedures The test is done using 51 mm long and 95 mm diameter cylindrical specimens cut from cores of concrete members taken with a diamond-dressed coring bit or using 51 mm long slices cut from 100 x 200 mm concrete cylinders, and the test values are normalized using the ratio of the standard.

After water cure of 27 days , the specimens were dried for one hour. Then, the curved surface of the test specimen was coated with rapid setting epoxy. After coating was dried, the specimen was vacuum saturated with water and then soaked for 4 hours in de-aerated water in vacuum desiccators with a vacuum pump. Then the specimen was soaked in water for 18 hours. The specimen was placed in the testing apparatus where one end of the specimen was exposed to a solution containing sodium chloride (NaCl) (3.0 per cent by mass) in distilled water) and the other end is exposed to a solution containing sodium hydroxide (NaOH) (0.3 N in distilled water) as shown in Figure 3.7. A 60 V potential was applied across the specimen to stimulate the permeation of chloride ions penetration through the specimen. The current across the specimen was measured at least at every 30 minutes during the 6-hour test duration. As the chlorides penetrated into the concrete, the pore solution became more conductive and the current readings increased. The total charge passing through the specimen (in coulombs) was found by calculating the total area under the plot of time versus current. Therefore, higher coulomb values at the completion of the test indicated higher permeability as shown in Table 3.6.

Table 3.6. Chloride ion penetrability based on charge passed

Charge Passed (coulombs)	Chloride Ion Penetrability
>4.000	High
2.000-4.000	Moderate
1.000-2.000	Low
100-1.000	Very Low
<100	Negligible

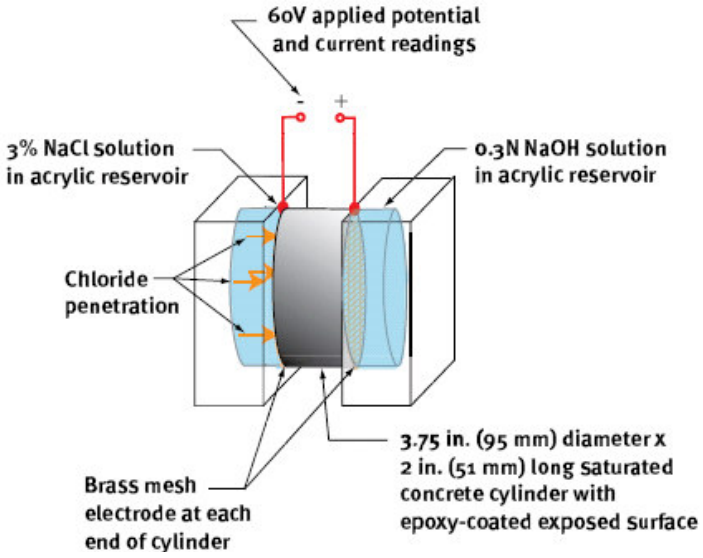

Figure 3.7. Rapid chloride permeability test setup

3.3.8. Sulphate Resistance Test

$MgSO_4$ was soluted in water as 75 gr per liter. This corresponds to 60 gr of SO_4 per liter of solution. The specimens were kept in the solution and weighed every 15 days. The solution was changed every month. The weight change of the specimens was continuously observed and recorded versus time to determine the resistance of concrete to sulphate deterioration.

3.3.9. Microscopic Analyses

Microscopic analysis was done to view the cracks via the optical microscope and also to observe the self healing effects on cracks by electron scanning microscope. The microscopic analysis was done on specimen before and after curing. The specimens were prepared according to apparatus.

3.3.9.1. Electron Scanning Microscopy

Electron scanning microscope was used to view the process of further hydration on the crack surfaces of the specimen through the self healing procedure. The pictures were taken at 5000 times magnifying. Small specimen of 1cm3 were prepared without harming

the specimen. The specimen were dried and both crack surface and sliced surface is investigated with 5000 magnifying. The filling of the voids were investigated comparing the specimen before and after cure.

3.3.9.2. Optical Microscopy

Microscopic analysis was done using an optical microscope with 70 and 150 times magnifying. The cracks were observed before and after cyclic loading and the measurements were taken. The specimen were sliced and the sliced surface was cleaned to see the cracks thoroughly. After cyclic loading the cracks were investigated then some of the specimen were kept in water cure and some in air cure. The crack size changes before and after cure was measured.

3.3.10. Mercury Intrusion

Mercury intrusion test was done by introducing mercury under pressure in to the concrete pores and the extrusion of it. With the pressure and the quantity of the mercury the computer can analyze pore diameters and sizes. Critical pore diameter at which there is a need to increase the pressure to increase the pores that intrude mercury was also determined from the analysis.

3.3.11. Post Peak Response Analyses

The tests were performed on cylindrical specimens of d =100 mm diameter and h = 200 mm height. The bottom steel platen was fixed while top steel platen was allowed to provide full contact with the specimen surface. Both surfaces were sulphur capped. Two linear variable differential transformer (LVDTs) type displacement transducers with ±0,001 mm range were used to measure the platen-to-platen displacement. The LVDTs were attached on the middle 100 mm part of the concrete cylinder ring assembly. Load was recorded using a pressure transducer. The LVDTs and pressure transducer were interfaced with a computer for signal conditioning and data acquisition.

Initially a load of 20 -30 per cent of the maximum load was applied. If the second loading used the same path loading was started loading was done at a stable loading strain rate so that a sudden failure did not occur. The tests were done on a manually controlled compression machine. After peak stress is reached unloading and then reloading was applied to the specimen.

Fracture energy was calculated taking area under stress strain curve in post peak analysis. Under compression it was hard to obtain full curve so upto $0.6f_{max}$ after post peak is taken as the limit.

3.4. Self Healing

In this study effect of curing conditions on self healing was also investigated. Water cure and laboratory curing conditions were chosen. The water in water cure was at 20-25°C. The specimen in laboratory conditions were kept between 40-60 per cent relative humidity level and at 20-25°C. The specimens were kept in different curing conditions for 28 days after cyclic loading and after this curing period the specimens were investigated for their mechanical and permeability properties.

4 . EXPERIMENTAL RESULTS AND DISCUSSION

The purpose of this thesis is to investigate the mechanical and permeability properties of concrete subjected to low cyclic compressive loading at different loading amplitudes. The tests done on specimens are explained in previously. After cyclic loading the changes in mechanical and permeability properties of concrete were investigated as well as the effects of self - healing due to additional curing applied to the specimens.

The test program consisted of testing 10x20 cm concrete cylinders under uniaxial cyclic loading at different amplitudes after the specimens were water cured for 28 days. The concrete cylinders were tested after being sulphur capped in the compression testing machine which was manually controlled. At the first stage of testing some of the specimens were loaded up to failure under constant compressive stress loading rate to determine the maximum stress. Afterwards other specimens were loaded cyclically at stress levels of 0.6, 0.8 and 0.9 of the maximum stress up to 100 cycles.

At the second stage of testing some of the specimens were tested to identify the changes occurred in some mechanical and permeability properties of concrete. The tests applied were compressive and splitting tensile strengths, modulus of elasticity, ultrasonic pulse velocity, water absorption, mercury intrusion, rapid chloride permeability and sulphate resistance of concretes. Additionally, micro-structural examinations of concrete sections for cracking after cyclic loading were also inside.

As the third stage of the study some of the specimens after cyclic loading were kept in different curing environments to investigate the self healing capability of cracks formed during the cyclic loading. Then these additionally cured specimens were tested for changes in concrete properties as described above for cyclically loaded specimens.

4.1. Mechanical Properties of Cyclically Loaded Specimens

After cyclic loading the changes in various concrete properties were investigated. The degree of damage on the internal structure of concrete after cyclic loading was determined through testing for some of the mechanical properties.

Compressive strength, modulus of elasticity, splitting tensile strength, and ultrasonic pulse velocity of the specimens were also determined after cyclic loading. Figure 4.1 shows the stress strain diagram of the concrete specimen monolithically loaded until failure. Figures 4.2 to 4.4 show the stress strain diagrams for concretes cyclically loaded up to the stress levels of $0.6f_{max}$, $0.8f_{max}$ and $0.9f_{max}$, respectively.

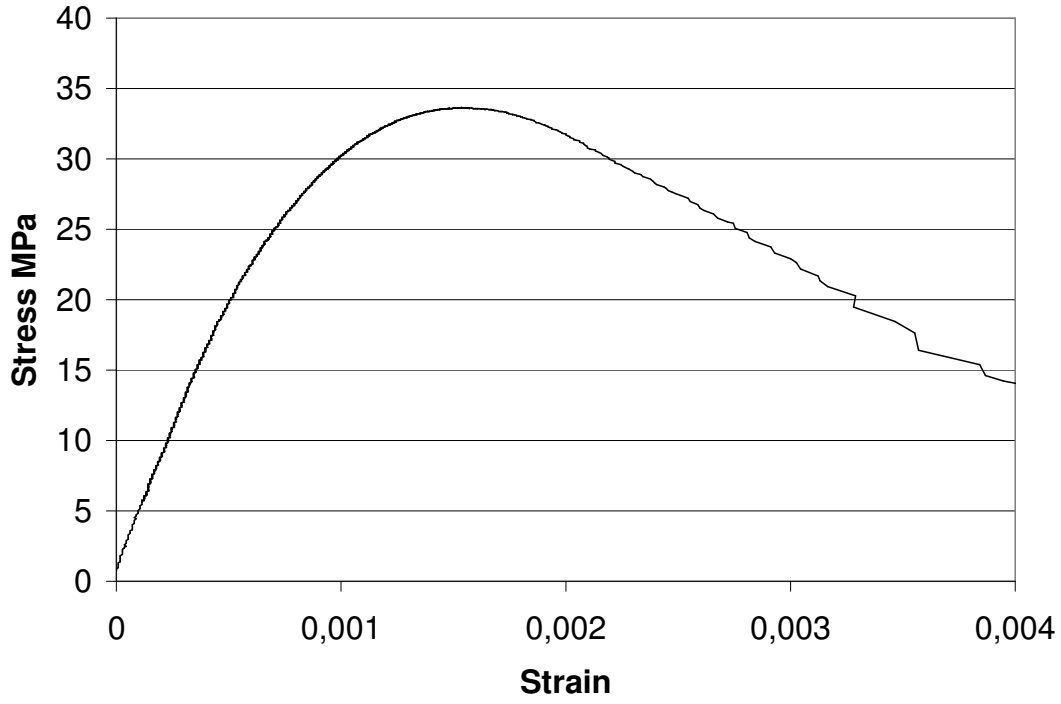

Figure 4.1. Stress – strain diagram for control specimen under static loading

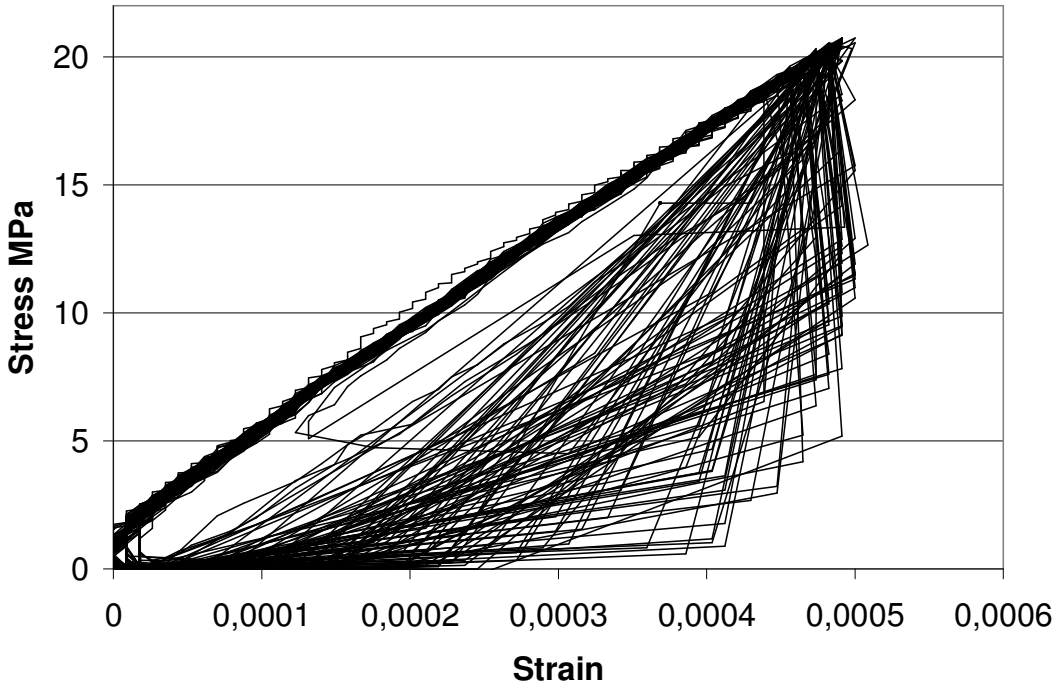

Figure 4.2. Stress - strain diagram for 0.6 f_{max} cyclic loading

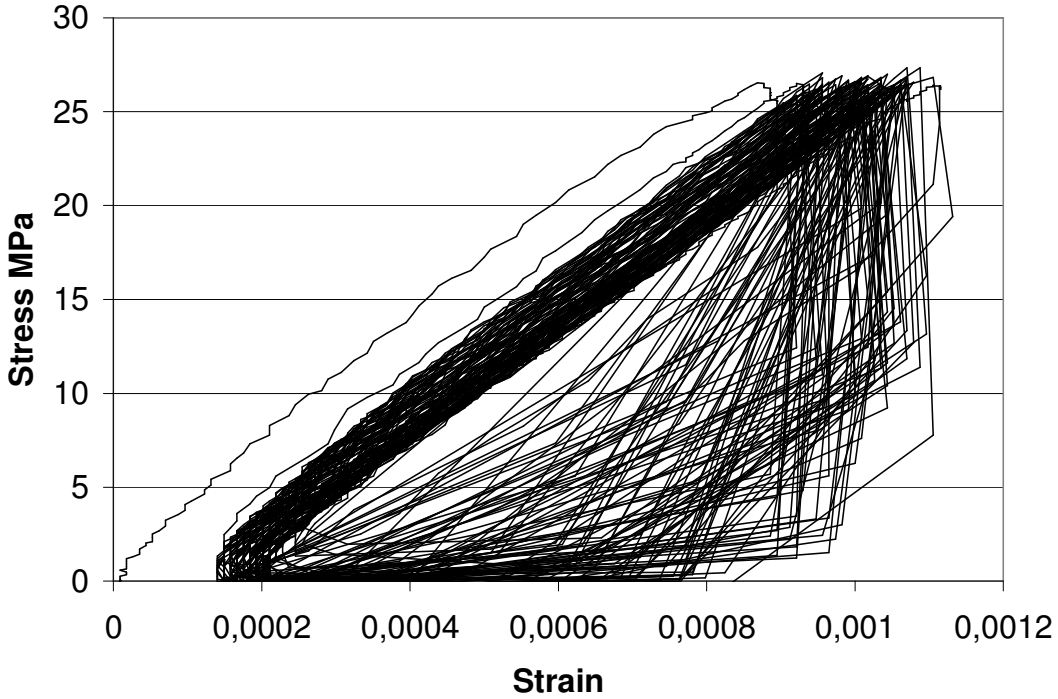

Figure 4.3. Stress – strain diagram for 0.8 f_{max} cyclic loading

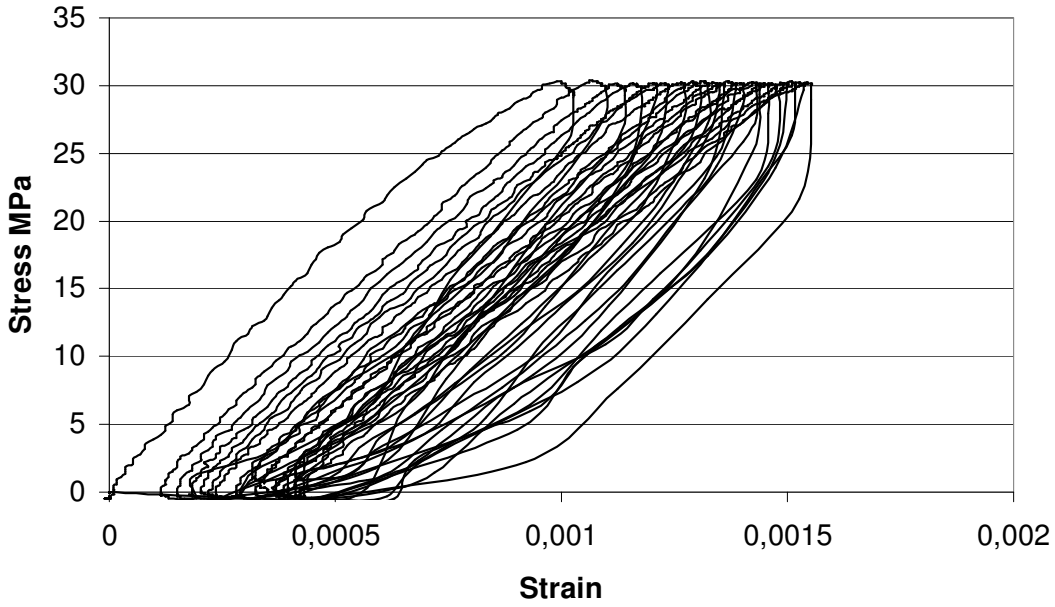

Figure 4.4. Stress – strain diagram for 0.9 f_{max} cyclic loading

4.1.1. Compressive Strength

Compressive strength of control specimens and specimens loaded up to 100 cycles at different stress levels were measured. The individual test results and the average of the four specimens are given in Table 4.1. The average compressive strengths were measured as 38.1 MPa, 37.4 MPa, 36.2 MPa and 35.8 MPa for the control, $0.6f_{max}$, $0.8f_{max,}$ and $0.9f_{max}$ loaded specimens, respectively. Cyclically loaded specimens had lower compressive strength and the compressive strength decreased with the increase in the stress level at cyclic loading. The maximum decrease in compressive strength was 6 per cent at $0.9f_{max}$ loaded specimen as also shown in Figure 4.5. The damage ratio defined as the ratio of the difference in compressive strengths of control specimen cyclically loaded specimen to the strength of control specimen, is given in Figure 4.6.

Table 4.1. Compressive strength of concrete specimen

After Cyclic Loading	Control	$0.6f_{max}$	$0.8f_{max}$	$0.9f_{max}$
Specimen 1	35.5	37.3	37.3	37.3
Specimen 2	37.9	37.2	34.9	34.2
Specimen 3	40.9	35.1	36.7	35.9
Specimen 4	38.1	39.8	36.1	35.8
Average	38.1	37.4	36.2	35.8
Standard Deviation	2.21	1.92	1.03	1.27

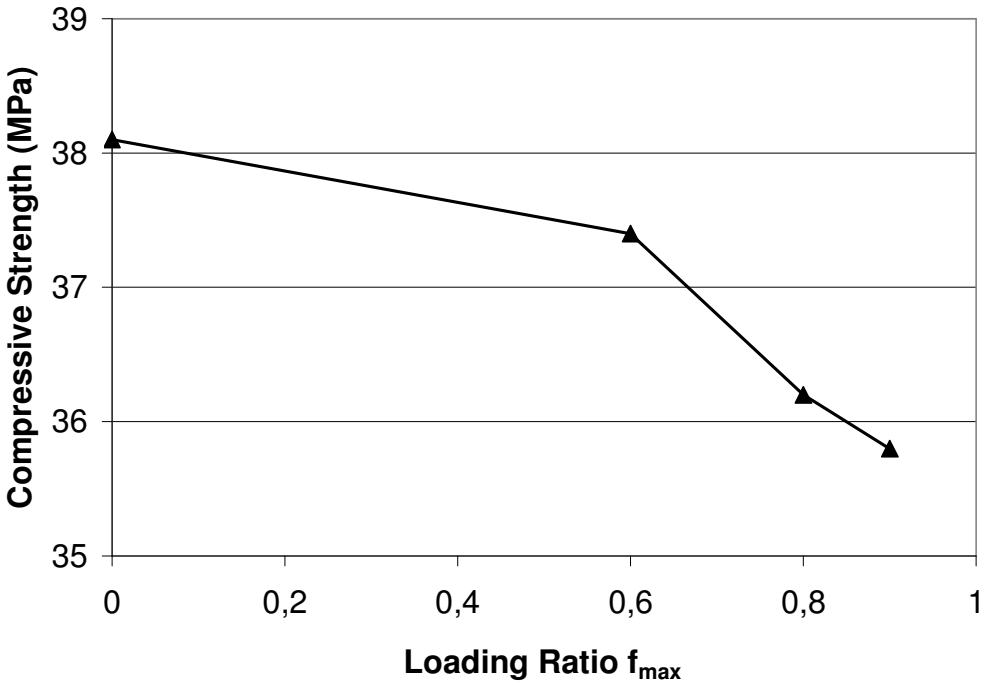

Figure 4.5. Variation of compressive strength of concrete with loading ratio

Residual strength of concrete after cyclic loading has also been investigated by Baluch et al [33] whose findings are given in Figure 4.7. In this research it was found out that the residual strength of concrete decreases after cyclic loading. As given in the research done by Baluch [33] there was a decrease in compressive strength with increasing number of cycles as given in Figure 4.6.

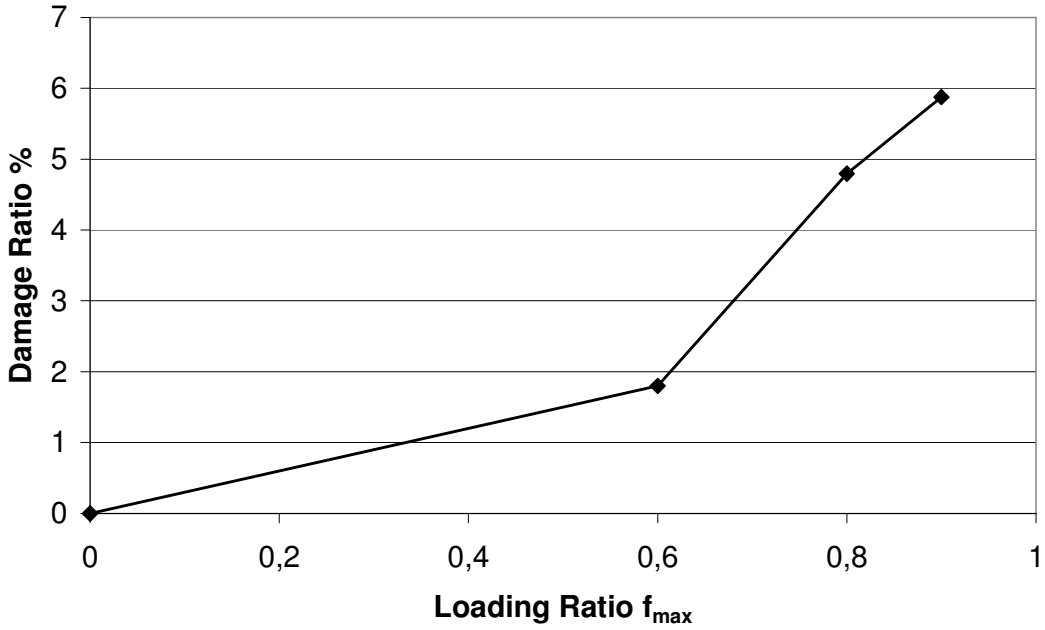

Figure 4.6. Damage ratio for compressive strength after cyclic loading

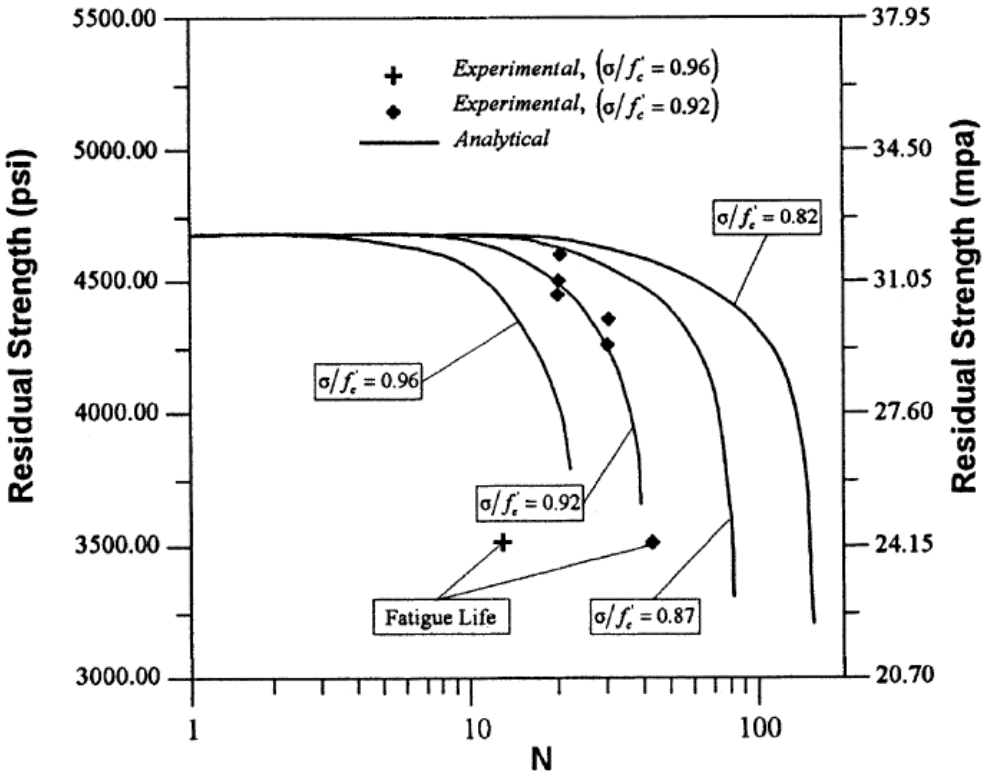

Figure 4.7. Residual compressive strength after cyclic loading [33]

Test results have also shown that stiffness of concrete experienced a clear degradation with cyclic loading. In each loading cycle residual strain increased. Also total strain at failure increased with increasing number of cycles as given in Figure 4.8 and plastic strain after cyclic loading also increased after cyclic loading as given in Figure 4.9. Table 4.2 summarizes the strain measurements after cyclic loading of concrete specimens. Some of the specimens were also loaded with a very slow rate of loading to get the full stress strain curve. The maximum strains obtained at maximum stresses for the control and $0.6f_{max}$, $0.8f_{max}$ and $0.9f_{max}$ cyclically loaded specimens are shown in Figure 4.8. It was observed that as the loading ratio was increased the strain at peak stress also increased. In Figure 4.10 the comparison of $0.9f_{max}$ loaded to control specimen is given.

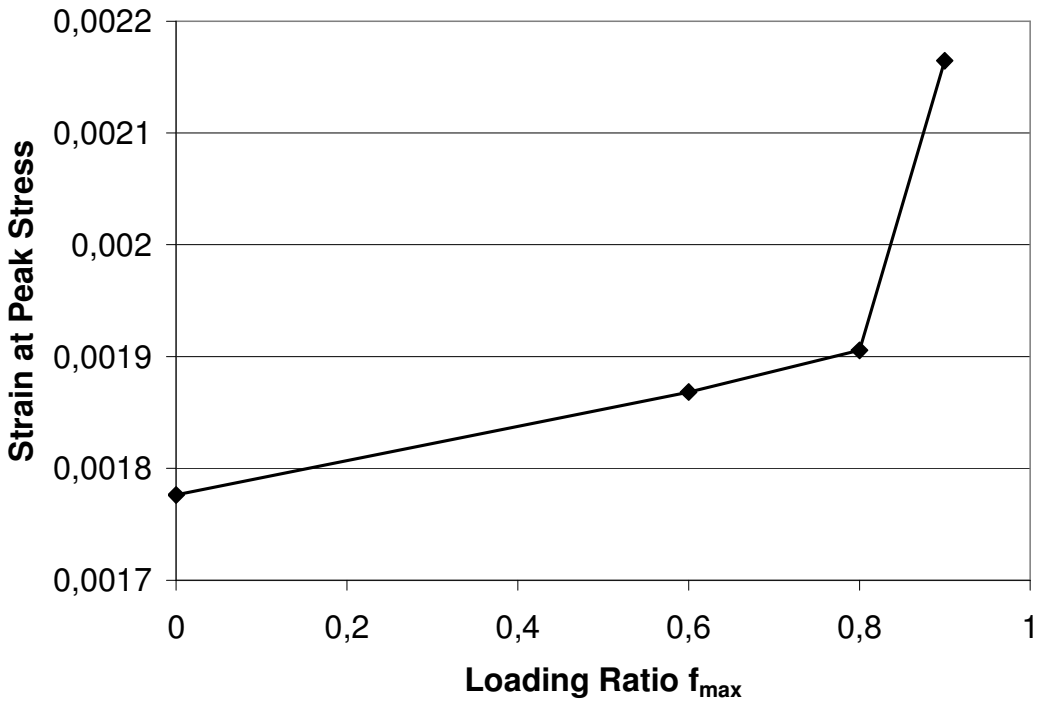

Figure 4.8. Strain at peak stress after cyclic loading.

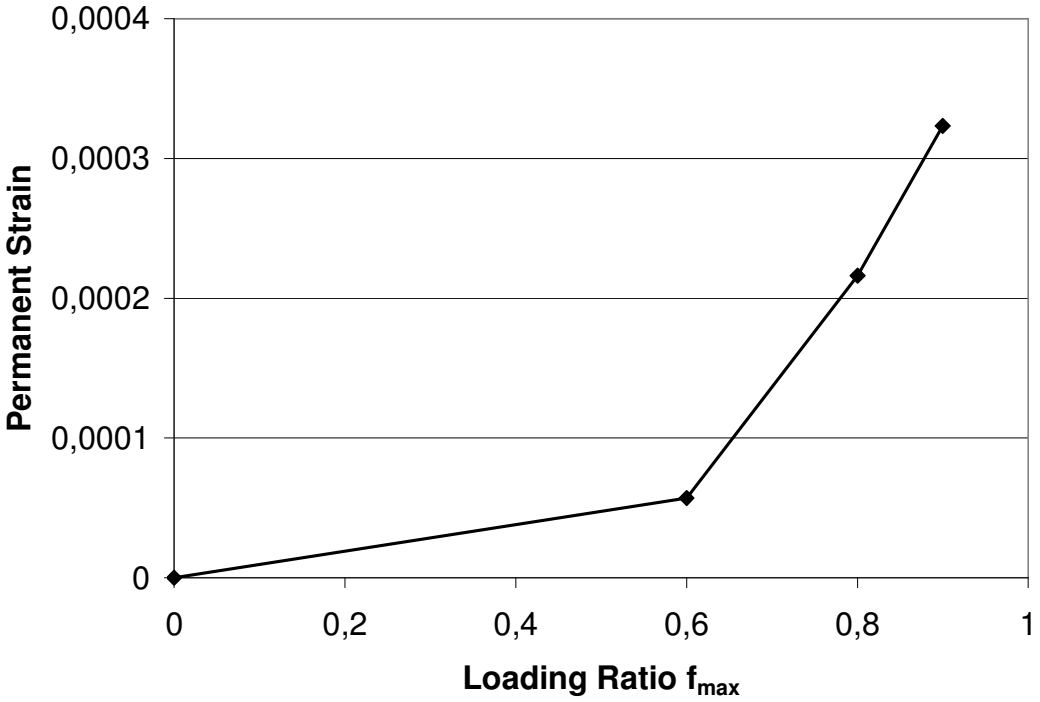

Figure 4.9. Strain at the end of cyclic loading

Table 4.2. Strain measurements after cyclic loading

	Control	**0.6f_{max}**	**0.8f_{max}**	**0.9f_{max}**
At maximum stress after cyclic loading	0.00177	0.00187	0.0019	0.00216
At the end of cyclic loading	0	0.000057	0.000216	0.000323

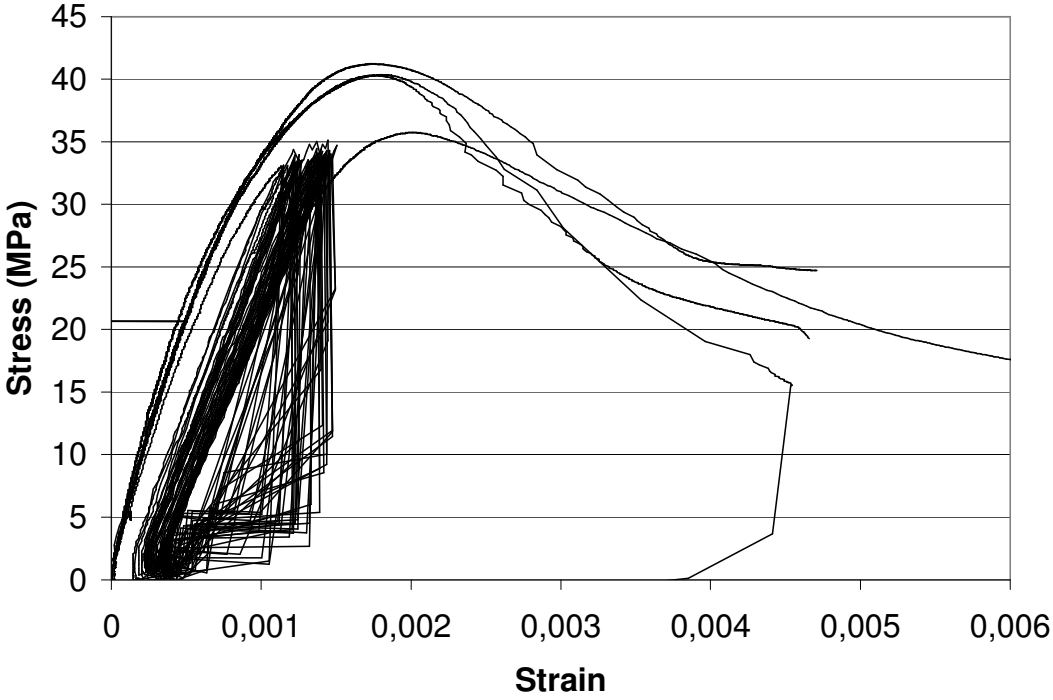

Figure 4.10. Stress - strain diagram of $0.9f_{max}$ loaded specimen and control specimen

4.1.2. Modulus of Elasticity

The moduli of elasticity the control specimens are given in Table 4.3. Modulus of elasticity measured from static compressive loading of the control specimens not subjected to cyclic loading varied between 36.0 GPa and 42.2 GPa with an average value of 38.9 GPa and a standard deviation of 2.22 GPa. The moduli of elasticity of the concrete specimens which were cyclically loaded to $0.6f_{max}$, $0.8f_{max}$ and $0.9f_{max}$ are given in Tables 4.4, 4.5 and 4.6 respectively, calculated after each of the first 5 cycles and after the 100^{th} cycle. The decrease in modulus of elasticity can be observed graphically in Figure 4.4 which is similar as given in Figure 4.11 [12].

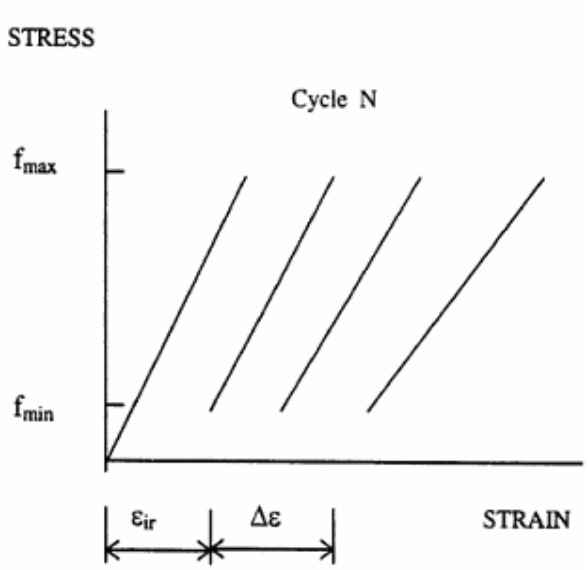

Figure 4.11. The decrease in modulus of elasticity with cyclic loading [12]

Table 4.3. Control specimen moduli of elasticity of control specimens

Specimen Number	Modulus of Elasticity (GPa)
1	36.0
2	39.9
3	37.5
4	37.8
5	42.2
6	40.0
Average	38.9
Standard Deviation	2.22

The moduli of elasticity of the cyclically loaded specimens decreased with the increase in the number of cycles applied, as shown in Figure 4.11 [12]. In this thesis work it was found that modulus of elasticity after the 100^{th} cycle was reduced to 47 per cent of the value after the first cycle for the concrete specimen loaded to $0.9f_{max.}$ There were approximately 22 per cent and 9 per cent decrease in the $0.8f_{max}$ and $0.6f_{max}$ loaded specimens, respectively. Increasing the load ratio (applied load-to-strength ratio) also caused a decrease in the modulus of elasticity determined after the same number of cycles. The difference was more in the specimens loaded to $0.9f_{max}$. Variation of the modulus of elasticity in the first five cycles with different loading ratios is given in Figure 4.12. As the loading ratio increases there is a larger decrease in modulus of elasticity. The highest reductions with increasing load ratio were observed after 100^{th} cycle of loading. Modulus

of elasticity were reduced by 12, 21 and 47 per cent with respect to the control concrete at $0.6f_{max}$, $0.8f_{max}$, and $0.9f_{max}$ loaded specimens, respectively, as measured at the end of the 100^{th} cycle, as shown Figure 4.13.

Table 4.4. 0.6 f_{max} loaded specimen modulus of elasticity (GPa)

Specimen \Cycle No	**1**	**2**	**3**	**4**	**5**	**100**
1	40.1	40.0	39.8	39.6	39.5	35.8
2	36.2	35.9	35.7	35.6	35.1	33.1
3	37.3	36.3	36.0	36.0	36.0	34.9
4	36.9	36.8	36.7	36.7	36.7	33.6
Average	37.6	37.2	37.1	37.0	36.8	34.3
Standard Deviation	1.71	1.87	1.88	1.81	1.9	1.23

Table 4.5. 0.8 f_{max} loaded specimen modulus of elasticity (GPa)

Specimen No \Cycle No	**1**	**2**	**3**	**4**	**5**	**100**
1	40.2	36.3	33.7	33.5	33	29.3
2	39	37.7	37.9	37.1	37.3	31.7
3	39.2	37.8	37.9	37	37.1	31.1
Average	39.5	37.3	36.5	35.9	35.7	30.7
Standard Deviation	0.64	0.84	2.43	2.05	2.43	1.25

Table 4.6. 0.9 f_{max} loaded specimen modulus of elasticity (GPa)

Specimen No \Cycle No	**1**	**2**	**3**	**4**	**5**	**100**
1	43.4	35.7	30.7	28.9	26.8	23.2
2	39.6	30.8	27.4	27.3		24.5
3	43.3	38.3	38	37.6	37.1	19.2
4	44.3	40.1	30.3			15.9
Average	42.7	36.3	31.6	31.3	32.0	20.7
Standard Deviation	2.08	4.04	4.52	5.54		3.91

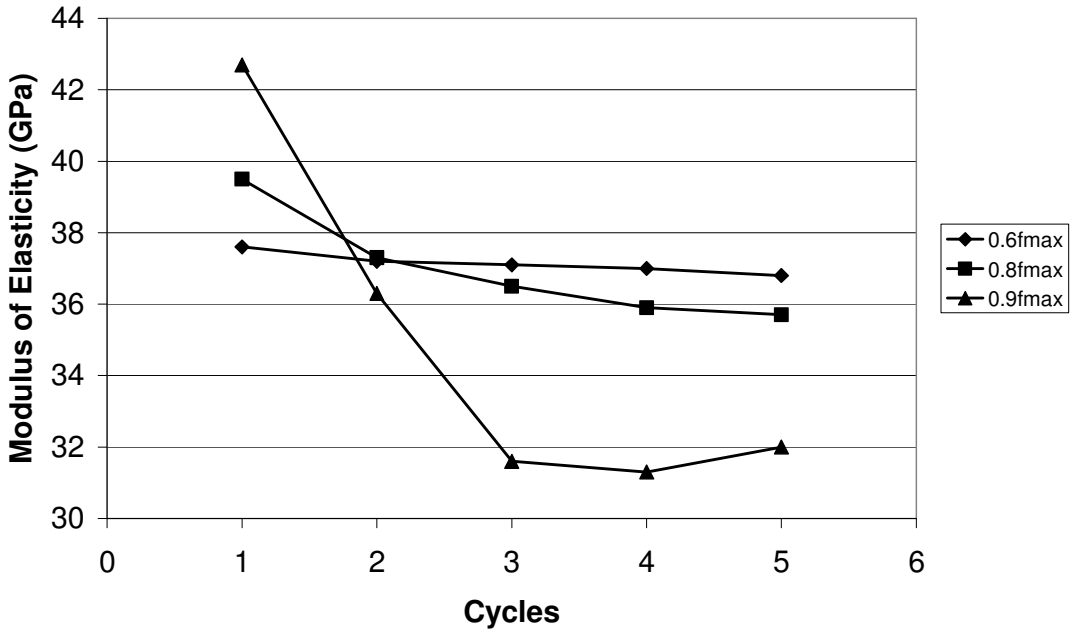

Figure 4.12. Variation of modulus of elasticity of concrete with loading ratio at 1-5 cycles

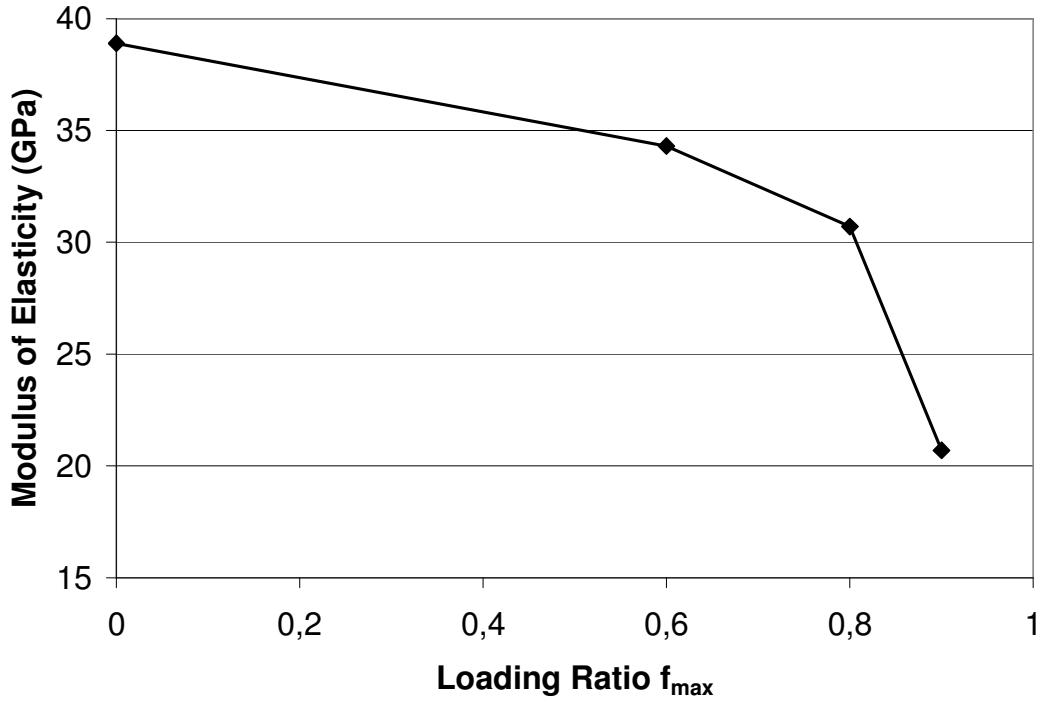

Figure 4.13. Variation of modulus of elasticity of concrete with loading ratio at 100th cycle

The increase in cyclic loading stress level ratio caused a decrease in modulus of elasticity which can be also observed in Figure 4.14 in terms of damage ratio.

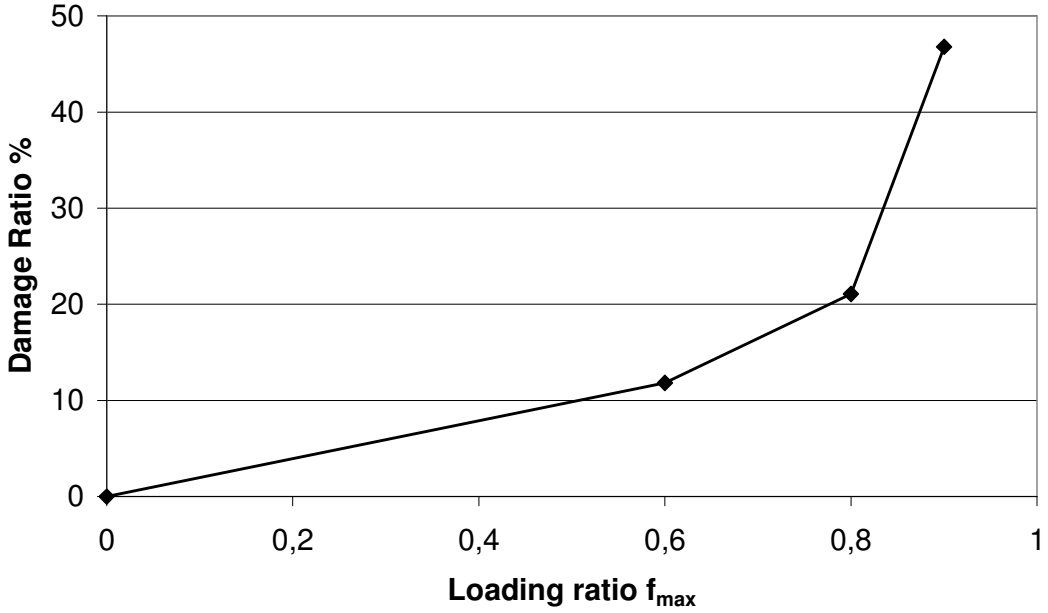

Figure 4.14. Damage ratio for modulus of elasticity after cyclic loading

TS 500 and Eurocode 2 relate the modulus of elasticity to the compressive strength of concretes by the Equations (4.1) and (4.2). Modulus of elasticity of concretes were also calculated from Equation (4.1) and Equation (4.2) given by TS 500 and Eurocode 2 as given in Tables 4.8 and 4.9, respectively. The values calculated from the code equations were higher than the experimental results. This may be due to the type of aggregates used in concretes. This effect of aggregate type is illustrated in Table 4.7 which indicates approximately 20 per cent increased for crushed limestone aggregate to gravel. The use of dense crushed limestone in this study might have caused an increase of approximately 14 per cent as calculated from the values in Table 4.8 and 4.9. In Eurocode 2 the modulus of elasticity of the concrete subjected to cyclic loading is decreased 40 per cent of design value [11]. The decrease in Eurocode will supply enough margin for the design since only at $0.9f_{max}$ loading 50 per cent decrease could be observed.

Table 4.7. Modulus of elasticity correction factor[58]

Aggregate	**k_1**
River Gravel	1.005
Crushed Graywacke	1.002
Crushed Quartzitic Aggregate	0.931
Crushed Limestone	1.207
Crushed Andesite	0.902
Crushed Basalt	0.922
Crushed Clayslate	0.928
Crushed Cobbel Stone	0.955
Blast Furnace Slag	0.987
Calcined Bauxite	1.163
Lightweight Coarse Aggregate	1.035
Lightweight Fine and Coarse Aggregate	0.989

$$E_{cj} = 3250\sqrt{f_{ckj}} + 14000(MPa) \text{ (TS 500)} \quad (4.1)$$

$$E_{cm} = 22(\frac{(fcm+8)}{10})^{0.3} GPa \text{ (Eurocode 2)} \quad (4.2)$$

Table 4.8. Modulus of elasticity values according to TS 500

Compressive Strength MPa	38.1	37.4	36.2	35.8
Modulus of Elastisity GPa	34.1	33.9	33.6	33.5

Table 4.9. Modulus of elasticity values according to Eurocode 2

Compressive Strength MPa	38.1	37.4	36.2	35.8
Modulus of Elastisity GPa	34.8	34.6	34.4	34.3

It has been found out by many researchers [12, 29] that modulus of elasticity and strength of concrete decreases after cyclic compressive loading. However, it was shown by Ballatore [28] that cyclic compressive loading increased the strength and the modulus of elasticity of concrete. But, in the study of Ballatore [28], the cyclic compressive loading

ratio was as low as 10-20 per cent of the maximum compressive strength. In low stress levels such as 10-20 per cent of the failure load increased the compressive strength about 10-15 per cent [28]. However, as it was observed in this study that, with higher stress levels as 0.6 – 09f_{max}, the cyclic loading caused decrease both in compressive strength and modulus of elasticity.

4.1.3. Splitting Tensile Strength

Splitting tensile strength test was done according to TS EN 12390-6 on the control and cyclically loaded specimens after the application of the 100^{th} cycle. The test results are presented in Table 4.10 and Figure 4.15 and damage ratio is given in Figure 4.16. The results showed that low cycle fatigue loading caused a reduction on the splitting tensile strength of the concrete. It was also observed that the splitting tensile strength decreased with the increase in the applied load ratio. The decrease in the splitting tensile strength at 0.6f_{max}, 0.8f_{max} and 0.9f_{max} load ratios were obtained as 9, 28 and 30 percentages, respectively, compared to the control specimen. There was a greater decrease in the splitting tensile strength beyond 0.6f_{max} loading, where as the difference in the drop between 0.8f_{max} and 0.9f_{max} was not that much significant.

Table 4.10. Splitting tensile strength of concrete at cyclic loading (MPa)

Specimen	**Control**	**0.6 f_{max} Loaded**	**0.8 f_{max} Loaded**	**0.9 f_{max} Loaded**
1	4.08	3.57	2.61	2.79
2	3.95	3.34	2.04	2.16
3	3.76	3.57	3.57	2.96
4	3.47	3.34	2.81	2.71
Average	3.81	3.46	2.76	2.64
Standard Deviation	0.26	0.13	0.63	0.35

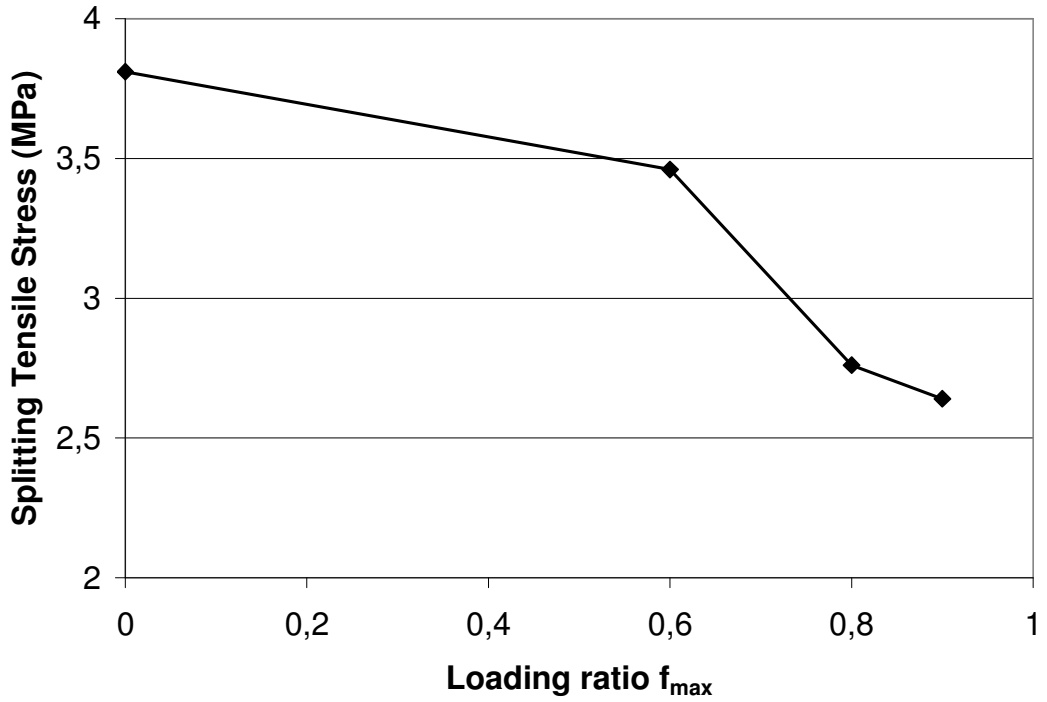

Figure 4.15. Variation of splitting tensile strength of concrete with loading ratio

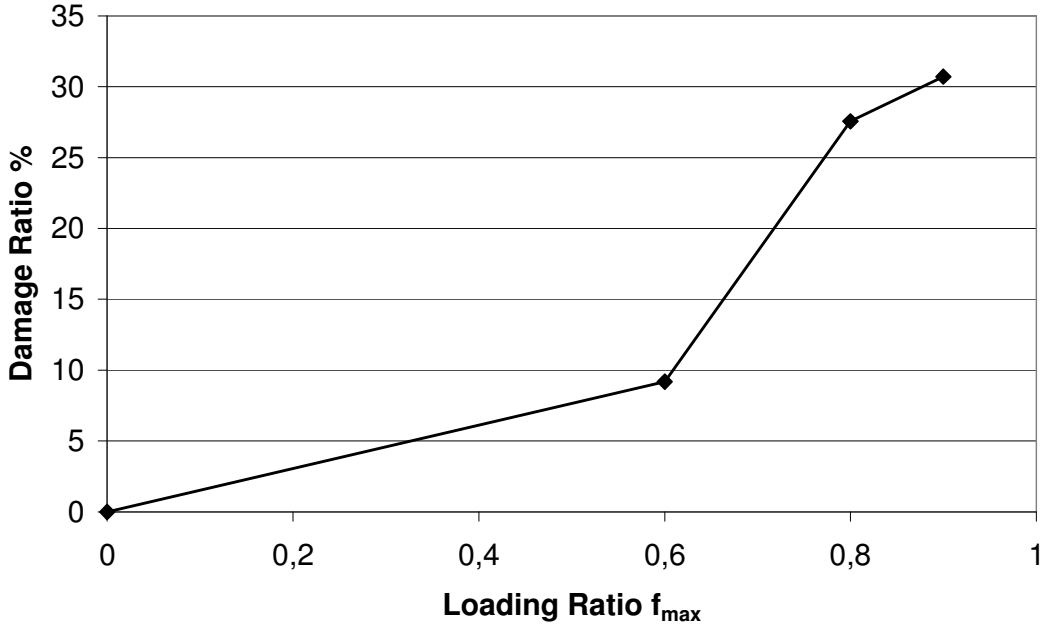

Figure 4.16. Damage ratio for splitting tensile strength after cyclic loading

According to TS 500 splitting tensile strength can be estimated via compressive strength by Equation (4.3.)

$$f_{ctm} = 0.3 \times f_{ck}^{(2/3)} MPa \tag{4.3}$$

The splitting tensile strength for 38.1 MPa compressive strength was found as 3.4 MPa which is fairly close to the undamaged concrete specimens test result which is 3.8 MPa. But for $0.9f_{max}$ loaded specimen which has an average compressive strength of 35.8 MPa, the calculated splitting tensile strength is 3.26 MPa . However, test result is found out to fall more below that, which is 2.64 MPa. It can be concluded that although $0.9f_{max}$ damaged concrete specimens had lower tensile strength compared with the value calculated from its compressive strength, the damage in concrete was probably parallel to the loading direction and lowered the tensile strength.

It can be concluded that the equations in the standards for the prediction of modulus of elasticity and splitting strength are derived for the undamaged specimens, and they are not applicable for the damaged concrete. There is a limit for concrete material for cyclically loaded concrete elements in the modulus of elasticity. Only 60 per cent can be taken into account in design and this limit is in the safe margin since the values found are above this value.

4.1.4. Ultrasonic Pulse Velocity

After cyclic loading ultrasonic pulse velocity measurements were done on the concrete specimens. This was done for the purpose of observing the effects of cyclic loading on the porosity of concrete resulting from cracking due to loading. The cracks formed through cyclic loading should have been expected to increase the porosity of the concrete and cause a decrease in the ultrasonic pulse velocity. The measured values are given in Table 4.11. and Figure 4.17 and damage ratios are given in Figure 4.18.

Table 4.11. Ultrasonic pulse velocity of concrete after cyclic loading (m/sec)

Specimen No	**Control**	**0.6f_{max}**	**0.8f_{max}**	**0.9f_{max}**
1	4,700	4,730	4,540	4,450
2	4,650	4,690	4,610	4,260
3	4,760	4,680	4,600	4,140
4	4,720	4,620	4,340	4,470
Average	4,720	4,680	4,520	4,330
Standard Deviation	45.7	45.5	126	158

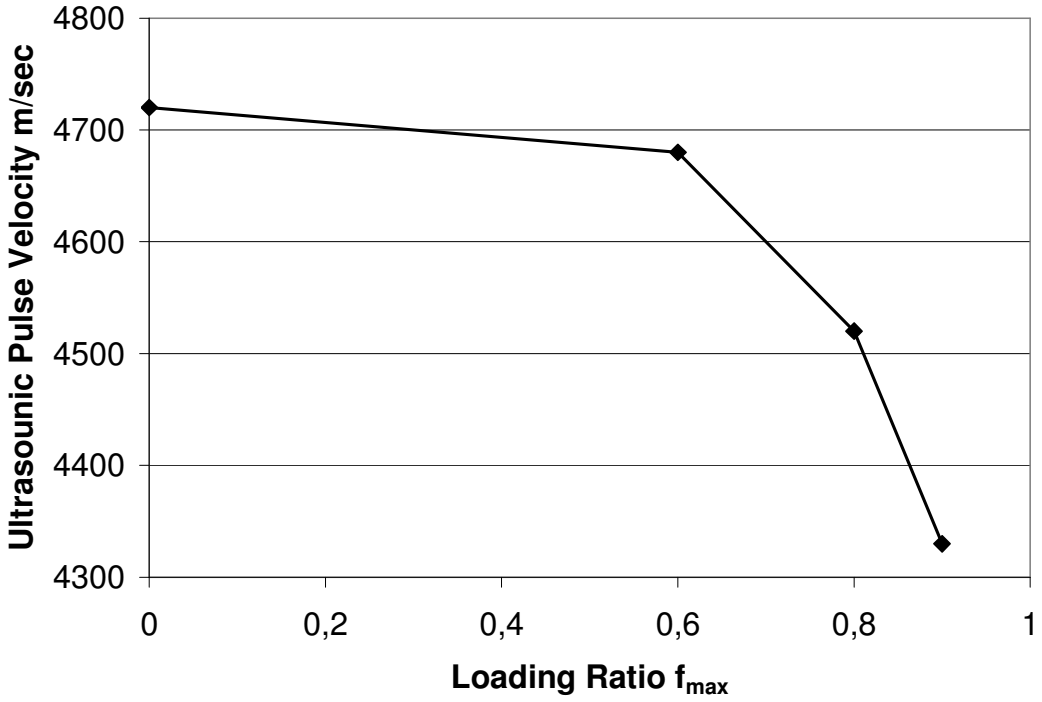

Figure 4.17. Variation of ultrasonic pulse velocity of concrete with loading ratio

Test results have shown that ultrasonic pulse velocities dropped with the increase of stress level in the cyclic loading. In 0.9f_{max} loading the ultrasonic pulse velocities dropped nearly 10 per cent compared with the control specimen. While almost no change has been observed up to 0.6f_{max} loading, a sharp decrease was reported after 0.6f_{max} to 0.9f_{max} loading of concrete. This may be due to growth of cracks in the cement paste after the latter level of stress.

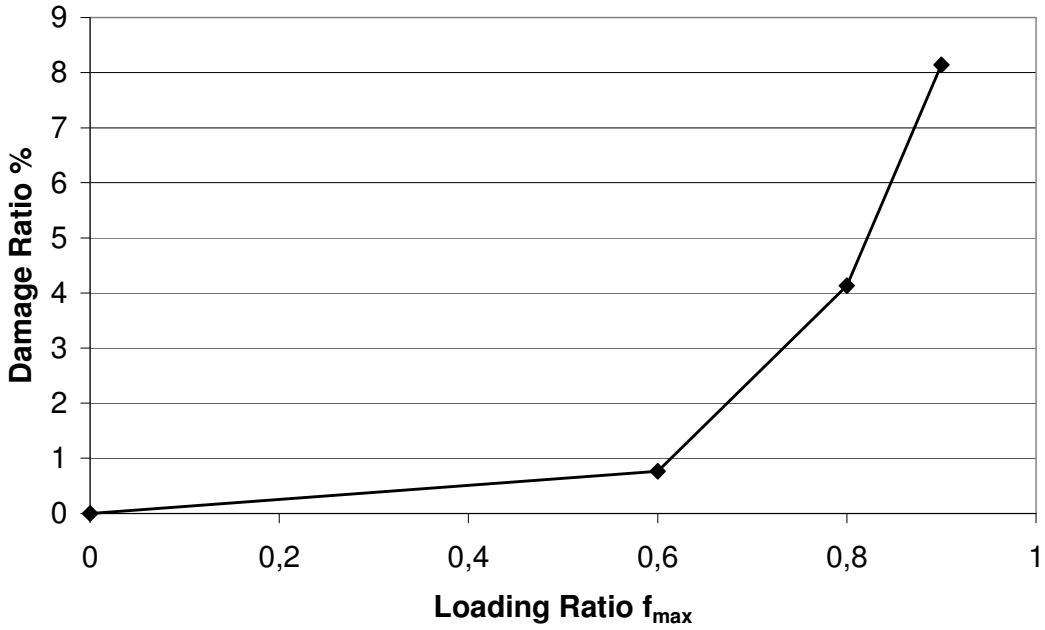

Figure 4.18. Variation of damage ratio for ultrasonic pulse velocity after cyclic loading

4.1.5. Total Mechanical Property Changes

When we review the effects of cyclic loading on the studied mechanical properties of concrete there is relation between modulus of elasticity and splitting tensile strength and compressive strength and ultrasonic pulse velocity test results as given in Figure 4.19. The stress strain properties of the damaged concrete specimen were illustrated in Figure 4.2-4.4. It can be seen that the modulus of elasticity values were much more affected than the compressive strength results from the cyclic loading. This is due to the the larger increase in strain compared to stress at $0.9f_{max}$ loaded specimens. Thus, decreases up to 50 per cent have been observed for the modulus of elasticity under cyclic loading.

These results show that under compression the cracks are parallel to the loading path since ultrasonic pulse velocity does not change in that direction. However the splitting tensile strength is affected more because the specimen can fail easily through the crack path that occurred during compressive loading.

The empirical formulas for tensile splitting strength and modulus of elasticity can not be applied to the concrete members that are subjected to cyclic loadings.

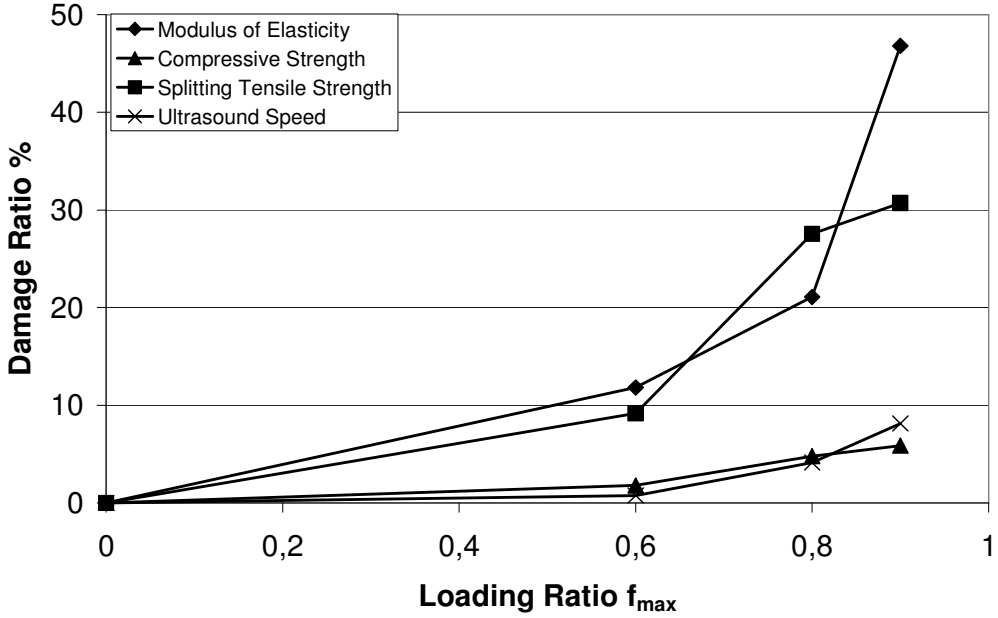

Figure 4.19. Damage ratio of mechanical properties of concrete after cyclic loading

4.2. Permeability Properties of Cyclically Loaded Specimens

Effects of cyclic loading on the permeability of concretes were investigated in this thesis through capillary water absorption and rapid chloride permeability tests. Because of close interaction between the permeability properties and porosity of concrete, mercury intrusion test was also conducted on the cyclically loaded concrete specimens to investigate the effects of cyclic loading on the porosity and pore structure of concrete. Additionally, effects of cyclic loading on durability of concrete against sulphate attack were also investigated.

4.2.1. Water Absorption and Sorptivity

Water absorption test was done according to the method given previously. Test results in terms of water absorbed in gr. by the concrete specimens through capillary suction are given in Table 4.12 , Table 4.13 and Figure 4.20 .

Table 4.12. Capillarity test results (gr)

Loading Ratio/Time minutes	1	4	9	16	25	36	49	60	120	720
Control	1.3	2.3	3.1	3.7	4.7	5.7	6.2	6.5	7.3	13.5
$0.6f_{max}$	2.0	2.8	4.0	4.8	5.3	5.8	6.8	6.8	8.3	13.8
$0.8f_{max}$	2.0	3.0	4.0	4.8	5.8	6.2	7.2	7.6	8.4	14.6
$0.9f_{max}$	2.8	4.5	6.0	7.2	8.2	9.2	10.2	10.8	13.0	20.7

Table 4.13. Sorptivity of specimens after cyclic loading($mm/min^{1/2}$)

Loading Ratio/k	Sorptivity
Control	0.055
$0.6f_{max}$	0.057
$0.8f_{max}$	0.059
$0.9f_{max}$	0.083

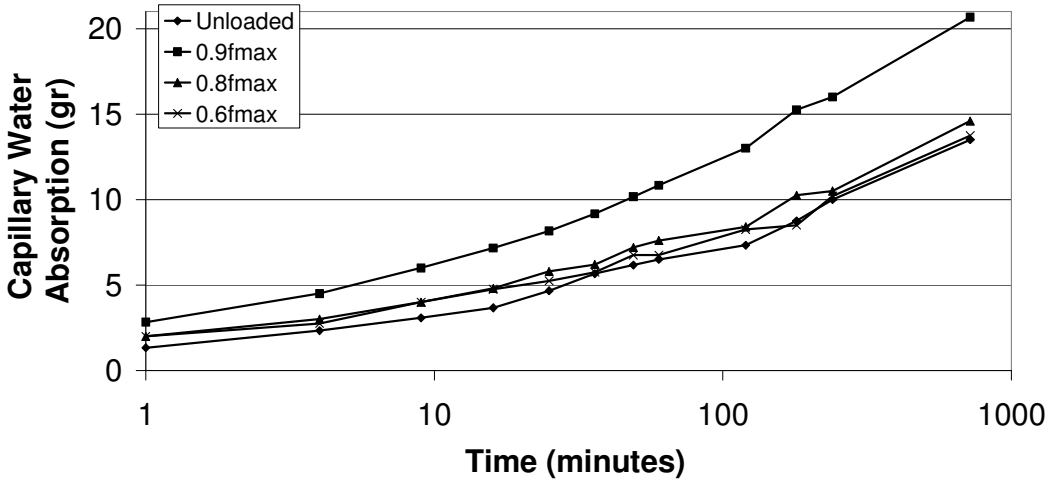

Figure 4.20. Capillary water absorption of concrete after cyclic loading

It was observed that cyclic loading had an effect on capillary test results. The damage in concrete resulted in higher water absorption values. $0.9f_{max}$ loaded specimens had 53 per cent more water absorption than control specimen. As the amplitude of cyclic loading increased the damage in the specimen increased and the absorption of water increased. The water absorption of the specimen after cyclic loading is given in Figure 4.20 and increase in water absorption compared with control specimen is given in Figure 4.21. The sorptivity

results for 0.6 w/c ratio concrete for 28 day water cure is found 0.46 x 10^{-3} cm/$s^{1/2}$ (0.036mm/$min^{1/2}$) are similiar with our results [60].

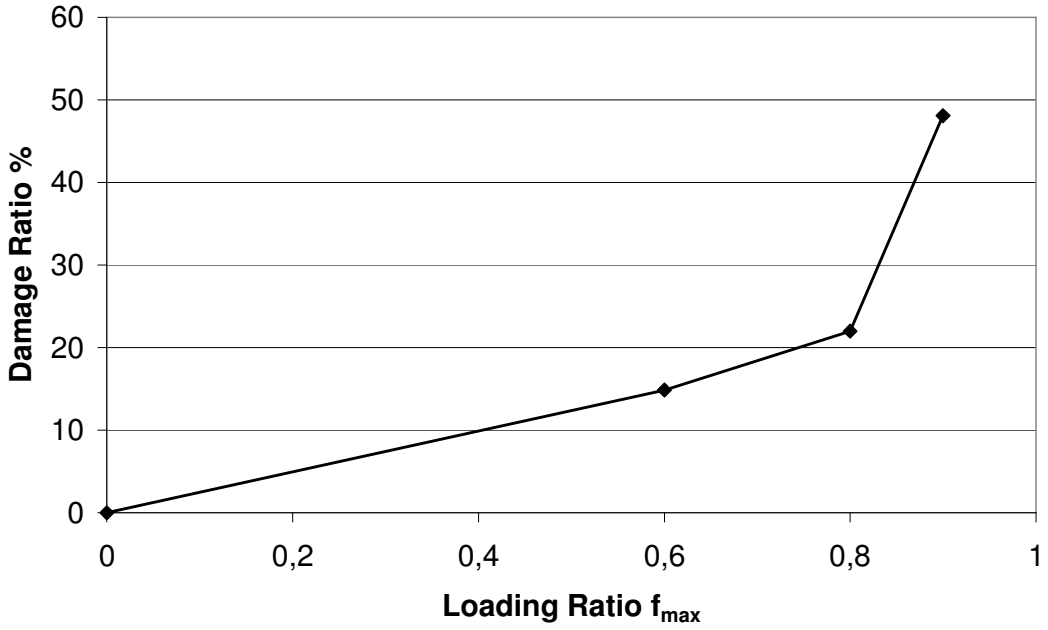

Figure 4.21. Damage ratio for water absorption after cycling loading

4.2.2. Rapid Chloride Permeability

Rapid chloride permeability tests were done according to ASTM C1202. The results are given in Table 4.14 and Figure 4.22 and damage ratio is given in Figure 4.23.

Table 4.14. Rapid Chloride Permeability test results (Coulombs)

	Control	**0.6f_{max}**	**0.8 f_{max}**	**0.9 f_{max}**
Specimen1	5,770	6,090	6,950	10,400
Specimen2	6,390	5,310	6,540	7,380
Specimen3	5,050	6,420	6,040	6,640
Specimen4	5,950	5,940	6,000	9,630
Specimen5	5,870		6,100	6,730
Specimen6	5,750			
Average	5,800	5,940	6,310	8,160
Standard Deviation	434	465	410	1740

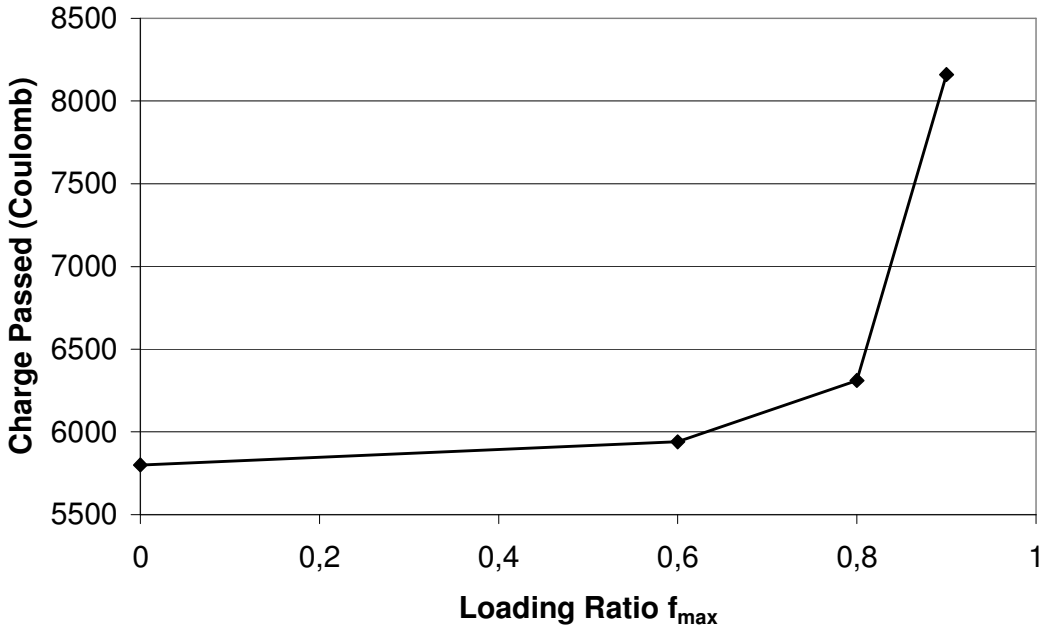

Figure 4.22. Rapid chloride permeability of concrete after cyclic loading

Test results have shown that the rapid chloride permeability of concrete subjected to cyclic loading were higher than the control concrete. It was also observed that the chloride permeability increased with the increase in the loading ratio. There were recorded 2.5, 8.5 and 41.0 percentages increase in chloride permeability, compared to control concrete , at $0.6f_{max}$, $0.8f_{max}$ and $0.9f_{max}$ loading ratios, respectively. As it was true for the other concrete properties, the great increase in the rapid chloride permeability was at $0.9f_{max}$ loading ratio. This showed that as the loading ratio in cyclic loading reached to the level of discontinuity limit of concrete the damage in the internal structure of concrete was greater which caused a distinguished increase in the porosity of the system.

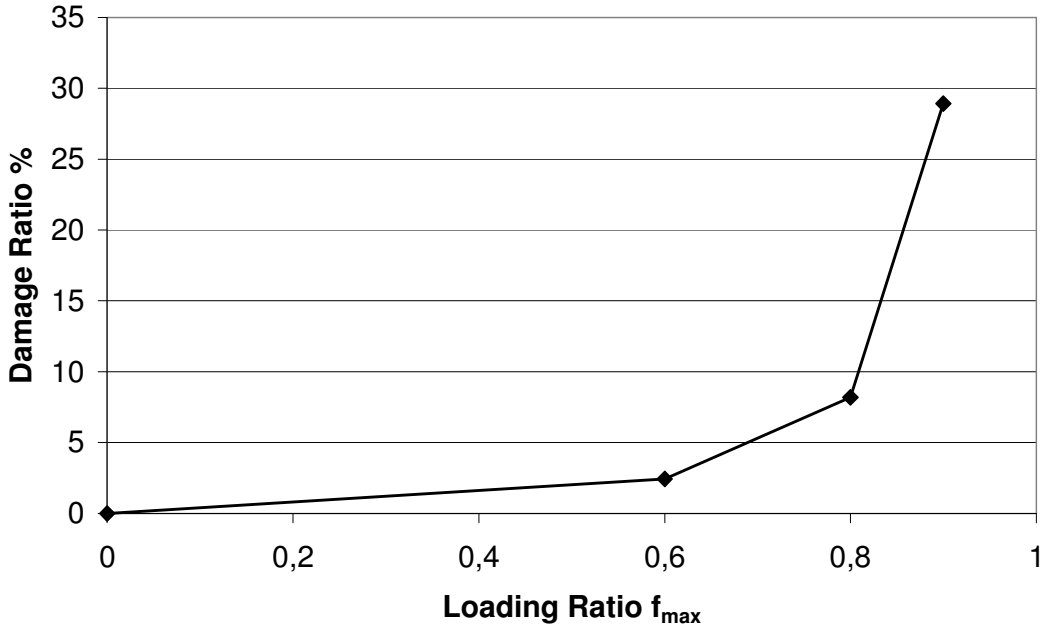

Figure 4.23. Damage ratio for rapid chloride permeability after cycling loading

4.2.3. Mercury Intrusion Porosity

Portland cement-based material is a porous construction material. This porous mechanism causes capillary porosity and connectivity of these capillary pores is an important characteristic of pore system related to the diffusivity of concrete. The critical pore diameter represents the grouping of the largest fraction of interconnected pores influencing the transport properties so the critical pore diameter can be used to assess the connectivity of cement-based materials. The critical pore diameter (dc) is defined as the inflection point on the intrusion pore volume (V) versus diameter (d) curve, or the maximum of the V versus log d curve.

Effect of cyclic loading on the pore structure of concrete was investigated by the mercury intrusion porosity measurements. Test results were expressed in terms of pore diameter and total volume of pores as illustrated in Figure 4.24, 4.25, 4.26 and Table 4.15. Damage ratios are given in Figure 4.27.

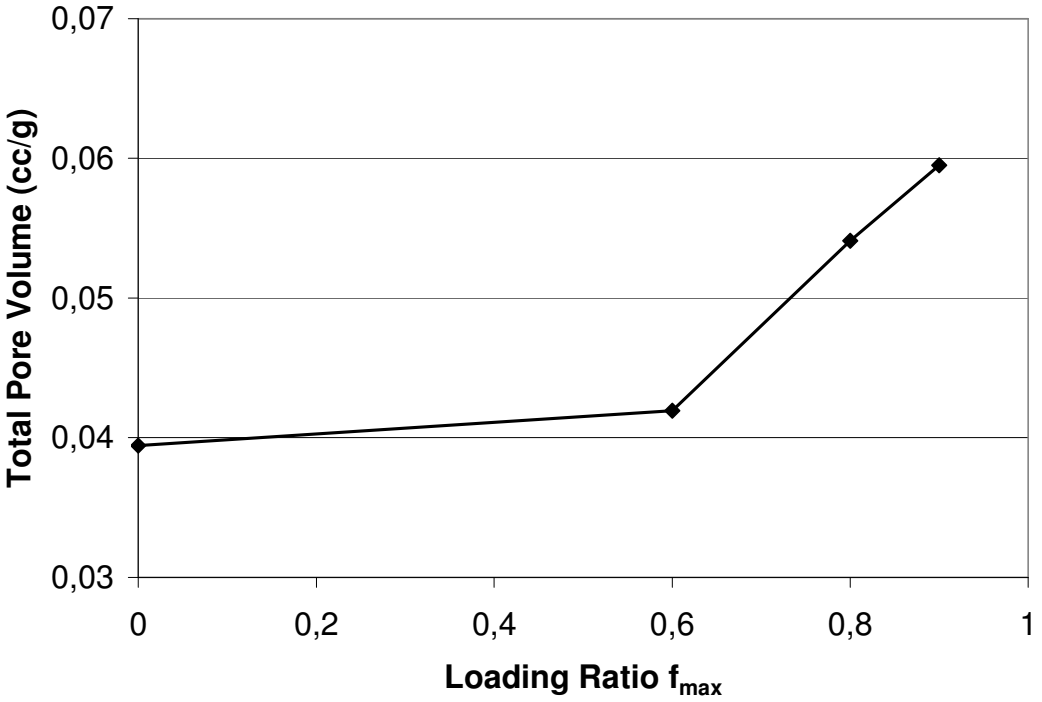

Figure 4.24. Total pore volume of concrete after cycling loading

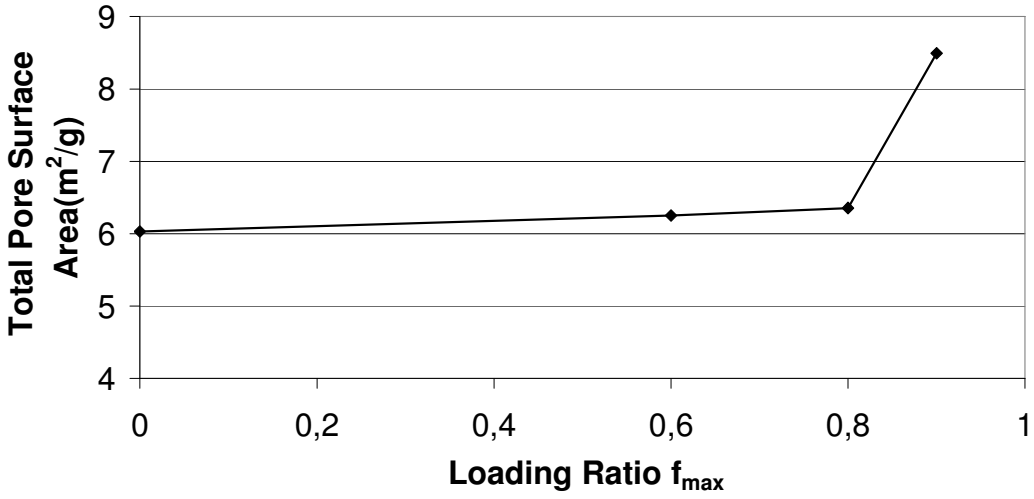

Figure 4.25. Pore surface area of concrete after cycling loading

Table 4.15. Mercury intrusion test – Pore volume and surface area of pores

	Volume(cc/g)	Surface Area(m^2/g)	Critical Pore Diameter(nm)
0.9f_{max}	0.059	8.49	38
0.8 f_{max}	0.054	6.35	55
0.6 f_{max}	0.042	6.25	65
Control	0.039	6.03	69

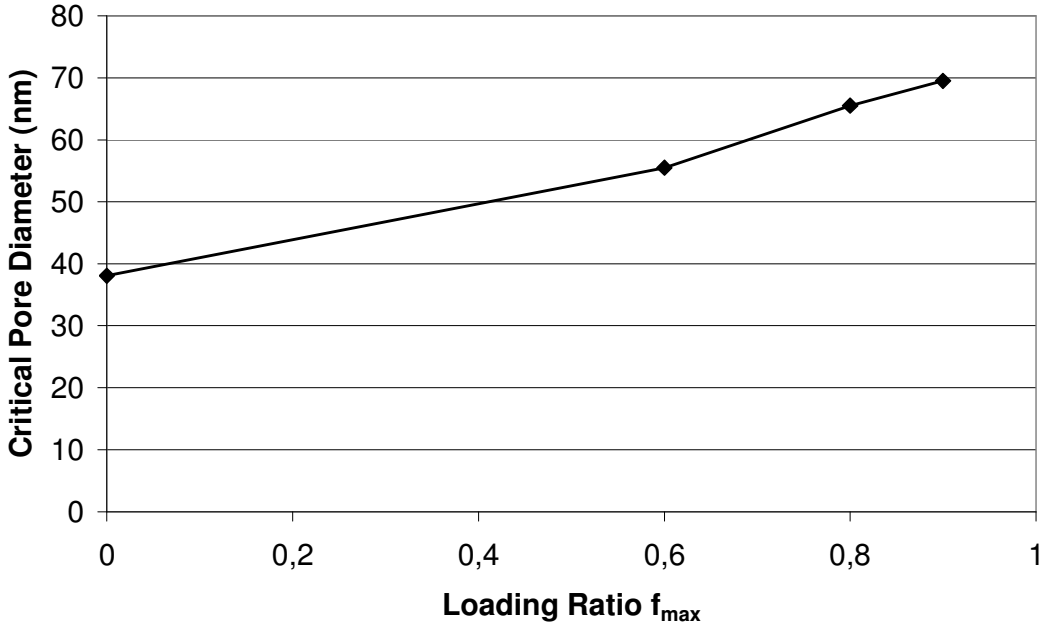

Figure 4.26. Mercury intrusion tests critical pore diameter versus loading ratio

With cyclic loading surface area and diameter of pores increased. The cyclic loading caused damage in the specimen as cracks in the cement paste and/or within the transition zone and the surface area of the pores and pore diameters as measured by mercury intrusion test. The volume of pores in 0.9f_{max} loaded specimen was twice of the Control specimen. Total area was also 50 per cent increased for the 0.9f_{max} loaded specimen compared to the control specimen.

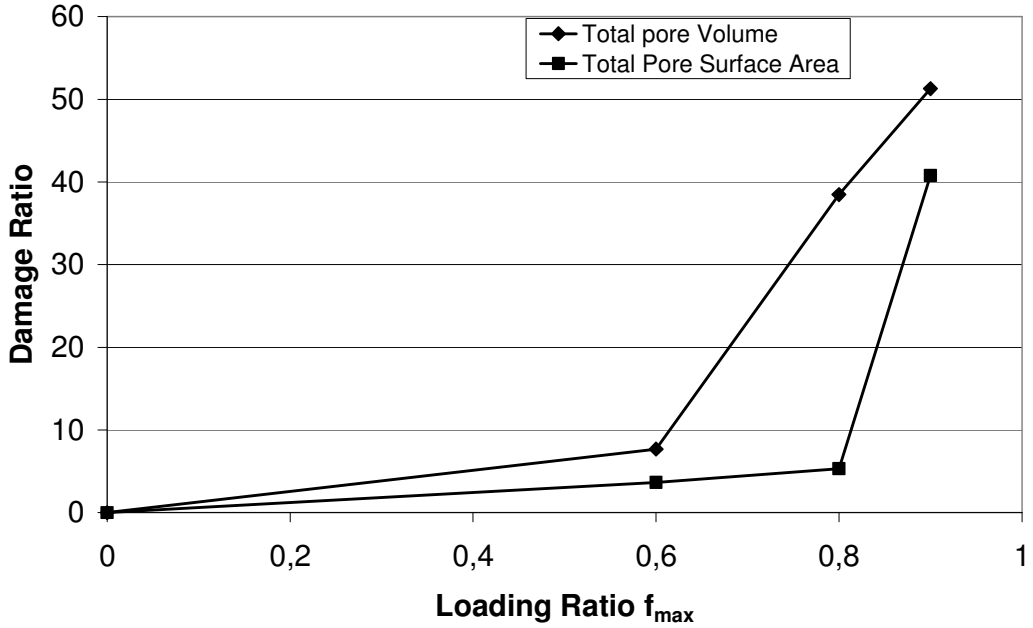

Figure 4.27. Damage ratio for mercury intrusion after cycling loading

4.2.4. Sulphate Resistance

Concrete in sulphate environment may be deteriorated due to the chemical reaction. The sulphate attack to the concrete is mainly related to the permeation of sulphate ions into concrete through the pores. Thus, it was also aimed to investigate the effect of cyclic loading on concrete's porosity, in relation to the deterioration of concrete due to sulphate attack. Weight of the control and cyclically loaded concrete specimens kept in sulphate solution were continuously measured through a sufficiently long duration of time as shown in Figure 4.28.

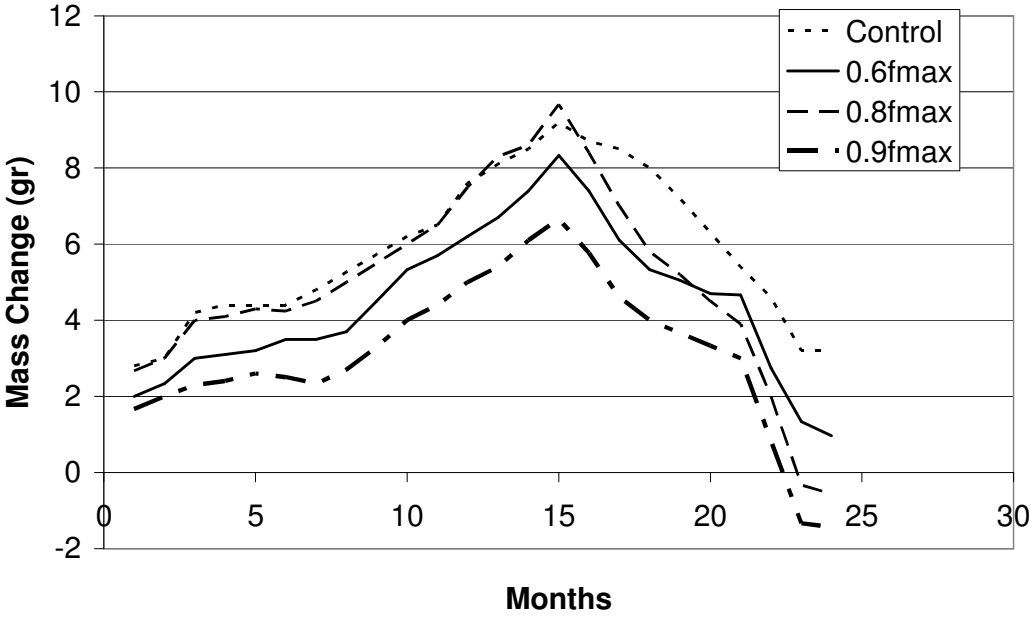

Figure 4.28. Mass changes due to sulphate attack

All specimens gained weight after the initiation of the test for a period about 15 months after which all concrete specimens started to loose weight till the end of approximately 24 months when the test has been terminated. Trend for gain and loss of weight were almost parallel for all specimens. Initial gain in weight of the specimens is attributable to the absorption of the specimens till saturation and then filling up of the pores by the expansive reaction products, then by densifying the hardened concrete and increasing its weight. Subsequently, the disruption of the cement paste by the expansive reaction products resulted in a decrease in the weight of the specimens, thus increasing the weight loss with the immersion period.

The mass losses in $0.9f_{max}$ loaded specimen were the highest which was followed by the $0.8f_{max}$ and $0.6f_{max}$ loaded specimens where as the control specimens had the lowest mass loss. So with the increase in amplitude of cyclic loading the mass loss was also increased. The reason for this was the larger number and size of cracks which were formed in the concrete with the increase in the stress level to which the concrete specimen was cyclically subjected.

4.3. Mechanical Properties of Self Healed Specimens

After cyclic loading some of the specimens were kept in water for curing and some in laboratory environment for 28 days to investigate the self healing properties of concrete. This was done to investigate the effect of water curing on healing of the micro cracks formed in the aggregate-cement paste interface and/or in the cement paste after low cycle fatigue loading of concrete specimens. Then these specimens were tested for compressive strength, modulus of elasticity and splitting tensile strength.

4.3.1. Compressive Strength

Compressive strengths of specimens, which were additionally either water or laboratory cured after being cyclically loaded at different levels of stress were measured. The individual results and the average of the measured compressive strengths are given in Table 4.16. Figure 4.29 shows the variation of compressive strength with loading ratio.

Table 4.16. Compressive strength of cyclically loaded concrete after additional curing

After Water Cure	**Control**	**$0.6f_{max}$**	**$0.8f_{max}$**	**$0.9f_{max}$**
Specimen 1	41.0	39.3	39.4	36.9
Specimen 2	39.8	38.6	38.6	37.6
Specimen 3	43.7	41.3	38.3	38.2
Specimen 4	41.5	39.7	38.7	37.5
Average	41.5	39.7	38.7	37.6
Standard Deviation	1.63	1.14	0.47	0.53
After Laboratory Cure	**Control**	**$0.6f_{max}$**	**$0.8f_{max}$**	**$0.9f_{max}$**
Specimen 1	40.6	36.3	36.2	33.5
Specimen 2	38.1	38.3	36.2	36.4
Specimen 3	38.3	38.2	37.3	35.9
Specimen 4	39.2	37.5	36.5	35.3
Average	39.1	37.6	36.5	35.3
Standard Deviation	1.14	0.92	0.53	1.27

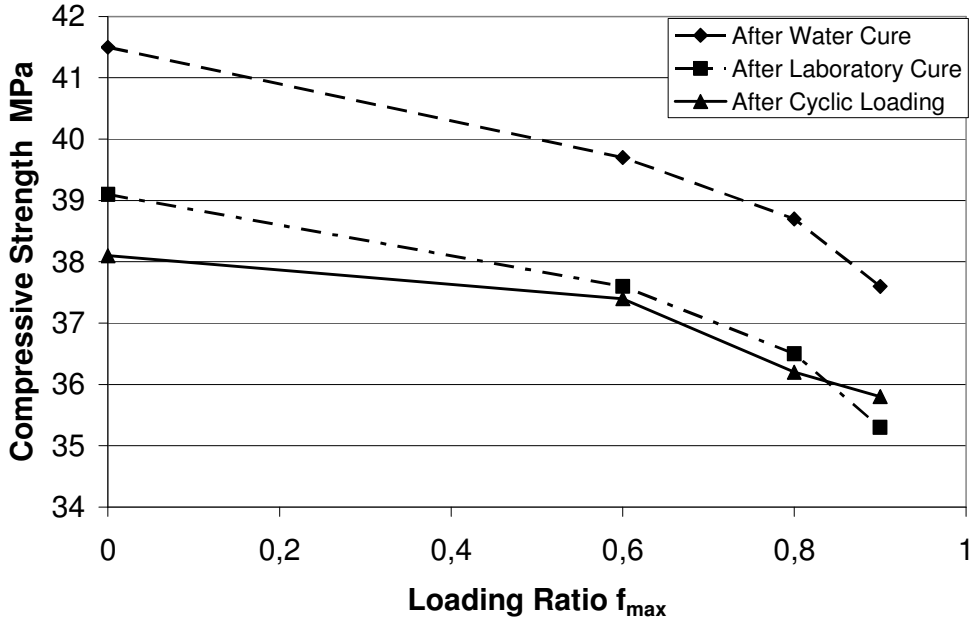

Figure 4.29. Effect of curing on the compressive strength of cyclically loaded specimens

The average compressive strengths of concrete specimens, water cured and laboratory cured after cyclic loading, were 41.5 MPa, 39.7 MPa, 38.7 MPa, 37,6 MPa and 39.1 MPa, 37.6 MPa, 36.5 MPa, 35.3 MPa for the control, $0.6f_{max}$, $0.8f_{max}$, $0.9f_{max}$ loaded specimens, respectively. Concretes, water cured after cyclic loading, had higher compressive strengths than laboratory cured specimens which had slightly higher compressive strengths compared to compression test results conducted just after cyclic loading of concrete specimens. Compressive strength of concretes for all cases decreased with increasing loading ratio.

Beneficial effect of water curing for self healing of cracks formed during cyclic loading through further hydration of still unhydrated cement particles in the cement paste were clearly observed. There was an improvement of about 5 per cent in the compression strength of water cured $0.9f_{max}$ cyclically loaded specimens where as the increase for the control specimens reached to 9 per cent. Air curing, however, showed almost no improvement in the compressive strength of cyclically loaded specimens although approximately 3 per cent increase in strength was observed with respect to control specimens due to further hydration of cement. Gain ratios of concrete specimens, water and air cured after cyclic loading, for different loading ratios are given in Figure 4.30.

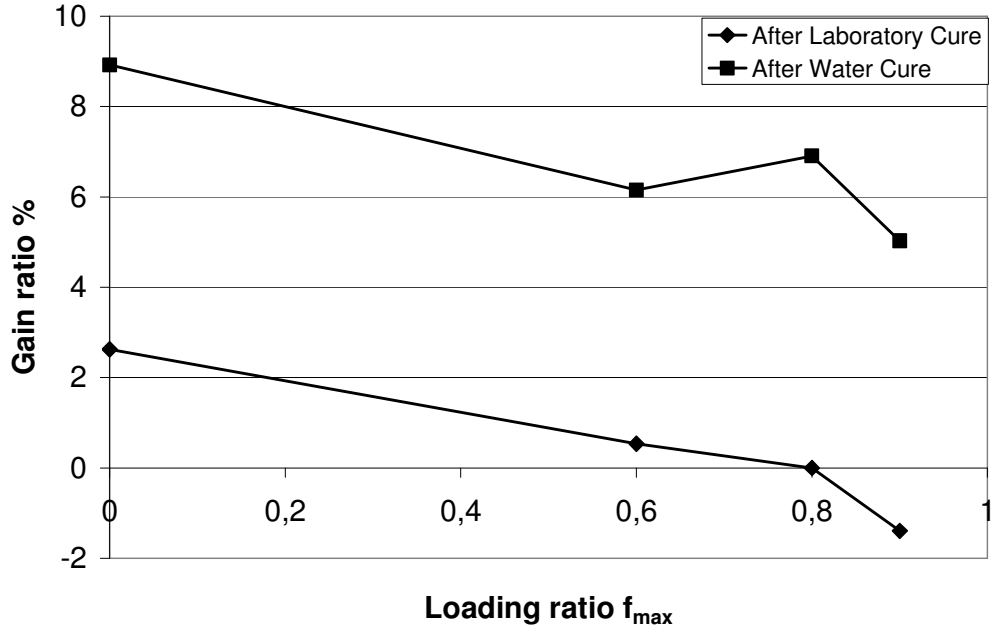

Figure 4.30. Gain ratios for compressive strength for specimens water cured and laboratory cured after cyclic loading

5.3.2. Modulus of Elasticity

The modulus of elasticity of the cyclically loaded specimens after water and laboratory curing conditions are given in Table 4.17. Modulus of elasticity measured from static compressive loading of concrete specimens subjected to laboratory curing after cyclic loading were 37.2 GPa, 37.9 GPa, 33.9 GPa, and 29.6 GPa control, $0.6f_{max}$, $0.8f_{max}$ and $0.9f_{max}$ loaded concretes respectively. On the other hand, the values for water cured specimens were 42.1 GPa, 41.5 GPa, 34.5 GPa and 33.3GPa for the control, $0.6f_{max}$, $0.8f_{max}$ and $0.9f_{max}$ loaded concretes, respectively. The variation of modulus of elasticity with curing conditions and loading ratio is given graphically in Figure 4.31.

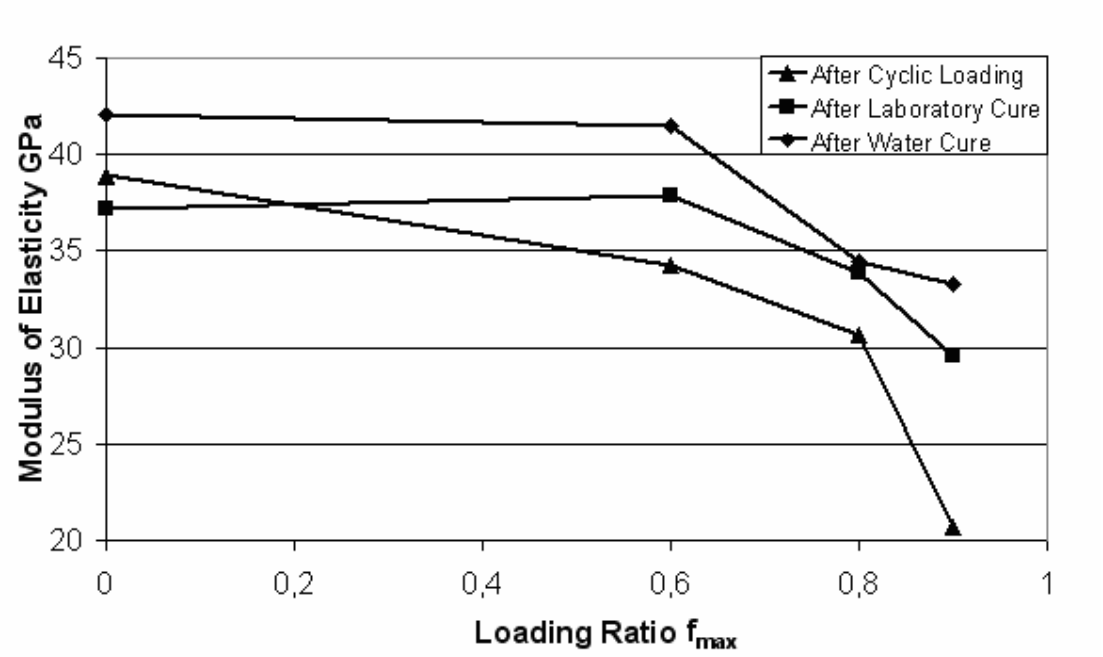

Figure 4.31. Effect of curing on the modulus of elasticity of cyclic loading

Modulus of elasticity of cyclically loaded specimens recovered with 28 days curing in both water and air after cyclic loading. However, water curing was more effective in healing of the cracks enhancing the modulus of elasticity. The increase varied from 8 per cent for the control to 60 per cent for the $0.9f_{max}$ loaded specimens after water curing of cyclically loaded specimens. The improvement for the air cured concrete specimens reached at most to 44 per cent for the $0.9f_{max}$ loaded specimens. Gain ratios of concrete specimens, water and air cured after cycling loading, for different loading ratios are given in Figure 4.32.

Table 4.17. Modulus of elasticity comparisons at different curing conditions(GPa)

Loading Ratio	**After Cyclic Loading**	**After Laboratory Cure**	**After Water Cure**
Control	38.9	37.2	42.1
$0.6f_{max}$	34.3	37.9	41.5
$0.8\ f_{max}$	30.7	33.9	34.5
$0.9\ f_{max}$	20.7	29.6	33.3

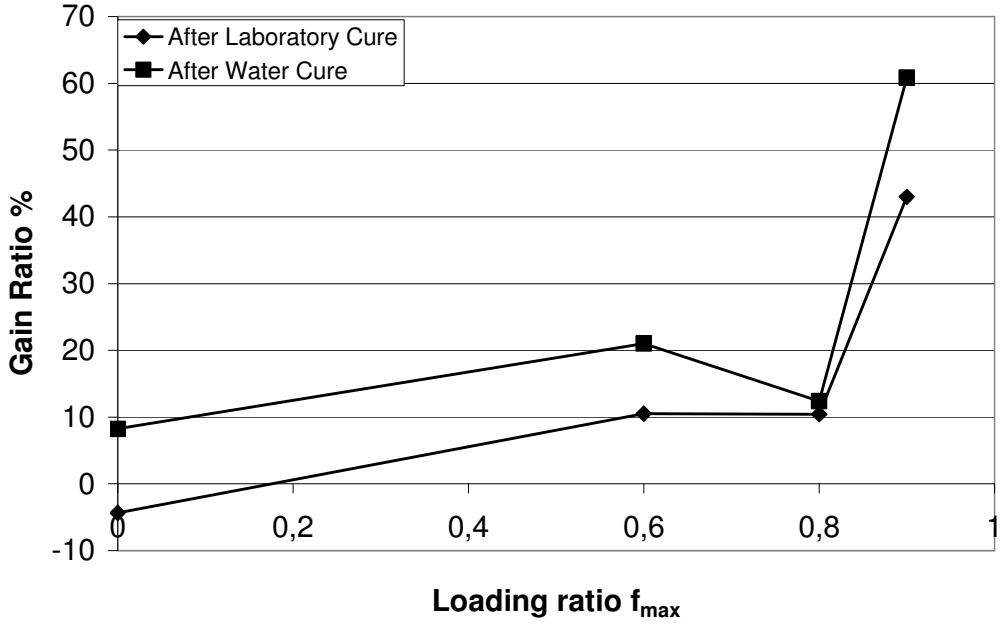

Figure 4.32. Gain ratio for modulus of elasticity specimens water cured and laboratory cured after cyclic loading

5.3.3. Splitting Tensile Strength

The splitting tensile test results of the cyclically loaded specimens after water and laboratory curing are presented in Table 4.18. The results showed that additional curing after low cycle loading of concrete specimens did not cause a considerable improvement on the splitting tensile strength of the concrete. It was also observed that the splitting tensile strength was lower for laboratory cured specimens compared to the water cured specimens. The splitting tensile strength for water cured specimens at $0.9f_{max}$ load ratio were 23 per cent higher than the laboratory cured specimen. Only slight increases for $0.6f_{max}$ and $0.8f_{max}$ stress levels could be observed for the water cured specimens. Thus, it may be concluded that self healing through additional curing of cyclically loaded specimens did not have a significant effect on tensile strength of concrete as observed in Figure 4.33. In Figure 4.34 the comparison of gain ratios with the laboratory cured and with water cured specimens given.

Table 4.18. Splitting tensile stress after water cure (MPa)

Specimen	**Control**	**0.6f_{max}**	**0.8f_{max}**	**0.9f_{max}**
1	4.01	3.54	3.25	2.17
2	3.60	3.73	2.54	1.82
3	3.85	3.31	3.08	2.33
Average	3.82	3.53	2.96	2.11
Standard Deviation	0.21	0.21	0.37	0.26

Table 4.19. Splitting tensile stress after laboratory cure (MPa)

Specimen	**Control**	**0.6f_{max}**	**0.8f_{max}**	**0.9f_{max}**
1	3.25	2.67	2.38	2.44
2	3.95	3.12	2.71	1.63
3	3.66	2.56	2.37	1.11
Average	3.60	2.77	2.48	1.72
Standard Deviation	0.35	0.3	0.19	0.67

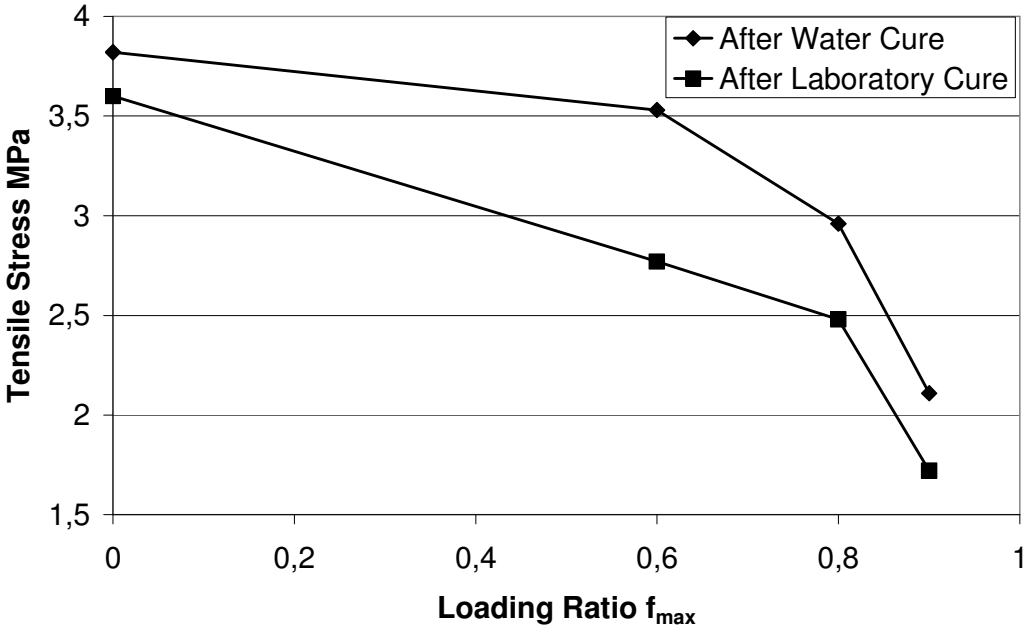

Figure 4.33. Splitting tensile strength of cyclically loaded specimens after curing

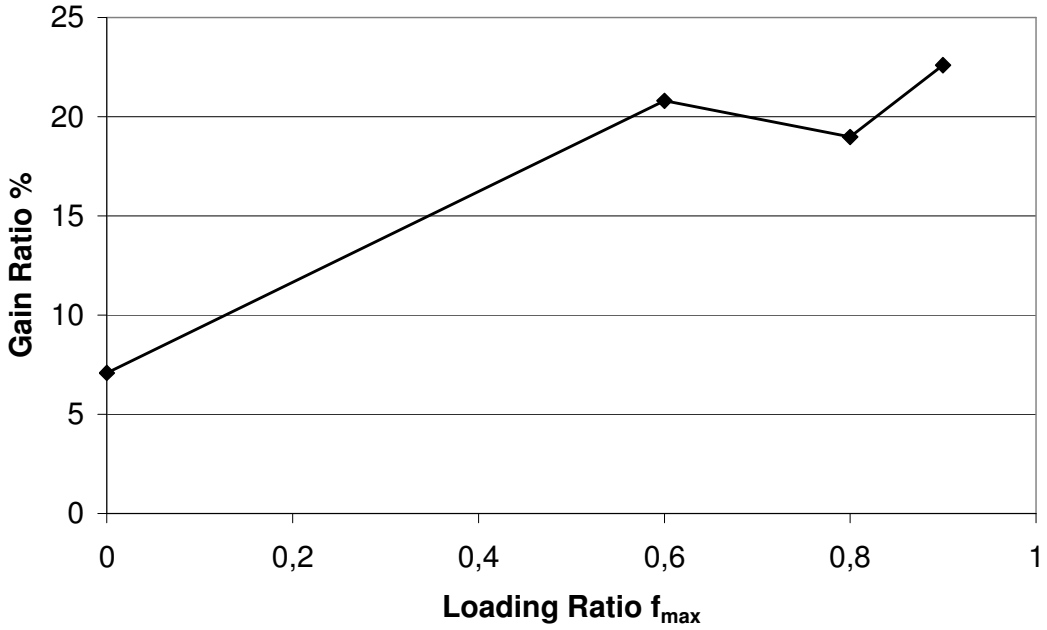

Figure 4.34. Gain ratio of splitting tensile strength water cured to laboratory cured specimens

4.3.4. Ultrasonic Pulse Velocity

After cyclic loading of the specimens, some of them were subjected to additional water and air curing after which ultrasonic pulse velocity measurements were done on these concrete specimens. Thus, the effects of self healing of cracks on the porosity of concrete were observed through ultrasonic pulse velocity measurements. The cracks formed through cyclic loading was expected to increase the porosity of the concrete and cause a decrease in the ultrasonic pulse velocity The measured values are given in Table 4.20, 4.21, 4.22 and Figure 4.35, 4.36.

Table 4.20. Ultrasonic pulse velocity test results (m/sec)

Loading Ratio	After Cyclic	After Water Cure	After Lab Cure
Control	4,720	4,920	4,810
0.6 f_{max}	4,630	4,850	4,740
0.8 f_{max}	4,530	4,780	4,690
0.9 f_{max}	4,390	4,760	4,670

Table 4.21. The change in ultrasonic pulse velocity after cyclic loading (m/sec)

Loading Ratio	After Cyclic Loading	Before Cyclic Loading
0.6	4,700	4,830
0.6	4,690	4,900
0.6	4,710	4,820
0.6	4,640	4,740
0.6	4,510	4,880
0.6	4,530	4,710
Average	4,630	4,810
0.8	4,630	4,820
0.8	4,590	4,600
0.8	4,640	4,840
0.8	4,560	4,770
0.8	4,610	4,760
0.8	4,160	4,690
Average	4,530	4,750
0.9	4,310	4,600
0.9	4,420	4,780
0.9	4,320	4,810
0.9	4,460	4,810
0.9	4,290	4,620
0.9	4,520	4,640
Average	4,390	4,710
Control	4,870	4,840
Control	4,670	4,720
Control	4,650	4,650
Control	4,690	4,720
Control	4,740	4,770
Average	4720	4,740

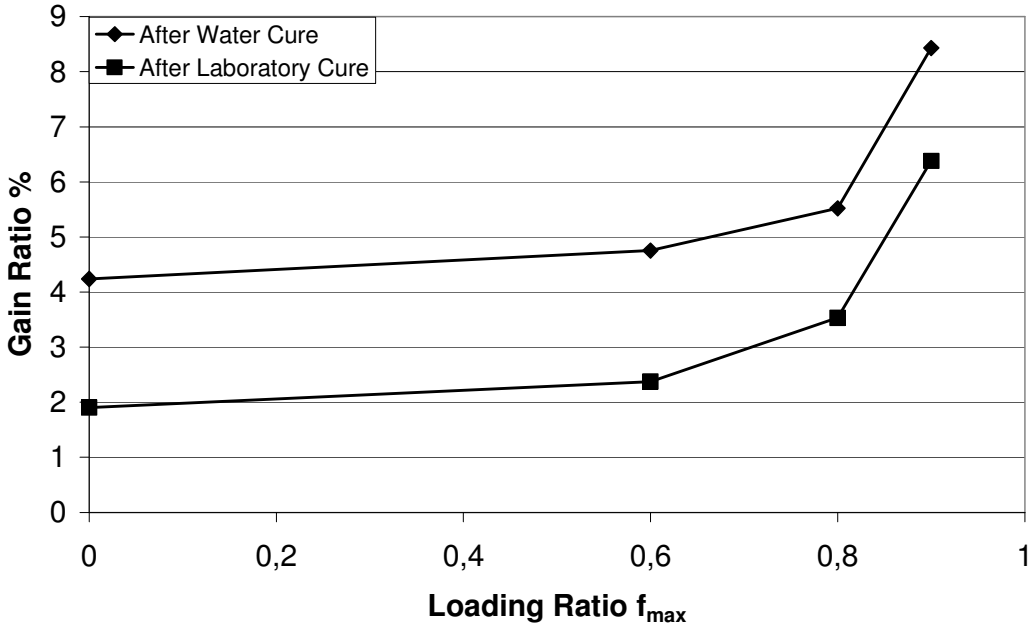

Figure 4.35. Gain ratio for ultrasonic pulse velocity of specimens water cured and laboratory cured after cyclic loading

Table 4.22. The change in ultrasonic pulse velocity after curing(m/sec)

Loading Ratio	After Water	Loading Ratio	After Laboratory Cure
Control	4,920	**Control**	4,819
Control	4,840	**Control**	4,808
Control	5,000		
Standard Deviation	80		8
0.6	4,890	**0.6**	4,762
0.6	4,900	**0.6**	4,762
0.6	4,770	**0.8**	4,695
Standard Deviation	72		37
0.8	4,810	**0.8**	4,662
0.8	4,790	**0.8**	4,739
0.8	4,730	**0.8**	4,673
Standard Deviation	42		42
0.9	4,840	**0.9**	4,556
0.9	4,880	**0.9**	4,785
0.9	4,550	**0,9**	4,464
Standard Deviation	180		162

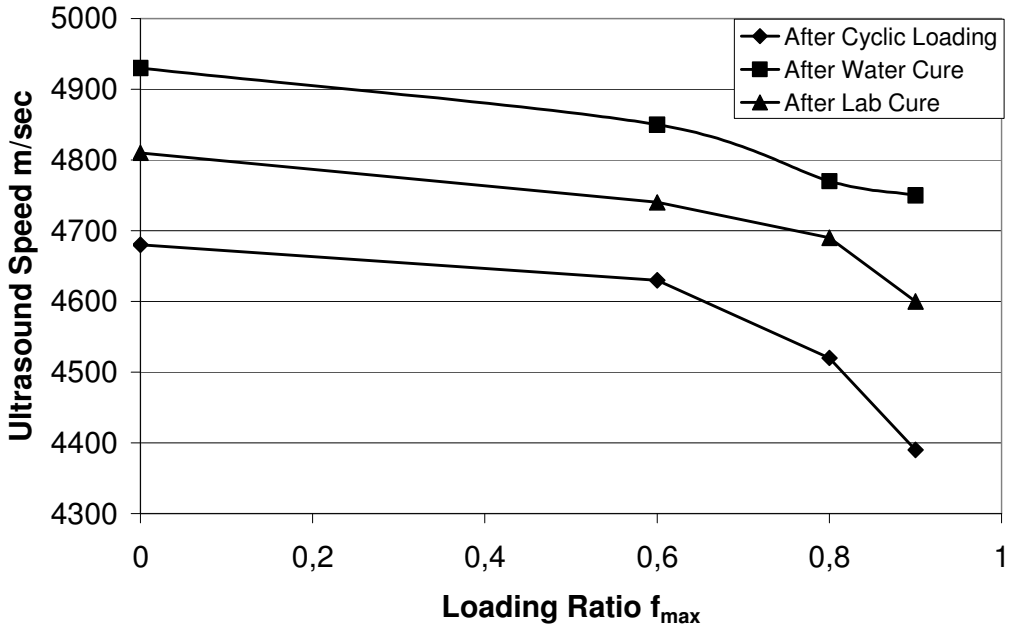

Figure 4.36. The change in ultrasonic pulse velocity after cyclic loading ratio and cure effect

After water curing, the concrete specimens had higher ultrasonic pulse velocities. Ultrasonic pulse velocity measured on $0.9f_{max}$ loaded specimen's increased from 4390 to 4750 m/sec with water cure. But even after laboratory cure ultrasonic pulse velocities increased compared with results that had been obtained after cyclic loading.

4.3.5. Mechanical Properties After Self Healing

The damaged specimens and the specimens kept in air, have the same mechanical behavior, which is the typical reloading after cracking. On the contrary, there is a difference with the mechanical behavior for the specimens stored in water. This result confirms that water is needed for the self-healing phenomenon.

Evaluating the beneficial effects of self healing on the mechanical properties of concrete has shown that compressive strength of first cyclic loaded and then water cured specimens exceeded the value of 28 day strength of undamaged concrete specimens in all cases. Also the ultrasonic pulse velocity test results for $0.9f_{max}$ loaded specimens were as high as those of the undamaged concrete specimens . Modulus of elasticity of the

specimens also increased with water curing compared with the laboratory cure. But this was not the case for the tensile strength; they showed only a few percent improvement and did not get over the value of the undamaged specimens with 28 days age.

4.4. Permeability Properties of Self Healed Specimens

Effects of cyclic loading and self healing of cracks formed during cyclic loading of concrete after different curing conditions on the permeability of concretes were also investigated in this study. For this purpose capillary water absorption and rapid chloride permeability tests were conducted on cyclically loaded concrete specimens where were additionally water and air cured for 28 days.

4.4.1. Water Absorption and Sorptivity

Capillary water absorption test was done after different curing conditions being applied to the cyclically loaded concrete specimens. It was observed that there were effects additional air and water curing on the capillarity test results of the cyclically loaded specimens. The water absorption and sorptivity of the specimens after cyclic loading and at different curing conditions are given in Table 4.23 4.24, 4.25, 4.26 and Figure 4.37, 4.38.

Table 4.23. Capillary water absorption of specimens after water curing (gr)

Loading Ratio/Time (min)	**1**	**4**	**9**	**16**	**25**	**36**	**49**	**60**	**120**	**720**
Control	1.3	2.0	2.5	3.8	4.0	5.0	5.0	6.3	7.3	11.8
0.6 f_{max}	1.3	1.5	2.0	3.0	3.8	4.0	4.5	5.5	7.3	11.3
0.8 f_{max}	1.3	1.5	2.3	3.3	3.5	4.3	4.5	5.5	6.8	11.8
0.9 f_{max}	1.3	2.0	2.5	3.5	3.8	4.5	5.0	6.0	8.3	13.5

Table 4.24. Capillary water absorption of specimens after laboratory cure (gr)

Loading Ratio/Time (min)	**1**	**4**	**9**	**16**	**25**	**36**	**49**	**60**	**120**	**720**
Control	0.8	1.8	2.5	3.5	4.5	5.0	5.3	6.3	8.0	12.0
0.6 f_{max}	1.3	2.0	2.8	4.3	5.0	5.5	6.5	7.8	10.0	15.0
0.8 f_{max}	1.3	2.8	3.8	4.8	5.5	6.5	7.5	9.1	11.8	16.0
0.9 f_{max}	1.5	2.8	3.5	4.8	5.8	7.0	7.5	9.3	13.3	19.8

Table 4.25. Sorptivity of specimens after laboratory cure (mm/min$^{1/2}$)

Loading Ratio/k	**Sorptivity**
Control	0.053
0.6 f_{max}	0.067
0.8 f_{max}	0.071
0.9 f_{max}	0.091

Table 4.26. Sorptivity of specimens after water cure (mm/min$^{1/2}$)

Loading Ratio/k	**Sorptivity**
Control	0.05
0.6 f_{max}	0.051
0.8 f_{max}	0.052
0.9 f_{max}	0.06

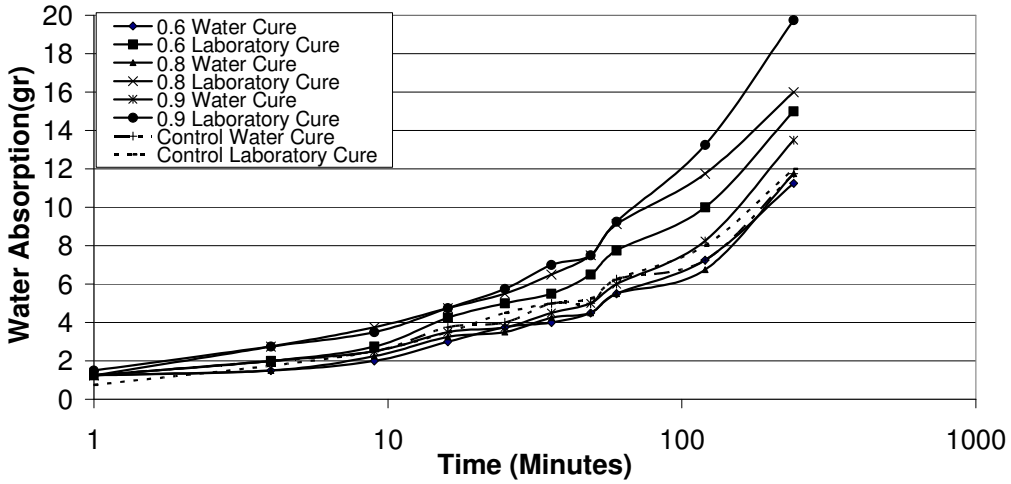

Figure 4.37. Capillary water absorption of concrete after cyclic loading and cure effect

With water curing water absorption of the specimens decreased. For 0.9f_{max} loaded specimen 27 per cent gain was observed in water absorption compared with specimen after cyclic Loading.The comparisons are given Table 4.25 and 4.26.

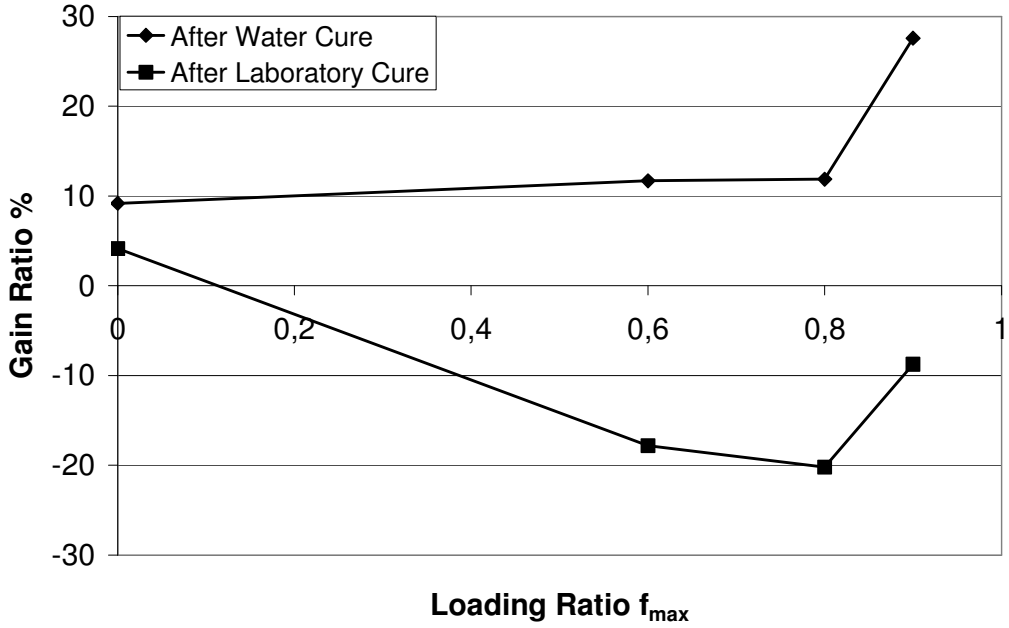

Figure 4.38. The Change water absorption after cyclic loading and curing effect

4.4.2. Rapid Chloride Permeability

Rapid chloride permeability tests on concrete specimens that were additionally cured after cyclic loading were also done according to ASTM C1202. The results are given in Figure 4.39 and Tables 4.27, 5.28 and 4.29.

Table 4.27. Rapid chloride permeability test results after water cure (coulombs)

	After Water Cure			
	Control	**0.6f_{max}**	**0.8f_{max}**	**0.9f_{max}**
Specimen1	4,860	5,420	5,510	6,530
Specimen2	5,300	5,340	5,940	5,510
Specimen3	5,380	4,850	5,830	6,380
Specimen4	5,000		5,940	5,800
Average	5,140	5,200	5,810	6,060
Standard Deviation	245	308	203	480

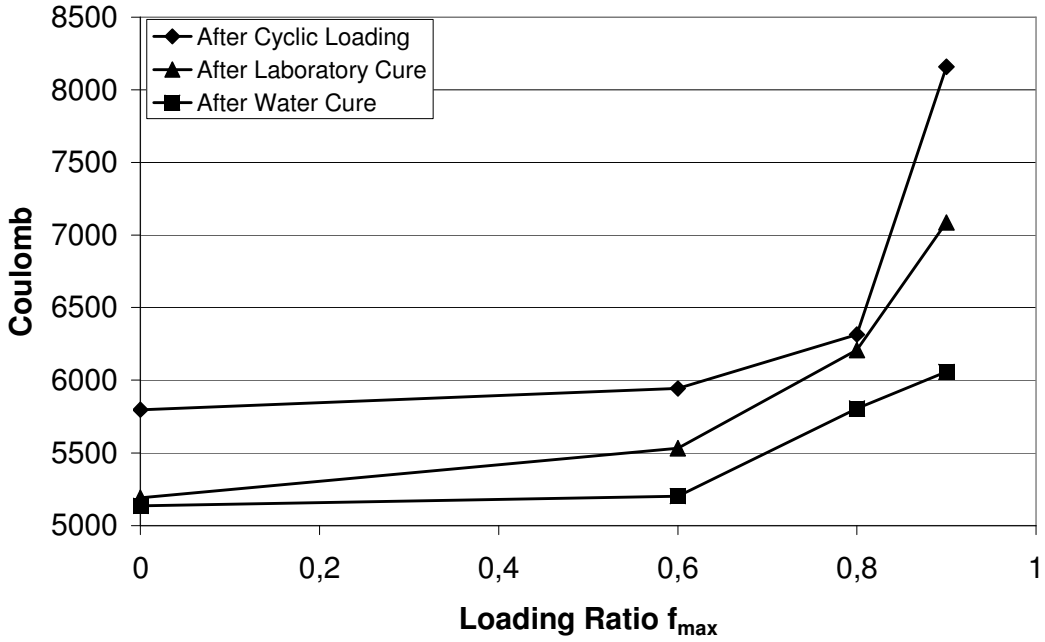

Figure 4.39. Rapid chloride permeability of concrete at different loading ratios after different cure conditions

Table 4.28. Rapid Chloride Permeability test results after laboratory cure (coulombs)

	After Laboratory Cure			
	Control	**0.6f_{max}**	**0.8f_{max}**	**0.9f_{max}**
Specimen1	5,016	5,309	5,905	7,095
Specimen2	5,376	6,086	6,750	7,101
Specimen3	4,884	5,202	5,970	7,066
Average	5,092	5,532	6,208	7,087
Standard Deviation	255	482	470	19

Table 4.29. Comparison of rapid chloride permeability of concretes (coulombs)

Coulombs	**Control**	**0.6f_{max}**	**0.8f_{max}**	**0.9f_{max}**
After Cyclic	5,798	5,943	6,315	8,158
After Lab Cure	5,192	5,532	6,208	7,087
After Water Cure	5,140	5,200	5,810	6,060

Test results have shown that the rapid chloride permeability of cyclically loaded concrete that were subjected to additional laboratory curing were higher than the water cured specimens. It was also observed that the chloride permeability increased with the increase in the loading ratio. There were recorded 5, 15 and 25 percentages increase in chloride permeability, compared to control concrete for laboratory cured specimen and 2, 7 and 27 percentages increase in chloride permeability, compared to control concrete for water cured specimen, at $0.6f_{max}$, $0.8f_{max}$ and $0.9f_{max}$ loading ratios, respectively. The results are given in Figure 4.40.

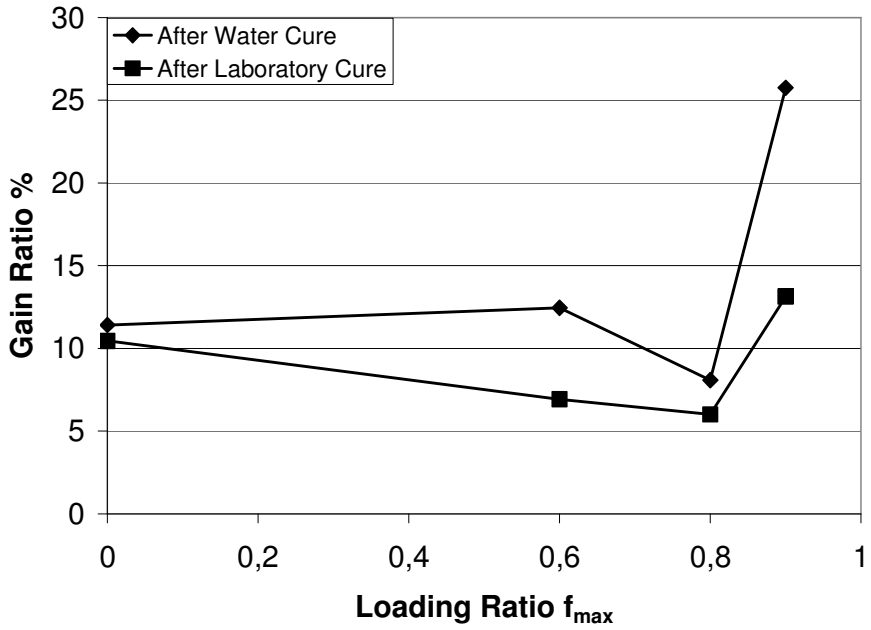

Figure 4.40. Rapid Chloride Permeability gain ratios at different loading ratios at laboratory cure

4.4.3. Sulphate Resistance

The effect of self healing of micro cracks formed after cyclic loading of concrete through additional water and air curing of the specimens was also investigated through by measuring the mass change of concrete specimens in sulphate solution. Mass changes in sulphate solution are given in Figure 4.41. Mass change of concrete specimens subjected to additional curing followed the same trends as the mass change of concrete specimens after cyclic loading.Specimens gained weight until 16 months after which losses in weight were measured due to destructive effect of expansive products formed through sulphate attack

into pores of concrete. The beneficial effect of water curing over air curing was observed comparing the mass loss data of the concrete specimens. It was also observed that highest mass losses were measured with $0.9f_{max}$ loaded specimen than $0.8f_{max}$ and $0.6f_{max}$ loaded specimens, indicating that self healing of cracks through additional curing was less effective for $0.9f_{max}$ loaded specimens.

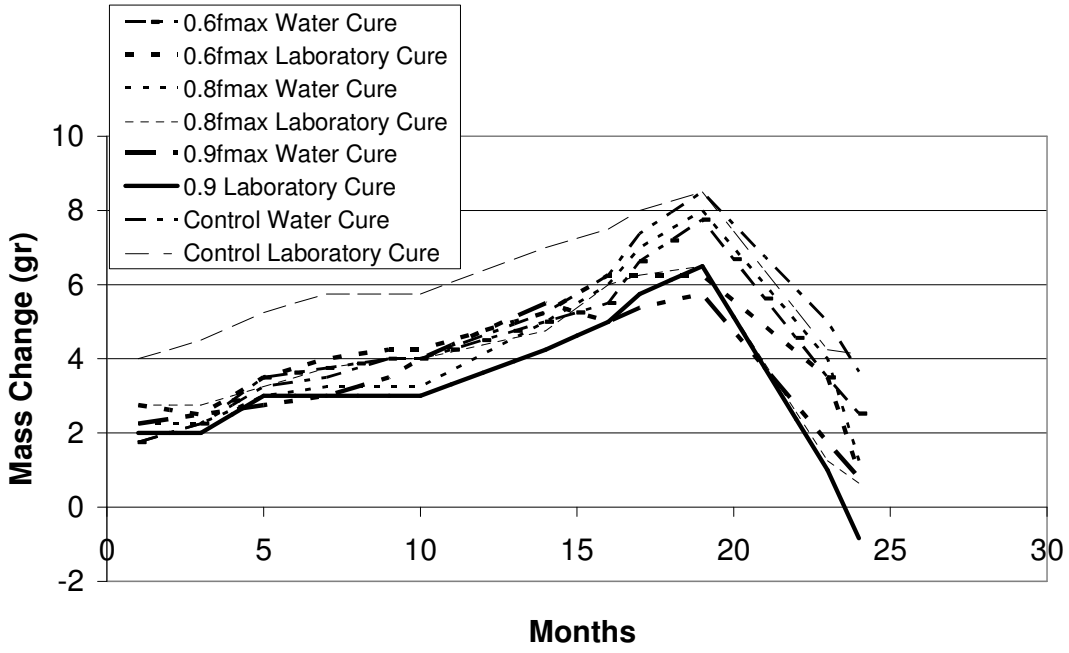

Figure 4.41. Mass change due to sulphate attack after different curing conditions

4.5. Microstructural Analyses

Microstructural analysis was done using electron microscope and optical microscope to investigate the cracks formed after cycling loading of concrete and the closing of these cracks through self healing after additional curing of concrete specimens.

4.5.1. Electron Scanning Microscopy Analysis

Electron scanning microscopy analysis was done to investigate the effect of additional curing on further hydration of cyclically loaded specimens to heal the cracks formed after cyclic loading of concrete specimens. The SEM photographs of control and $0.6f_{max}$, $0.8f_{max}$ and $0.9f_{max}$ loaded specimen after air and water curing are given in Table 4.30.

Table 4.30. Electron Scanning Microscopy analysis of different cured specimens

Loading Ratio	Laboratory Cured Specimen	Water Cured Specimen
Control	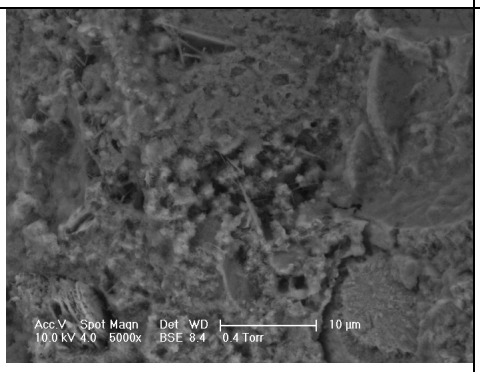	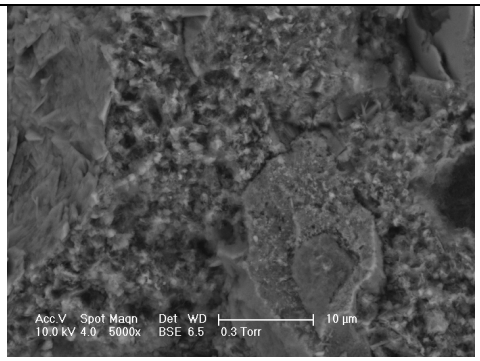
0.6 f_{max}	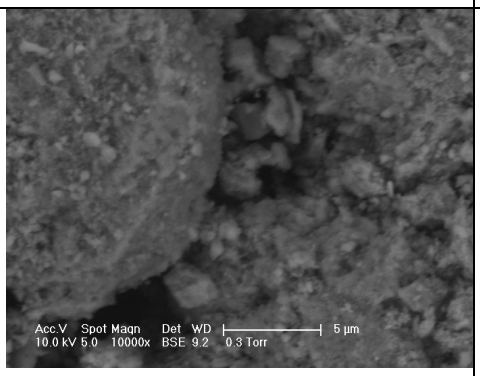	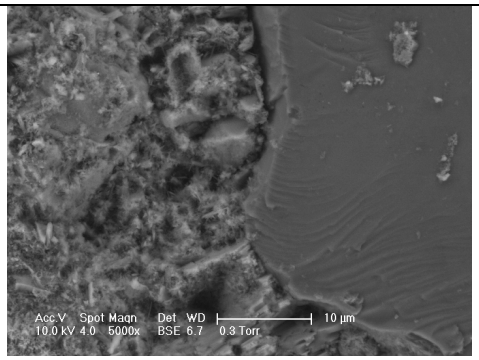
0.8 f_{max}	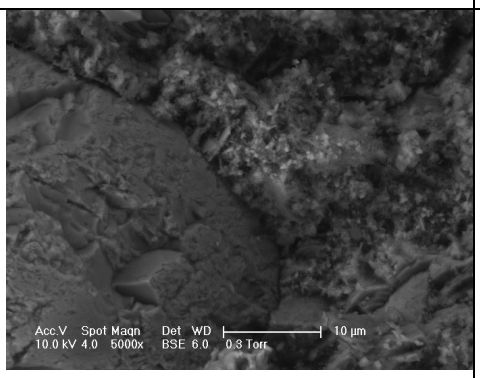	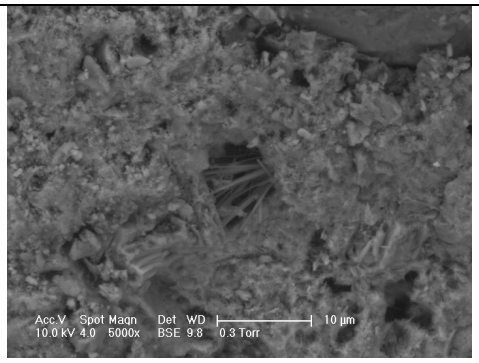
0.9 f_{max}	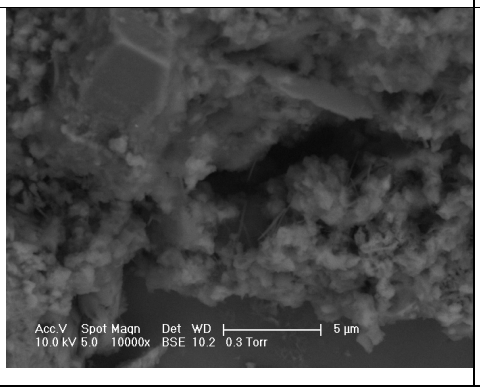	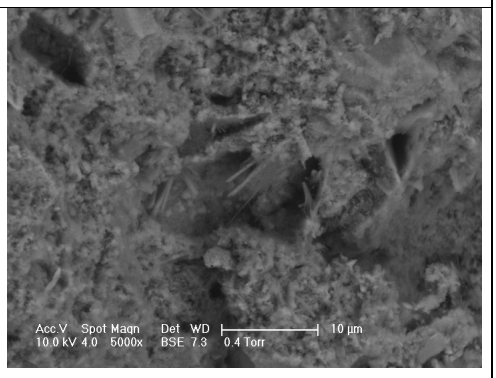

As it can be seen from Table 4.30 the hydration products are easily observed in water cured specimens than the air cured specimens. It was observed that needle like products filled the pores in especially the $0.8f_{max}$ and $0.9f_{max}$ loaded specimens. The air cured specimens appeared to be more porous than the water cured ones.

4.5.2. Optical Microscopy Analysis

The optical microscopy investigation was done on $0.6f_{max}$, $0.8f_{max}$ and $0.9f_{max}$ cyclic loaded specimens for the purpose of investigating the size of the cracks formed after cyclic loading. The crack openings are investigated. The crack openings for $0.9f_{max}$ loaded specimens were the largest as can be seen from the Table 4.31. The average crack widths of the cyclically loaded specimens as shown in Table 4.31 were calculated as 0.23 mm for 0.9fmax loaded, 0.15mm for 0.8fmax loaded and almost 0 mm for 0.6fmax loaded specimens.

Figures 4.42- 4.47 show the optical microscope photograph of water and air cured specimens. The crack width decreased from 0.28mm to 0.18mm with water curing are given in Figure 4.42- 4.43. The closing of cracks after cure was investigated and self healing effect can be observed. The laboratory cured specimens had larger crack openings which were not affected very much by air curing as shown in Figure 4.46- 4.47.

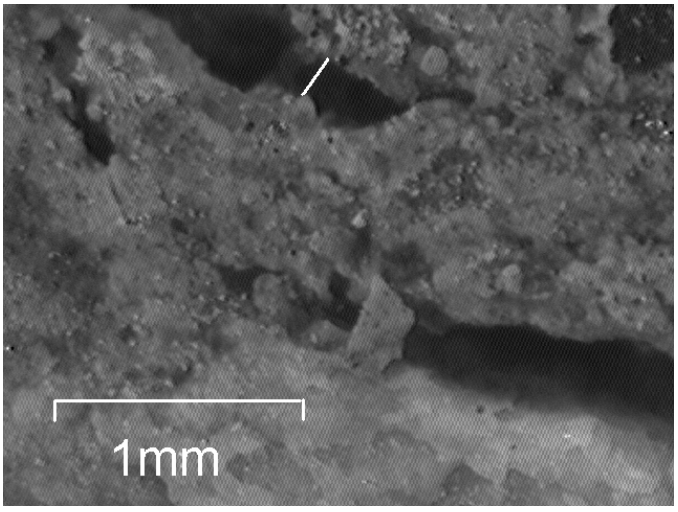

Figure 4.42. 0.9 f_{max} loaded specimen after water cure

Table 4.31. Optical Microscopy analysis of cyclically loaded specimen

$0.9f_{max}$ loaded	**$0.8f_{max}$ loaded**	**$0.6f_{max}$ loaded**
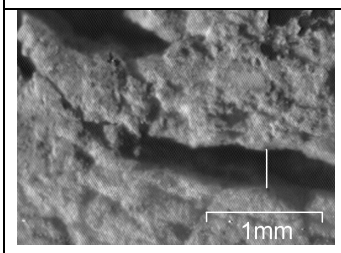 0,35mm crack width	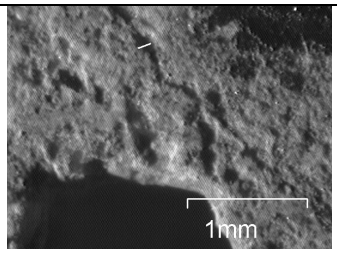 0,11mm crack width	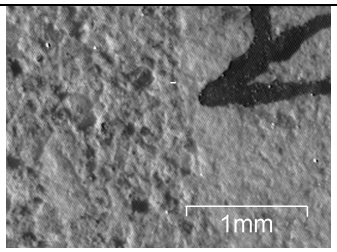 crack width 0,04mm
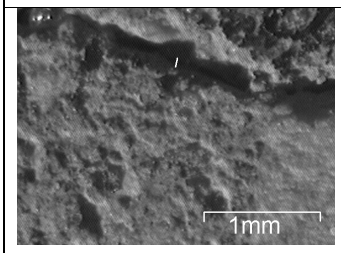 0,17mm crack width	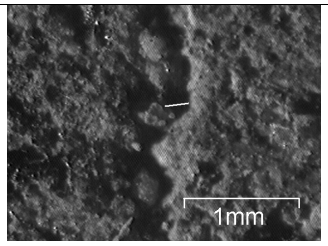 crack width 0,2mm	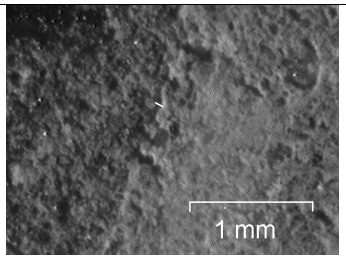 crack width 0,06mm
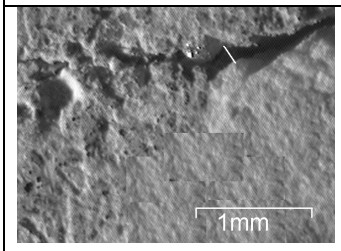 0,18mm crack width	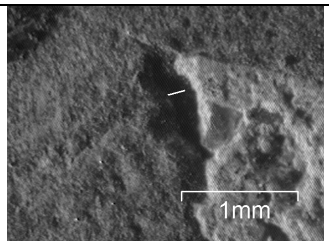 0,14mm crack width	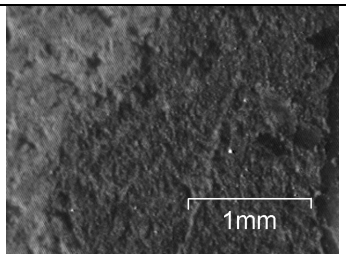 0 crack width

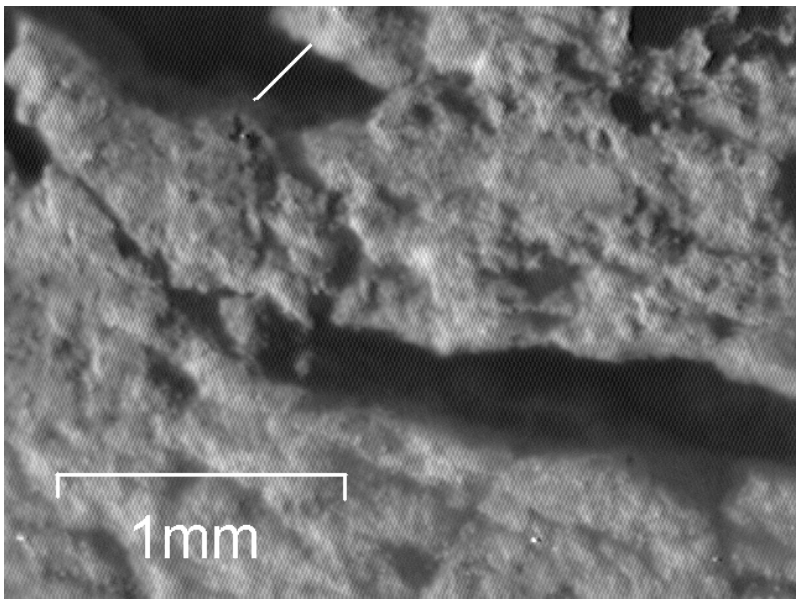

Figure 4.43. 0.9 f_{max} loaded specimen after cyclic loading

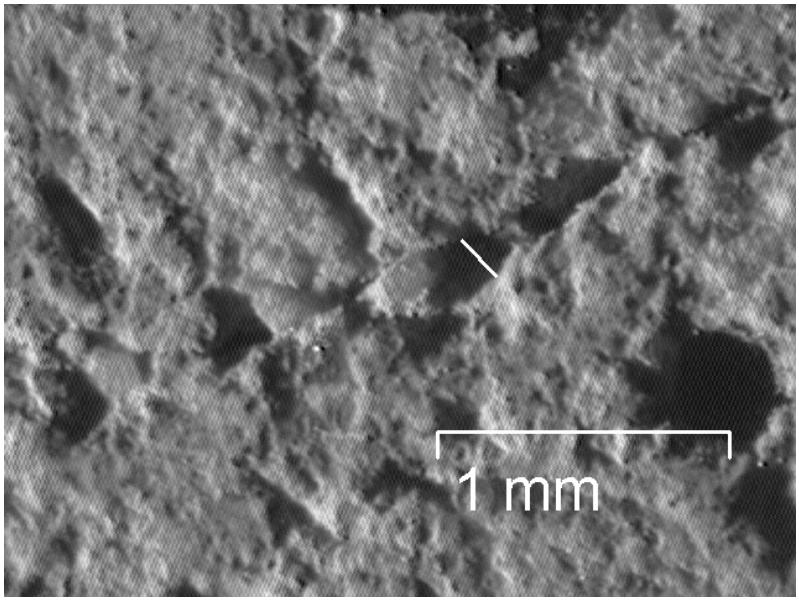

Figure 4.44. 0.9 f_{max} loaded specimen after cyclic loading

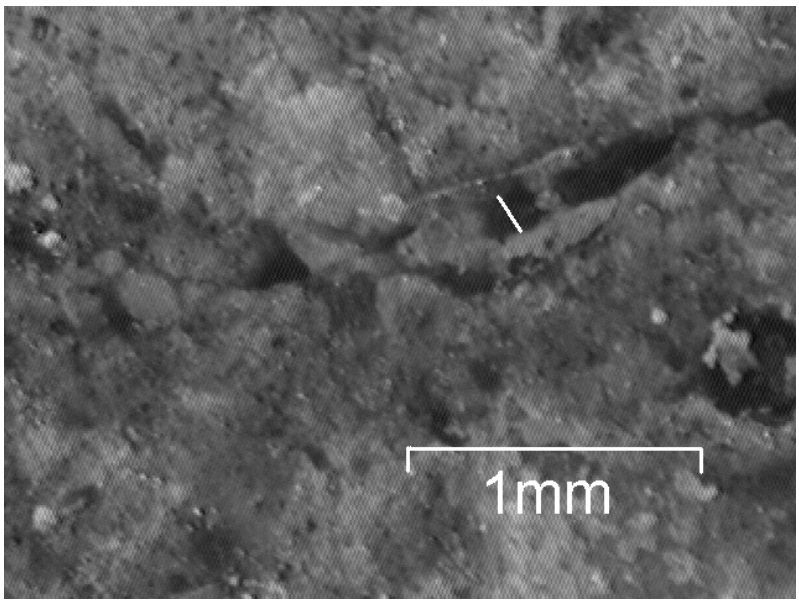

Figure 4.45. 0.9 f_{max} loaded specimen after water cure

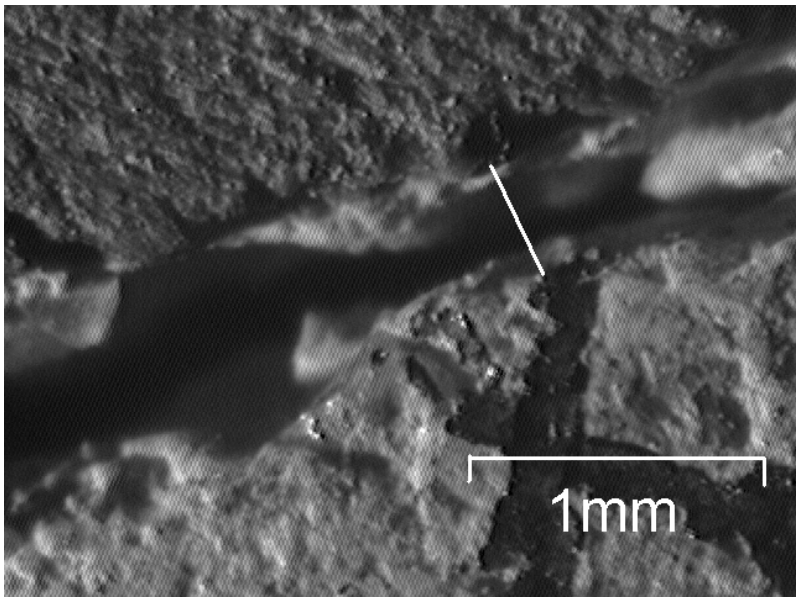

Figure 4.46. 0.9 f_{max} loaded specimen after cyclic loading

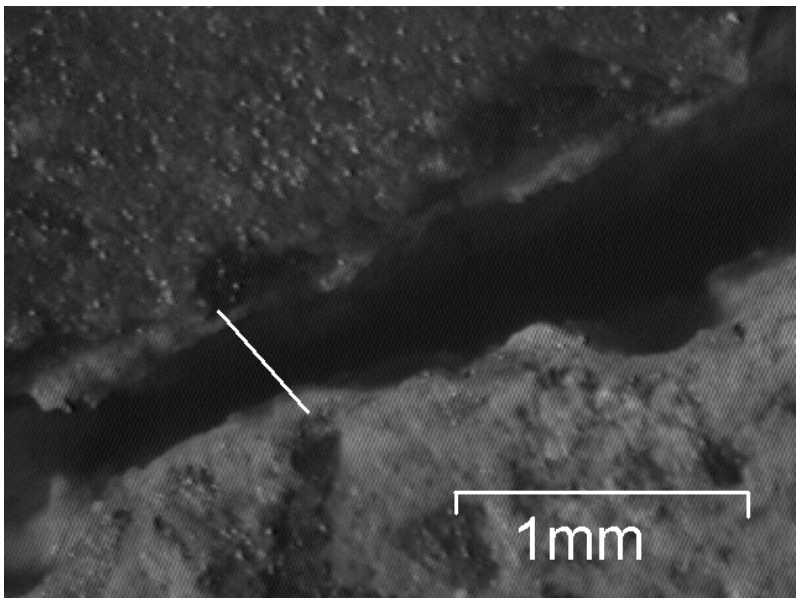

Figure 4.47. 0.9 f_{max} loaded specimen after laboratory cure

4.6. Post Peak Response Analysis

Post peak analyses was done to observe the change in properties with cyclic loading As discussed in previous sections, the specimens were cyclically loaded at different stress values and their behavior was observed.

Cylindrical specimens were loaded at different levels of maximum stress. After cyclically loading the mechanical and permeability properties were measured as explained and discussed before. In post peak response with the increase of cyclic loading ratio the concrete specimen showed a more ductile behavior. It was observed that higher level cyclically loaded specimens had higher damage levels.

4.6.1 Post Peak Response Results

After cyclic loading of concrete specimens at each of the three different loads, the cyclic loading has been extended to the post peak zone as illustrated in Figure 4.48. Focal point was found by taking parallels to loading modulus of elasticity from the peak stresses in the stress strain diagram it was found out that as the cyclic loading ratio increased the focal point deviated further from the control specimen focal point. This indicated that the

specimen behaved in a more ductile way and measurements have shown that modulus of elasticity decreased more than 50 per cent. The graphical representation of finding the focal point is shown in Figure 4.48. Table 4.32 includes thus found focal point coordinates in terms of stress and strain values for the concretes tested. Figure 4.49 and 4.50 shows the post peak response of $0.9f_{max}$ loaded and control specimens, respectively, for the purpose of locating the focal points. In locating the focal point only the lines to focal point untill the inflection point which was about 60 per cent of ultimate stress of concrete were taken into account.

Variation of focal point coordinates with the cyclic loading ratio are given in Figure 4.51 and 4.52. It is seen from these figures that as the loading ratio increased the stress and strain values achieved higher negative values. Figure 4.53 shows the locations of the focal points of control and $0.6f_{max}$, $0.8f_{max}$ and $0.9f_{max}$ loaded specimen.

Table 4.32. Focal point coordinates of different cyclic loaded specimen

	$0.9f_{max}$	**$0.8f_{max}$**	**$0.6f_{max}$**	**Control**
Stress MPa	-40.6	-28.3	-26.6	-23.3
Strain	-0.00127	-0.00065	-0.0006	0.00034

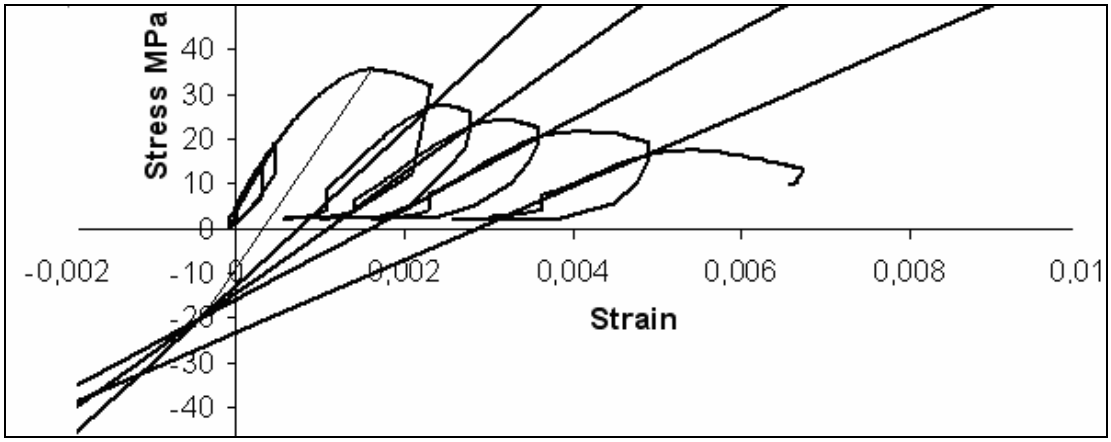

Figure 4.48. Example of finding the focal point.

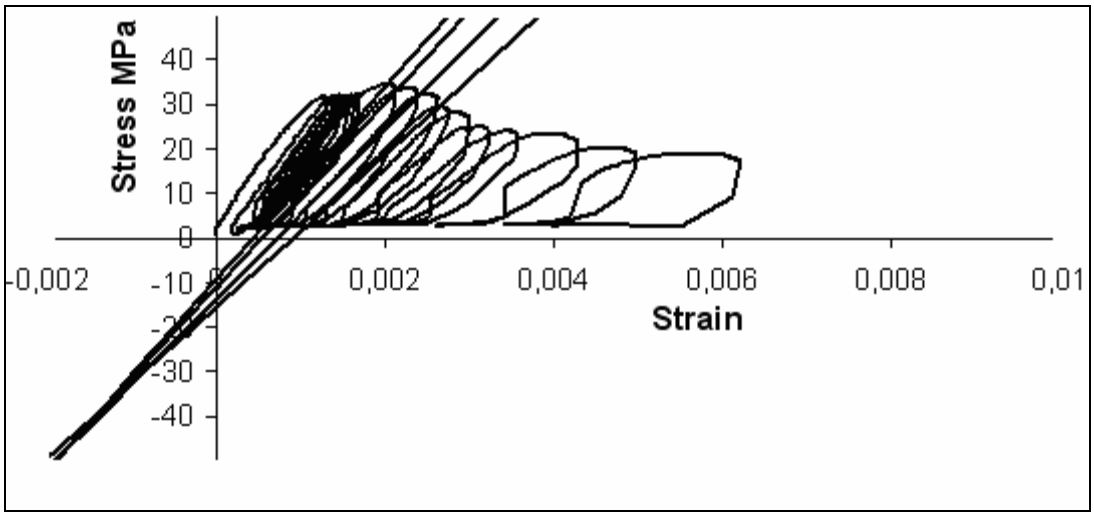

Figure 4.49. 0.9 f_{max} loaded specimen post peak response

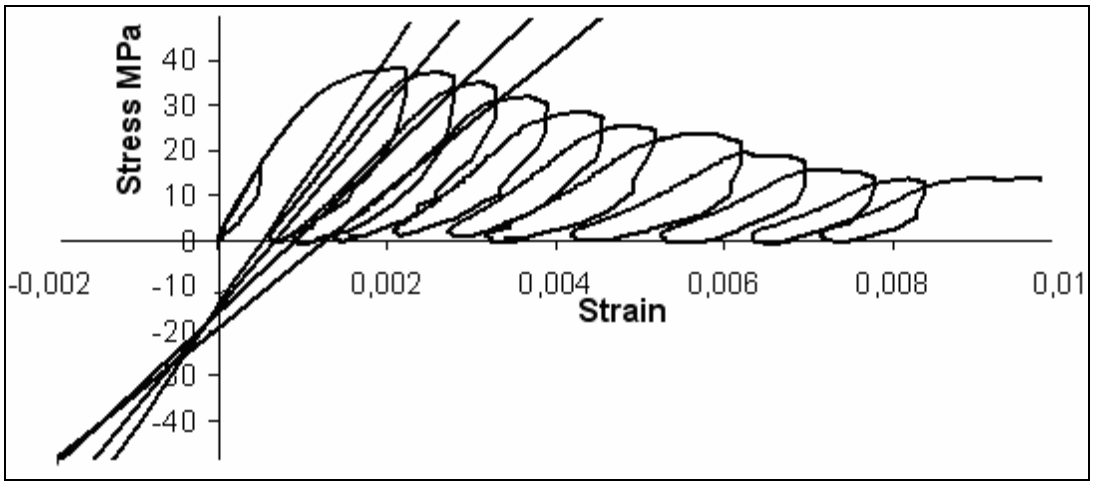

Figure 4.50. Control specimen post peak response

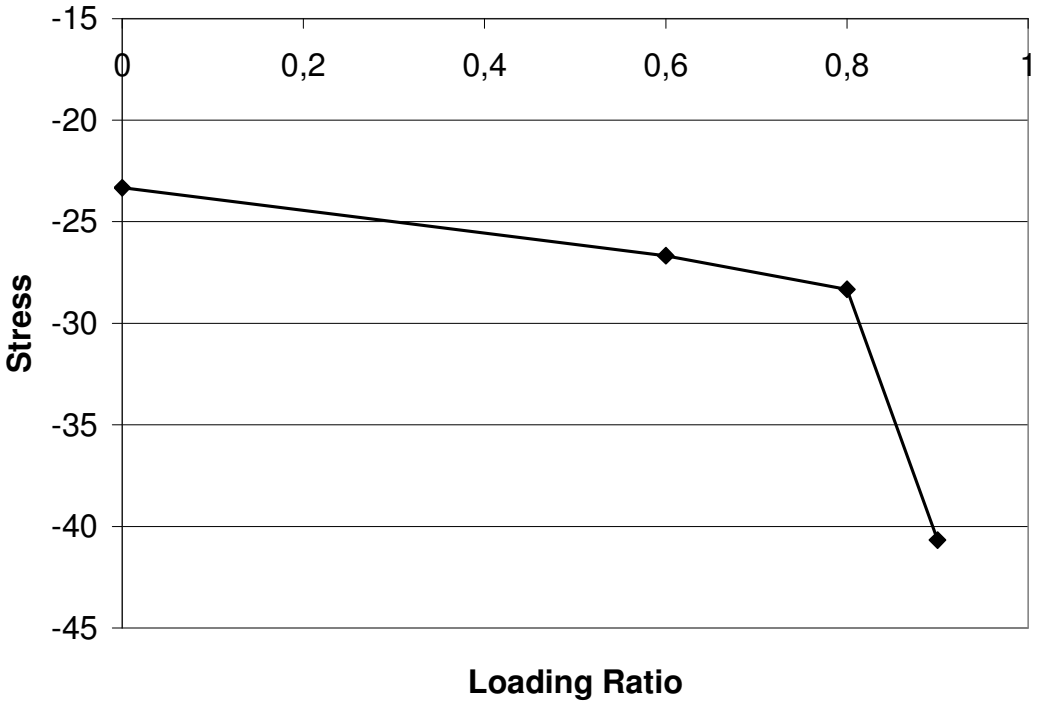

Figure 4.51. Variation of focal point stress value with loading ratio

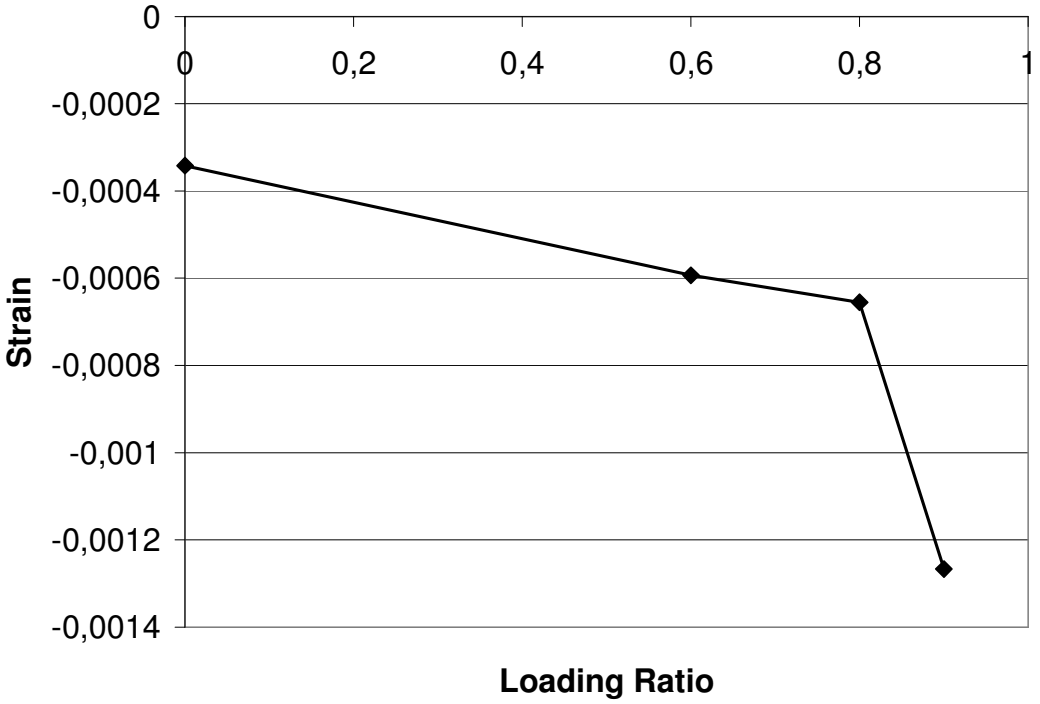

Figure 4.52. Variation of focal point strain value with loading ratio

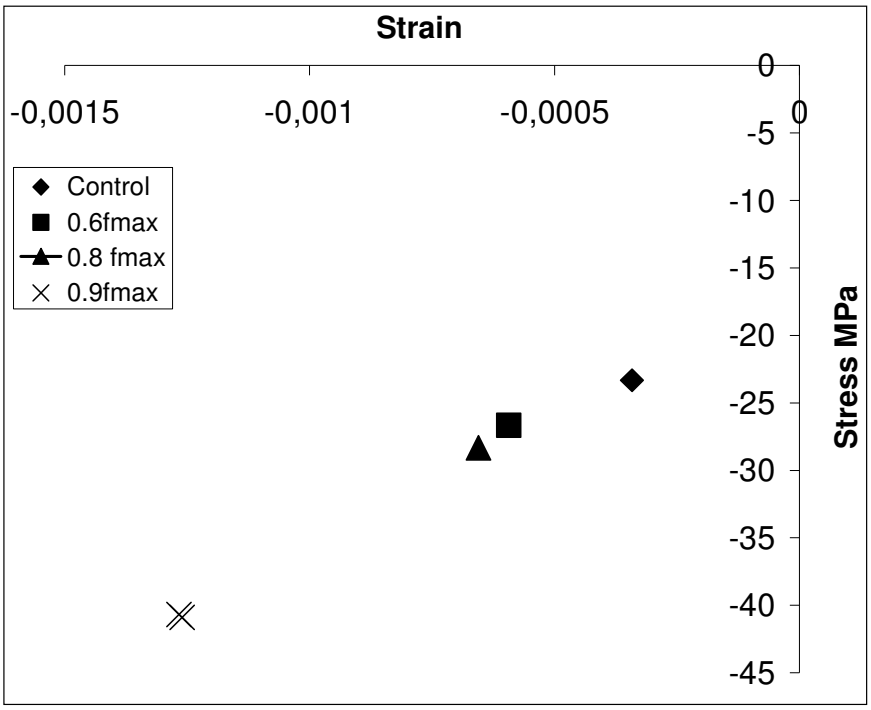

Figure 4.53. Location of focal points for different loading ratios

The fracture energy of concretes calculated as defined in Figure 2.23. The effect of cyclic loading on post peak response can be seen from the stress strain diagrams in Figure 4.48 and 4.49. It can be seen from Fig. 4.54 that fracture energy was lower compared to the control specimen's much higher fracture energy value. This decrease might be due to the comparatively larger damage accumulated during cyclic loading at higher loading stress levels. The decrease in fracture energy with cyclic loading ratio is also illustrated in Figure 4.54.

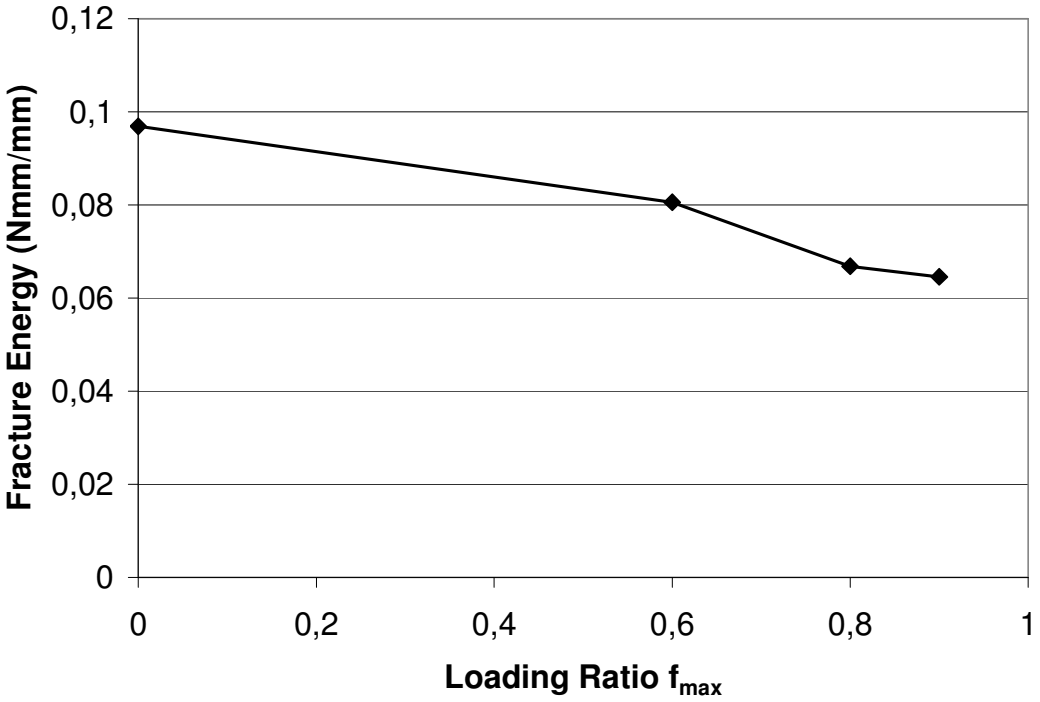

Figure 4.54. Variation of fracture energy with cyclic loading ratio

As the intensity of the cyclic loading increased the fracture energy also increased. It was also observed from Table 4.33 that focal point's coordinates also increased in absolute value which indicated a more ductile behavior of concrete at failure. Variation of modulus of elasticity of concrete with the peak stress is given in Figure 4.55. The modulus of elasticity increased with the peak stresses. The maximum stress and modulus of elasticity of the different cyclic loaded specimen are similar. But 0.9 f_{max} loaded specimen start at a lower stress level than other specimen. Maximum strength and modulus of elasticity are found for Control specimen. But after post peak the strength and modulus of elasticity are similar..

Table 4.33. Fracture energy of concretes after cyclic loading

Loading Ratio	**0**	**0,6f_{max}**	**0,8 f_{max}**	**0,9 f_{max}**
Fracture Energy N.mm/mm	0,097	0,080	0,067	0,064

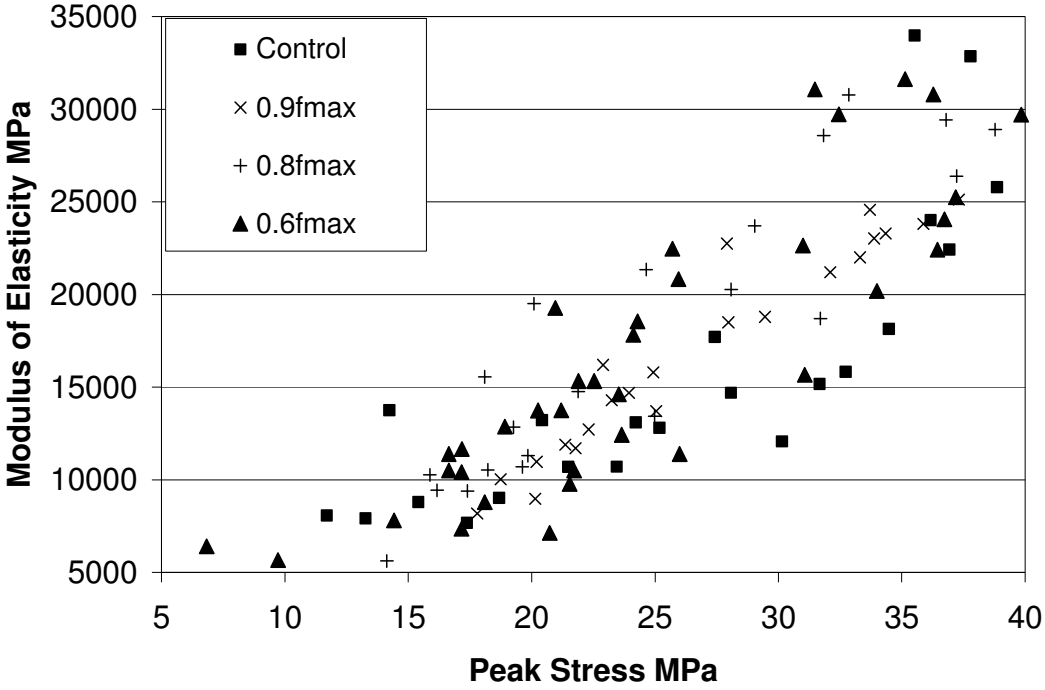

Figure 4.55. Variation of modulus of elasticity of concretes with maximum stress

The normalized modulus of elasticity and peak stress is given in Figure 4.56. The square of correlation coefficient for 0, 0.6,0.8 and $0.9f_{max}$ loading ratios are 0.85, 0.87, 0.95 and 0.93 respectively. The overall coefficient is 0.87. So we may conclude that peak response after cyclic loading is independent from loading history of the concrete.

The permanent strain after each post peak response was also measured. The relation of the permanent at strain with modulus of elasticity is given in Figure 4.57. The permanent strains for $0.9f_{max}$ loaded specimens largest where as their modulus of elasticity is lowest. The measured modulus of elasticity values scattered strongly except for very low strain values. But for lower strain values $0.9f_{max}$ loaded specimen have lower modulus of elasticity for the same permanent strain.

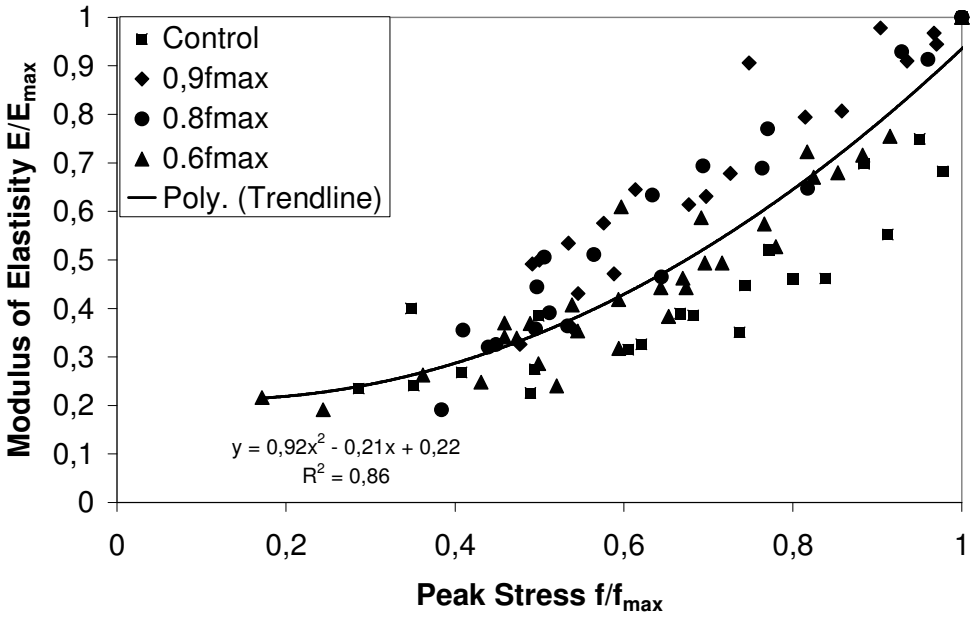

Figure 4.56. Normalized Modulus of Elasticity versus Peak Stress of cyclically loaded specimen

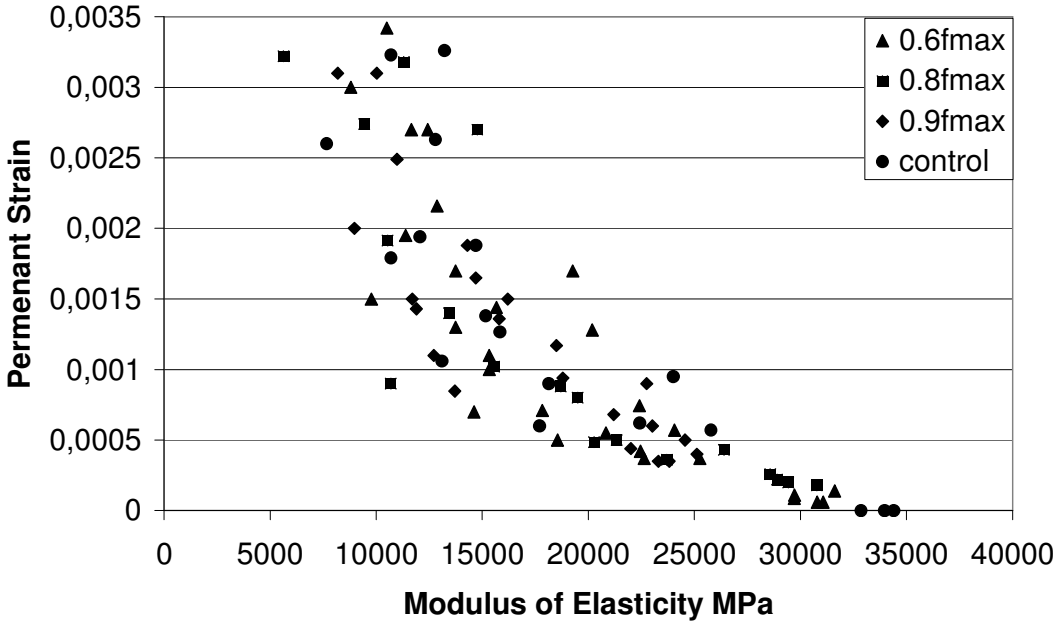

Figure 4.57. Variation of modulus of elasticity with permanent strain

Fracture energy was also calculated for different modulus of elasticity values after post peak response. The variation of fracture energy with modulus of elasticity is given in Figure 4.58. For the first few cycles $0.9f_{max}$ loaded specimen have lower fracture energy. As the post peak cycles increase the fracture energies become similar for the given modulus of elasticity.

The results of focal point investigation after cyclic loading showed that cyclic loaded specimens had lower fracture energy after the first few cycles of post peak zone but they also showed a more ductile behavior and had higher focal point strain values.

Normalized fracture energy versus modulus of elasticity are given in Figure 4.59. In this diagram maximum fracture energy is taken as the fracture energy at 3 times the peak strain. The square of correlation coefficients for 0, 0.6 , 0.8 and $0.9f_{max}$ loaded specimen are 0.93, 0.86 , 0.91 and 0.89 ,respectively. The overall square of correlation coefficient of the results is 0.87. So we may also conclude that fracture energy versus modulus of elasticity relationship is independent of the loading history of the concrete specimen.

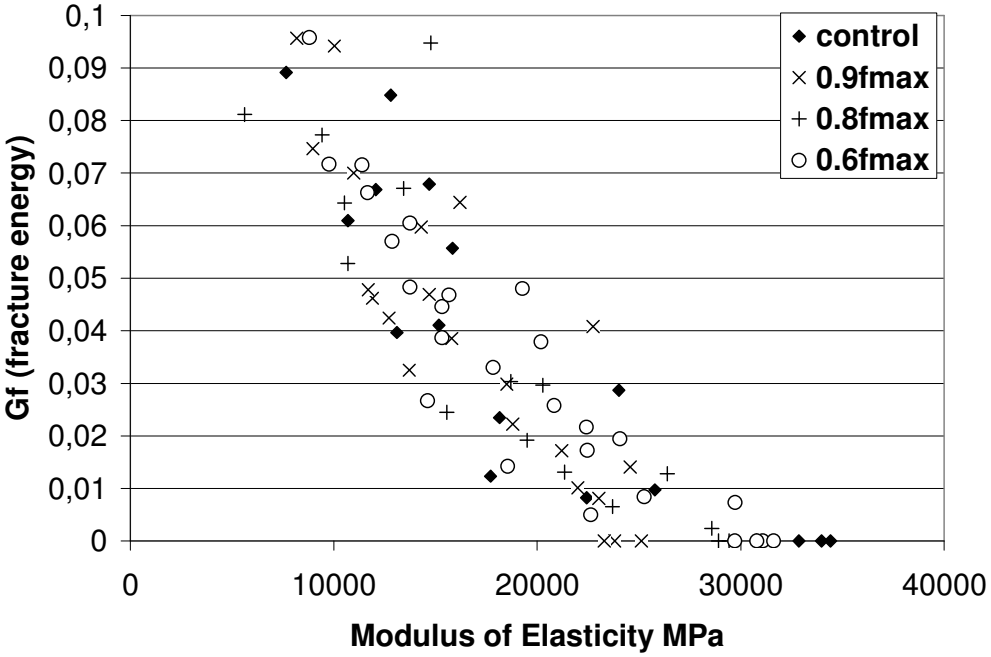

Figure 4.58. Variation of fracture energy with modulus of elasticity

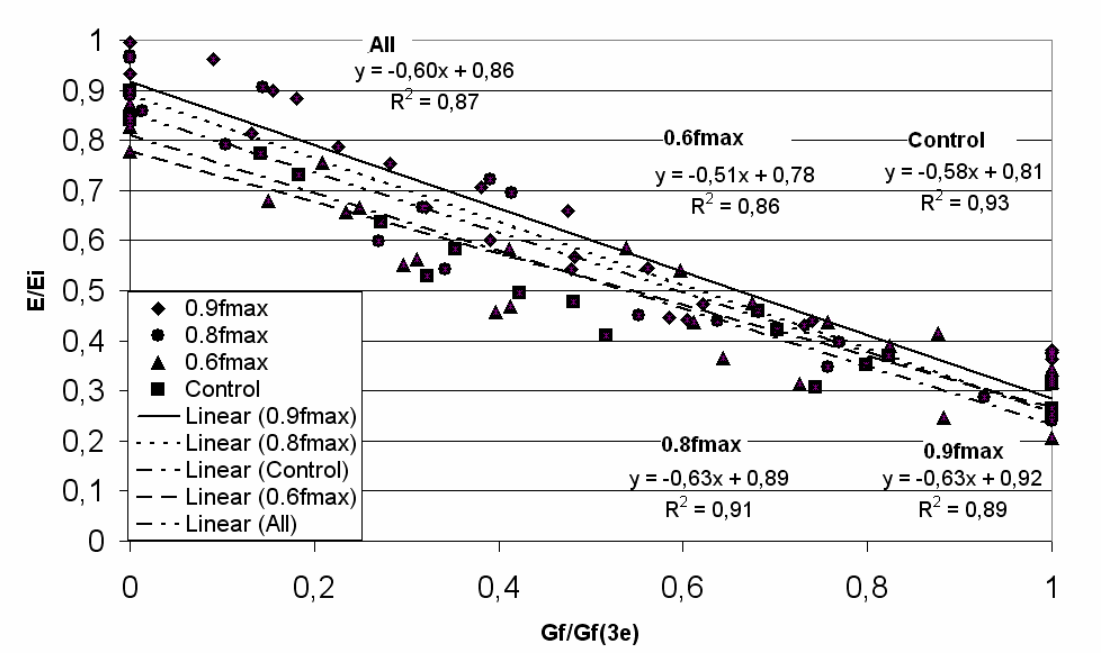

Figure 4.59. Normalized modulus of elasticity versus normalized fracture energy after cyclic loading

Autogenous curing effect was also investigated for the post peak response of cyclically loaded specimens. Focal point determination was done applying the same procedure for the specimens which were additionally water or air cured after cyclic loading. Focal points determined for air cured and water cured specimens are given, respectively, in Table 4.34 and 4.35. Focal point coordinates decreased in absolute value for the water and air cured specimens compared to the values determine after the cyclic loading of the specimens. Water cured specimens showed higher decrease in absolute value, including a more brittle behavior for concrete at failure. Location of focal points determined after cyclic loading and after water and air curing of cyclically loaded concrete specimens are shown in Figure 4.60. This figure also shows the effect of self healing of cracks due to additional water and air curing of concrete in terms of focal point coordinates which are actually incluzation of fracture energy and the mode of failure of concrete. Fracture energy of concretes after cyclic loading and after additional curing were shown in Figure 4.61. It was observed that fracture energy generally decreases with increasing loading ratio except that water cured concretes after $0.6f_{max}$ loading showed a slight increase.

Effect of water curing on fracture energy of cyclically loaded concretes was in the increasing way indicating a more brittle mode of failure where as air curing caused a slight decrease resulting in a more ductile behavior compared to cyclically loaded specimens. With water curing it may be said that the damage was repaired and thus the fracture energy of the concrete was increased making the material more brittle.

Table 4.34. Focal point values of different cyclic loaded specimen after laboratory cure

	$0.9f_{max}$	**$0.8f_{max}$**	**$0.6f_{max}$**	**Control**
Stress MPa	-47.5	-27.5	-20	-20
Strain	-0.0012	-0.0006	-0.00012	0.00019

Table 4.35. Focal point value of different cyclic loaded specimen after water cure

	$0.9f_{max}$	**$0.8f_{max}$**	**$0.6f_{max}$**	**Control**
Stress MPa	-32.5	-26.5	-17.5	-20
Strain	-0.0013	-0.0009	-0.00015	0.0005

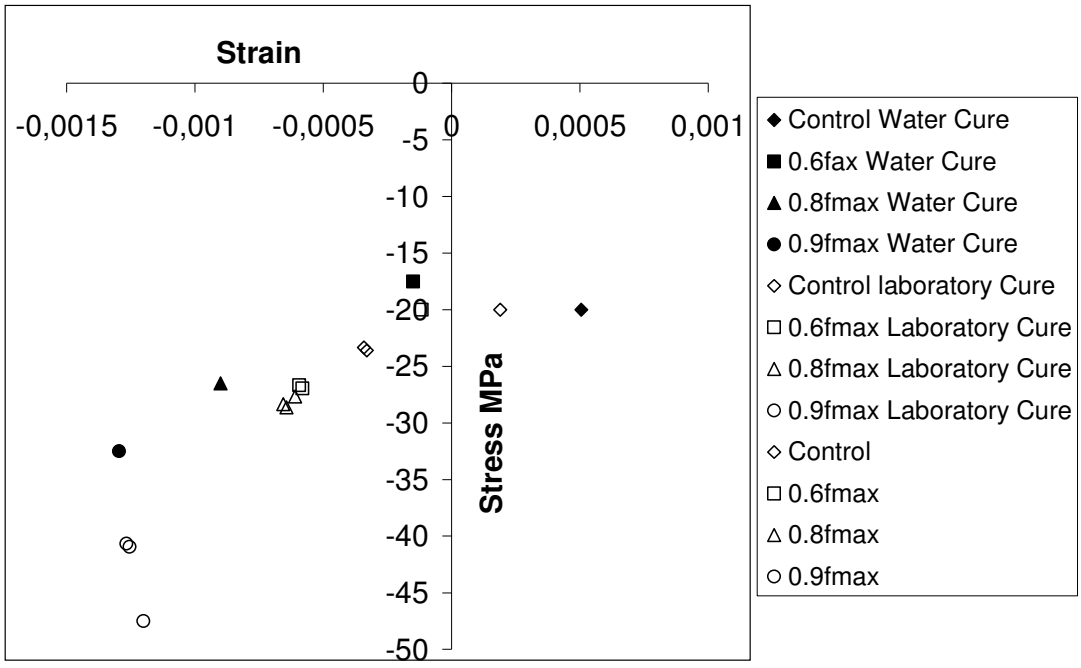

Figure 4.60. Focal point of specimen after water cure for different loading ratios

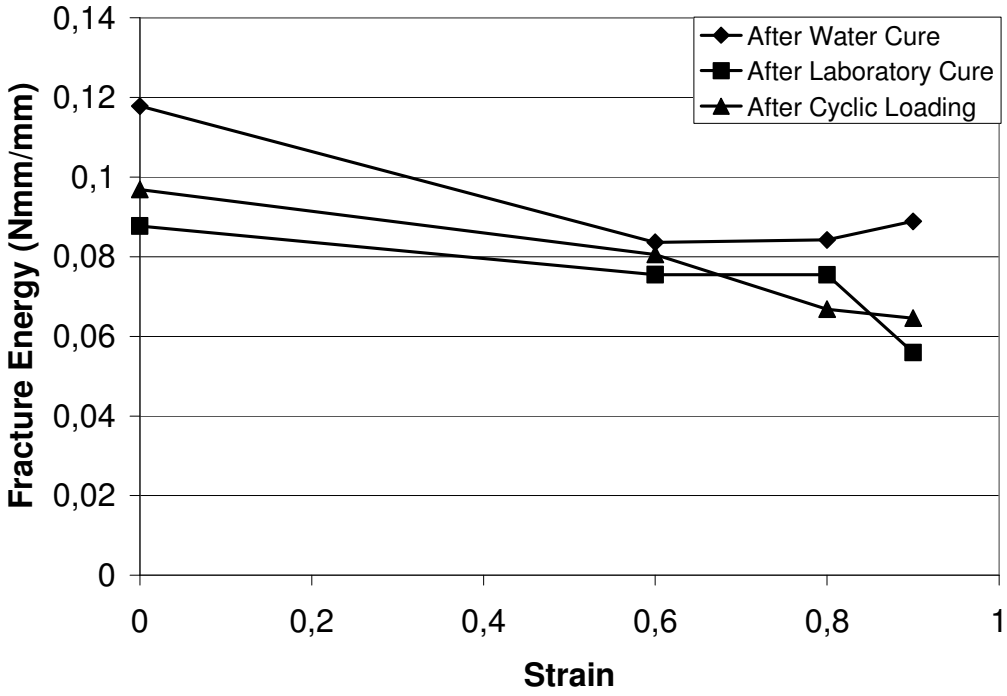

Figure 4.61. Variation fracture energy with cyclic loading ratio for different curing conditions

In Table 4.36 the square of correlation for each cyclic loading ratio after water and laboratory cure are given where as correlation for the overall data was shown in Figure 4.62. Overall square of correlation coefficient which was found 0.90. So we may conclude that the post peak response in terms of normalized fracture energy versus normalized modulus of elasticity is also independent of the curing of concrete after damage. Similar results and relations have been obtained by Taşdemir [54] as shown previously in Figure 2.25.

Table 4.36. Normalized fracture energy – modulus of elasticity R^2 correlation of results individually in post peak response

Loading Ratio	**After Water Cure**	**After Laboratory Cure**
Control	0.94	0.94
0.6f_{max}	0.94	0.93
0.8f_{max}	0.93	0.86
0.9f_{max}	0.95	0.94

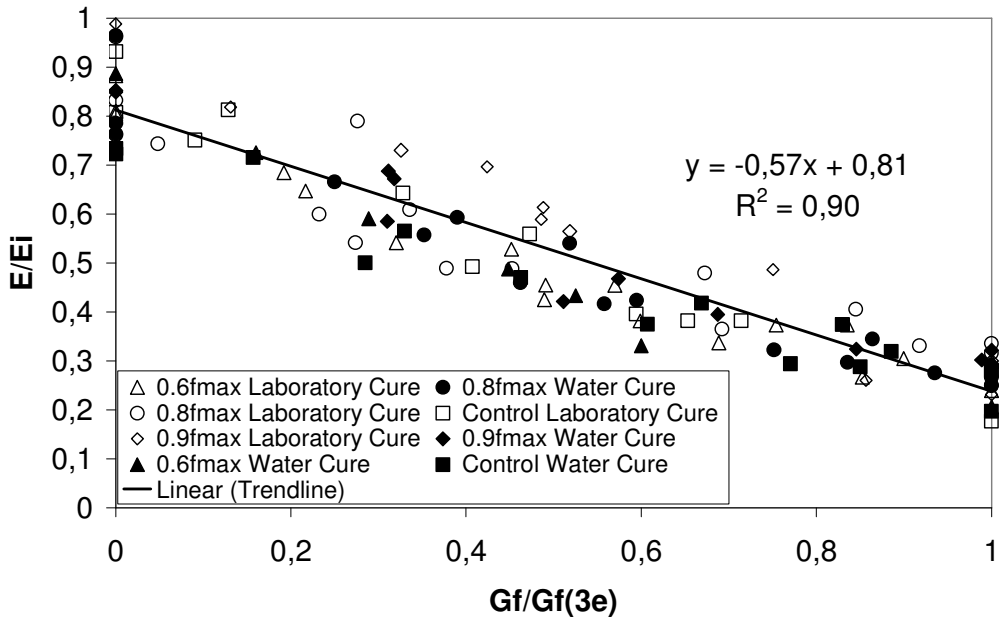

Figure 4.62. Normalized modulus of elasticity versus normalized fracture energy after water and laboratory cure

5. CONCLUSIONS

In this study mechanical and permeability properties of concrete which was subjected to compressive cyclic loading of $0.6f_{max}$, $0.8f_{max}$ and $0.9f_{max}$ were investigated. The healing effect of air and water curing after cyclic loading on the micro cracks formed due to cyclic loading were also investigated.

Some conclusions drawn from this study are:

- As expected compressive strength, splitting tensile strength, ultrasonic pulse velocity and modulus of elasticity decreased with cyclic loading. The decrease in splitting tensile strength and modulus of elasticity were higher with increasing loading ratio compared with the decrease in compressive and ultrasound speed.
- Each cyclic loading caused a permanent strain and permanent damage in the concrete. As the cyclic loading ratio increased the permanent strain increased. Also, with increasing cyclic loading ratios the strain at peak stress increased in the compression test of concrete.
- Water absorption , rapid chloride permeability of concrete , total pore volume and area , mass loss due to magnesium sulphate increased with increasing cyclic loading ratio. The increase in higher with $0.9f_{max}$ loading.

Self healing results are as follows;

- Compressive strength , modulus of elasticity, splitting tensile strength , ultrasonic pulse velocity increased more with water cure compared to laboratory air curing of cyclically loaded specimens.
- Water cure decreased the water absorption , rapid chloride permability and mass losses in magnesium sulphate solution of the cyclically loaded specimens compared with the laboratory curing
- It was observed that the hydration products filled the cracks with water cure in ESEM analyses.

- The crack openings were larger for higher cyclic loading ratios. Also with water cure the crack sizes decreased.
- Post peak responses of cyclically loaded specimen and water and laboratory cured specimen were investigated. Focal point stress strain coordinates changed to more negative values with increasing cyclic loading ratio.
- Fracture energy measured decreased with cyclic loading ratios.

Evaluation and discussion of the experimental results of the study indicates that:

- Cyclic loading at $0.6f_{max}$ appears to be a critical loading ratio for mechanical and permeability properties of concrete. Concretes which are subjected to low cycle loading at beyond $0.6f_{max}$ will exercise considerable reductions in mechanical and durability properties.
- In the case of an earthquake if the concrete in the structural elements is subjected to cyclic loading beyond this limit mechanical properties of concrete should be reevaluated for the further safety of the structure
- Self healing property of cracks caused after cyclic loading under appropriate curing conditions of early age concretes were beneficial for the mechanical and permeability properties of concrete to varying degrees.

6. REFERENCES

1. Hordjik, D. A., *Local Approach to Fatigue of Concrete*, Phd Thesis, Delft University, 1991

2. Glicerio, T., "The Fatigue Behaivor of Rolled Compacted Concrete", *Concrete Ways Symposium* , pp.155-165, Austria,1998

3. Tokyay, M., *Determination of The Tensile Fatigue Properties of Plain Concrete By Indirect Tension Tests*, M.Sc. Thesis , Middle East Technical University Engineering Faculty, 1980

4. Thun, H., *Assessment of Fatigue Resistance and Strength in Existing Concrete Structures*, Doctoral Thesis, Luleå University of Technology Department of Civil and Environmental Engineering Division of Structural Engineering, 2006

5. Spooner, D.C. and J.W. Dougwil, "A Quantitative Assessment of Damage Sustained in Concrete During Compressive Loading", *Magazine of Concrete Research*, Vol 27(92), pp151,160, 1975

6. Wöhler, A.,*Über die Festigkeitsversuche mit Eisen und Stahl*, Verlag von Ernst & Korn, Berlin, Germany, 1870

7. Carrasquillo, R. L., F. Slate and A.H. Nilson, "Micro Cracking and Behavior of High Strength Concrete Subject to Short Term Loading" , *ACI Materials Journal*, Vol 78, pp 179-186, May 1981

8. Gilkey, H.J., "Zig Zag Course of Concrete Progress", *ACI Journal*, Vol 21 No 8, pp573-579, Proceedings Vol 46, February 1950

9. Bazant, Z. P. and Y. Xiang, "Size Effect in Compression Fracture: Splitting Crack Band Propogation", *Journal of Engineering Mechanics*, Vol. 123 No 2, pp 162-172, February 1997

10. Buyukozturk, O., A. H Nilson and F. O. Slate, "Stress Strain Response and Fracture of a Concrete Model in Biaxial Loading" , *ACI Materials Journal* , Vol 68 No 52, pp 590-599, August 1971

11. European Union – Brite EuRam III EuroLightCon, *Fatigue of Normal Weight Concrete and Lightweight Concrete*, Document BE96-3942/R34, Netherlands, June 2000

12. Gao, L. and C. T. T. Hsu, "Fatigue of Concrete under Uniaxial Compression Cyclic Loading", *ACI Materials Journal* , pp575-581, Vol 95 No 5, September-October 1998

13. Maher, A. and D. Darwin, "Mortar Constituent of Concrete in Compression", *ACI Journal* , pp 100-109, March April 1982

14. .Chung, S., C. Meyer and M. Shinozuka, "Modelling of Concrete Damage" ,*ACI Structural Journal*, Vol 86, pp 259-271, 1989

15. Antoun, T. H., *Constitutive Failure Model for The Static and Dynamic Behaviors of Concrete Incorporating Effects of Damage and Anisotropy*, Ph.D. Thesis, The University of Dayton, 1991

16. Wang, K., D. J. Cansen, S. P. Shah and A. F. Karr, "Permeability Study of Cracked Concrete", *Cement and Concrete Research* , Vol. 27 No 3, pp 381-393, 1997

17. Shah, S. P. and S. Chandra,"Fracture of Concrete Subjected to Cyclic and Sustained Loading", *ACI Journal* , pp 816-827, Vol 67 No 49 , October 1970

18. Su, E. C. M., *Biaxial Compression Fatigue of Concrete*, Ph.D. Thesis, University of Houston , 1987

19. Xiaobin, L., *Uniaxial and Triaxial Behavior of High Strength Concrete With and Without Steel Fibers*, Ph.D Thesis, New Jersey Institute of Technology, 2005

20. Attiogbe, E. K. and D. Darwin, "Submicrocracking in Cement Paste and Mortar" *ACI Materials Journal,* pp 491-500, November December 1987

21. Alliche,A. and D. Francois, "Fatigue Behavior of Hardened Cement Paste", *Cement and Concrete Research* , V16, pp199-206,1986

22. Gököz Ü., *Ön Yorulmanın Yalın ve İnce Tellerle Donatılı Betonların Özelliklerine Etkisi* , Ph.D. Thesis , İTÜ Civil Engineering Faculty, 1978

23. American Concrete Institute, 215 "Fatigue Considerations For Design of Concrete Structures", *Manual of Concrete Practice*,2000

24. Kim, J. K. and Y. Y. Kim, "Experimental Study of The Fatigue Behavior of High Strength Concrete", *Cement and Concrete Research*, Volume 26, Issue 10, pp 1513-1523, October 1996

25. Cao, J. and U. Chung, "Defect Dynamics and Damage of Concrete Under Repeated Compression Studied by Electrical Resistance Measurement", *Journal of Materials Science*, Vol 31,pp 4351-4360, 2001

26. Ludirdja, D., R. L. Berger and J. F. Young, "Simple Method for Measuring Water Permeability of Concrete", *ACI Materials Journal,* Vol 86 No 5, pp433-439, September October 1989

27. Neville, A., "Autogenous Healing- A Concrete Miracle", *Concrete International*, pp 76-82, November 2002

28. Ballatore, E. and P. Bocca, "Variations in The Mechanical Properties of Concrete Subjected to Low Cyclic Loads", *Cement and Concrete Research* , Vol 27 No 3, pp 453-462, 1997

29. Mu, B., K. V. Subramaniam and S. P. Shah, "Failure Mechanism of Concrete Under Fatigue Compressive Load", *Journal of Materials In Civil Engineering* , ASCE , pp566-572, 2004

30. Moral, H., *Betonun Az Tekrarlı Bir Eksenli Basınç Altındaki Davranışına Bileşimin Etkisi*, Ph.D. Thesis, İstanbul Teknik Üniversitesi - Fen Bilimleri Enstitüsü, İstanbul , 1986

31. Award, M. E., Hilsdorf H.K., "*Strength and Deformation Characteristics of Plain Concrete Subjected to High repeated and Sustained Loads*", SP 41-1, ACI

32. Hasan, M.; T. Ueda and Y. Sato, "Stress-Strain Relationship of Frost-Damaged Concrete Subjected to Fatigue Loading", *Journal of Materials in Civil Engineering ASCE* Vol 1, pp 37-45 ,January 2008

33. Baluch, M.H., A. H. Algadhib and A. R. Khan, "CDM Model for Residual Strength of Concrete Under Cyclic Compression", *Cement and Concrete Composites*, Vol 25, pp 503-512, May –June 2003

34. Minh-Tan, D., C. Omar and A. P. Claude, "Fatigue Behaivor of High Performance Concrete", *ASCE Journal of Materials in Civil Engineering*, Vol 1, pp96-111, 1993

35. Byong, Y. B. C. and T. S. Tzu, "Stress Strain Behavior of Concrete Under Cyclic Loading", *ACI Materials Journal* , pp 178-193, 1998

36. Suaris, W. and F. Fernando, “Ultrasonic Pulse Attenuation as A Measure of Damage Growth During Cyclic Loading of Concrete”, *ACI Materials Journal*, pp 185-193, May-June 1987

37. Knab, L.I., G. V. Blessing and J. R. Clifton, “Laboratory Evaluation of Ultrasonics for Crack Detection in Concrete”, Vol 80 No 3, *ACI Materials Journal,* November December 1983

38. Gettu, R., A. Aguado and M.O.F. Oliveira, “Damage in High-Strength Concrete Due to Monotonic and Cyclic Compression—A Study Based on Splitting Tensile Strength” , *ACI Materials Journal ,*Vol 93 No 6, pp 1-5, November December 1996

39. Picandet, V., A. Khelidj and G. Bastian, “Effect of Axial Compressive Damage on Gas Permeability of Ordinary and High-Performance Concrete”, *Cement and Concrete Research*, pp1525-1532, Vol 31, 2001

40. Zhang, B., “Relationship Between Pore Structure and Mechanical Properties of Ordinary Concrete Under Bending Fatigue”, *Cement and Concrete Research* , V28 No 5, pp699-711, 1998

41. Sugiyama, T., T. W. Bremner and T. A. Holm, “Effect of Stress on Gas Permeability in Concrete”, *ACI Materials Journal* ,Vol 93 No 5, pp1-8, September October 1996

42. Edvardsen, C., “Water Permeability and Autogenous Healing of Cracks in Concrete” ,*ACI Materials Journal* , V. 96, No. 4, pp448-455, July-August 1999

43. Hearn, N., “Effect of Shrinkage and Load-Induced Cracking on Water Permeability of Concrete”, *ACI Materials Journal*, Vol 96 No 2, pp234-241, March April 1999

44. Kamran, M. N., P. J. M. Monteiro and K. L. Scrivener, “Analysis of Compressive Stress-Induced Cracks in Concrete”, *ACI Materials Journal*, Vol 95 No 5, pp 617-630, September October 1998

45. Abbas, A., M. Carcasses, J. P. Ollivier, “Gas Permeability of Concrete in Relation to Its Degree of Saturation”, *Materials and Structures/Matdriaux et Constructions*, Vol. 32, pp 3-8, January-February 1999

46. Samara, H.R. and K. C. Hover, “Influence of Microcracking on The Mass Transport Properties of Concrete”, Vol 89 M46, *ACI Materials Journal*, pp416-424, July August 1992

47. Kumara, R. and B. Bhattacharjee, “Porosity, Pore Size Distribution and In Situ Strength of Concrete” , *Cement and Concrete Research*, Vol 33, pp 155-164, 2003

48. Hearn, N. and G. Lok, “Measurement of Permeability Under Uniaxial Compression – A Test Method”, *ACI Materials Journal*, Vol 95 No 6, pp691-694, November December 1998

49. Lauer, K. R. and F. O. Slate, “Autogenous Healing of Cement Paste”, *ACI Journal*, V52-63, pp1083-1097, June 1956

50. Dhir, R. K., C. M. Sangha and J. G. L. Munday, “Strength and Deformation Properties of Autogenously Healed Mortars”, Vol 70-24, *ACI Journal*, pp 231-236, March 1973

51. Granger, S., A. Loukili, G. Pijaudier-Cabot and G. Chanvillard, “Experimental Characterization of The Self-Healing of Cracks in An Ultra High Performance Cementitious Material: Mechanical Tests and Acoustic Emission Analysis”, *Cement and Concrete Research*, Vol 37 ,pp 519–527, 2007

52. Zhong, W. and W. Yao, “Influence of Damage Degree on Self-Healing of Concrete”, *Construction and Building Materials*, in press

53. Reinhardt, H. W. and M. Jooss, " Permeability and Self-Healing of Cracked Concrete As a Function of Temperature and Crack Width", *Cement and Concrete Research* , Vol 33,pp 981–985, 2003

54. Tasdemir, C., M. A. Tasdemir, N. Mills, B. I. G. Barr and F. D. Lydon, "Combined Effects of Silica Fume, Aggregate Type, and Size on Postpeak Response of Concrete in Bending" , *ACI Materials Journal* , Vol 96, pp74-83, January February 1999

55. Lee, Y. H. and K. Willam, "Mechanical Properties of Concrete in Uniaxial Compression" , *ACI Materials Journal* , Vol 94 , pp 457-471, November December 1997

56. Köksal, H. O. and C. Karakoç, "An Isotropic Damage Model for Concrete", *Materials and Structures*, RILEM, Vol 32, pp 611-617, October 1999

57. Neville, A. M., *Properties of Concrete*, Longman Sc & Tech, 4th Ed., England, July 1996

58. Tomosawa, F. and T. Noguchi, "Relationship Between Compressive Strength and Modulus of Elasticity of High-Strength Concrete", *Third International Symposium on Utilization of High Strength Concrete, Symposium in Lillehammer*, Dept. of Architecture, Fac. of Engineering, Univ. of Tokyo, pp.1247-1254,Norway, June20-23, 1993

59. ERMCO (European Ready Mixed Concrete Organization), *Guidance to the Engineering Properties of Concrete*, Brussels, 2007

60. Tasdemir, C., "Combined Effects of Mineral Admixtures and Curing Conditions on The Sorptivity Coefficient of Concrete" , *Cement and Concrete Research* , Vol 33, pp1637–1642, 2003